Interaction Notes

Note 197

October 1974

Analytical and Numerical EMP Coupling Solutions for a Class of Structures Attached to the Wing of an Aircraft

by

M. I. Sancer and A. D. Varvatsis

Tetra Tech, Incorporated

Pasadena, California

Abstract

In this note we present a description of the analysis necessary to develop a large EMP coupling computer code. The analysis for two models of the wing is contained in this note; however, the code was only developed for the simpler wing model. The code calculates EMP induced surface current densities on the attached structure as well as aperture excited voltages and currents on a cable or cable bundle that is interior to the circular cylindrical portion of the structure. Also contained in the code is an option to isolate the circular cylinder and calculate new numerical results for this well studied and useful model.

ACKNOWLEDGMENT

We thank Carl Baum, Phil Castillo, and Mike Harrison for their continued interest and support of this work. Thanks go to Scott Siegel and Richard Sassman for their skillful computer programming. Special thanks go to Ray Latham whose presence always makes work a little easier.

CONTENTS

ILLUSTRATIONS

SECTION I

INTRODUCTION AND SUMMARY

The work reported in this note is a continuation of the effort presented in AFWL Interaction Note 148 (ref. 1) with essentially the following additional new tasks completed. Detailed solutions for surface current densities have been determined for a class of attached structures and the corresponding computer code has been developed. Solutions for aperture excited currents and voltages on a cable or cable bundle contained within the circular cylindrical portion of the attached structure are also presented and these solutions are contained within the computer code. In order to obtain an operating computer code we simplified the model of the wing and represented it as an infinite flat plane; however, the detailed analysis for the infinite elliptic cylinder model of the wing is also presented in detail.

In the process of completing the required work we made a significant discovery that will now be described. While debugging our computer code we built options into our program that would allow certain portions of the structure to be present while other portions could be made to vanish. In this manner we tested our program by calculating the surface current density induced on a finite circular cylinder with the intention of comparing our solution with the ones presented in references 2 and 3. In references 2 and 3 the total axial current is calculated and consequently we were required to integrate our calculated current density to make the comparison. We obtained excellent agreement for

---

1. Sancer, M. I., and A. D. Varvatsis, "Surface currents induced on structures attached to an infinite elliptic cylinder, Part I, Detailed magnetic field integral equation for an attached structure having an arbitrary shape," AFWL Interaction Notes, Note 148, December 1973.

2. Sassman, R. W., "The current induced on a finite, perfectly conducting, solid cylinder in free space by an electromagnetic pulse," AFWL Interaction Notes, Note 11, July 1967.

3. Sancer, M. I., and A. D. Varvatsis," Calculation of the induced surface current density on a perfectly conducting body of revolution," AFWL Interaction Notes, Note 101, April 1972.

the total current but observed that for essentially all frequencies in the EMP spectrum, including those whose associated wavelengths are much larger than the diameter of the cylinder, the surface current density was far from uniform around the circumference of the cylinder. The erroneous assumption of uniformity has been widely used in the past to justify the calculation of total currents in order to simply obtain current densities which are the necessary quantities for EMP coupling calculations. These debugging results have significant consequences and will be published as a separate AFWL Interaction Note. We have left this option in the code developed for the total attached structure problem with the additional option to calculate aperture excited currents and voltages induced on cables within the isolated cylinder.

In order to use the isolated cylinder code it is necessary to choose the appropriate source option, since there are two different sources one can choose in the attached structure code. One comes from a formal integral equation analysis and corresponds to the total field, incident plus scattered, in the presence of the infinite plane. This is the option presented in the text because it arises naturally in the derivation of the integral equation for the half plane model of the wing. The second option for the source term does not appear in the text because it is introduced based on physical rather than mathematical arguments. This source option is just the incident field and it should be used with the isolated cylinder option as well as with the total structure code for certain angles of incidence. The major part of the total code is independent of the form of the source; therefore, a useful continuation of this problem would be to include additional source options.

Thus far we have discussed the flexibility of the code developed for this problem in terms of options. There is another type of flexibility built into the code that enhances its usefulness. This is the large number and general character of the input parameters. These input parameters as well as the desired output parameters will now be listed.

Input Variables	Definition	Appropriate Figure(s)
φ_o, θ_o	incidence angles for the EMP	1,6
φ_p	polarization angle for the EMP	1,6
a_p	semi-major axis of the pylon	1
b_p	semi-minor axis of the pylon	1
h_p	height of the pylon	1
a_b	radius of the attached body	1
L_1	partial length of attached body	1
L_2	partial length of attached body	1
k_o	wavelength of Fourier transformed EMP	
φ_a^k	angular location of the k^{th} aperture	7
x_a^k	x coordinate of the k^{th} aperture	9
α_e^k	electric polarizability of the k^{th} aperture	
α_m^k	magnetic polarizability of the k^{th} aperture	
a	radius of the interior cable	7
δ	displacement of interior cable	7
φ_w	angular location of interior cable	7
Z_R	inpedance termination of interior cable	9
Z_L	impedance termination of interior cable	9
x_c	x coordinate of point where the voltage and current are measured on the interior cable	9

Output Variable	Definition
$J_{sF}(i), J_{tF}(i)$	two components of the surface current density at center of i^{th} zone on the $z > 0$ side of the attached structure

$J_{sB}(i), J_{t\,B}(i)$ — two components of the surface current density at center of i^{th} zone on the $z < 0$ side of the attached structure

$V(x_c), I(x_c)$ — values of the voltage and current induced on the interior cable at the specified location

Two comments regarding the input parameters are appropriate. One is that both k_o and all linear dimensions can be specified numerically as being normalized to some convenient length, d. That is k_o can be specified as $k_o d$, as long as all linear dimensions are divided by d when they are given numerical values. Finally, we note that the self zoning aspect of the code is a powerful capability in that a wide class of attached structures can be modeled by choosing different ratios of a_p, b_p, a_b, h_p, L_1 and L_2.

In Section II, the existing symmetry of the attached structure about the xy plane is utilized to reduce the matrix inversion time, and the appropriate analytical symmetry considerations are explained in detail. In Section III, the integral equations for the "reduced" current densities (introduced in Section II) are cast in component form and some preliminary calculations necessary for the next Section are performed. In Section IV, the integral equations for the two surface components of the "reduced" current densities are cast into a matrix equation form and the "incident" field components and matrix elements are presented in detail. In the final Section V, the necessary analysis is presented to obtain the aperture excited voltage and current on a cable or cable bundle contained in the circular cylindrical portion of the attached structure. In Appendix A, the numbering scheme of zones and subzones is developed along with detailed expressions for their coordinates and areas; and in Appendix B, the self-contributions to the matrix elements are cast in forms suitable for accurate numerical calculations.

SECTION II
SYMMETRY CONSIDERATIONS

In this section we use certain symmetry properties of the kernel of the magnetic field integral equation to derive a pair of integral equations defined only over half of all the surfaces involved. This is possible because the structure under consideration (fig. 1) possesses a plane of symmetry xy. This procedure is useful for numerical calculations in that it reduces the size of the matrix that must be inverted as will be discussed later. We start by recalling the integral equation derived in reference (p. 8, (21))

$$f(\Omega)\,\underline{J}(\underline{r}) = \underline{J}_T(\underline{r}) + \int_{S_A} \underline{\underline{K}}(\underline{r}, \underline{r}_o) \cdot \underline{J}(\underline{r}_o)\, dS_o \tag{1}$$

where S_A is the sum of all surfaces except the surface of the infinite elliptical cylinder (fig. 1) (this is so because of the specific choice of the Green's function as it was explained in reference 1) and $\underline{J}(\underline{r})$ is the unknown surface current density equal to $\hat{n} \times \underline{H}$ ($\hat{n}$ is the unit outward normal on the surface and $\underline{H}$ the unknown magnetic field). Also

$$\left.\begin{aligned} \underline{J}_T(\underline{r}) &= \hat{n} \times \underline{H}_T(\underline{r}) \\ \underline{H}_T(\underline{r}) &= \underline{H}_i(\underline{r}) + \underline{H}_s(\underline{r}) \end{aligned}\right\} \tag{2}$$

where $\underline{H}_i(\underline{r})$ is the incident magnetic field, $\underline{H}_s(\underline{r})$ is the magnetic field scattered by a perfectly conducting infinite elliptical cylinder illuminated by $\underline{H}_i(\underline{r})$ in the absence of other surfaces,

$$f(\Omega) = 1 - \Omega/4\pi \tag{3}$$

and Ω is the solid angle subtended by the surface S_A. If we don't choose $\underline{r}$ to approach at a discontinuity in curvature, then $\Omega = 2\pi$ and $f(\Omega)$ assumes the value of 1/2 which is usually seen in the magnetic field integral equation.

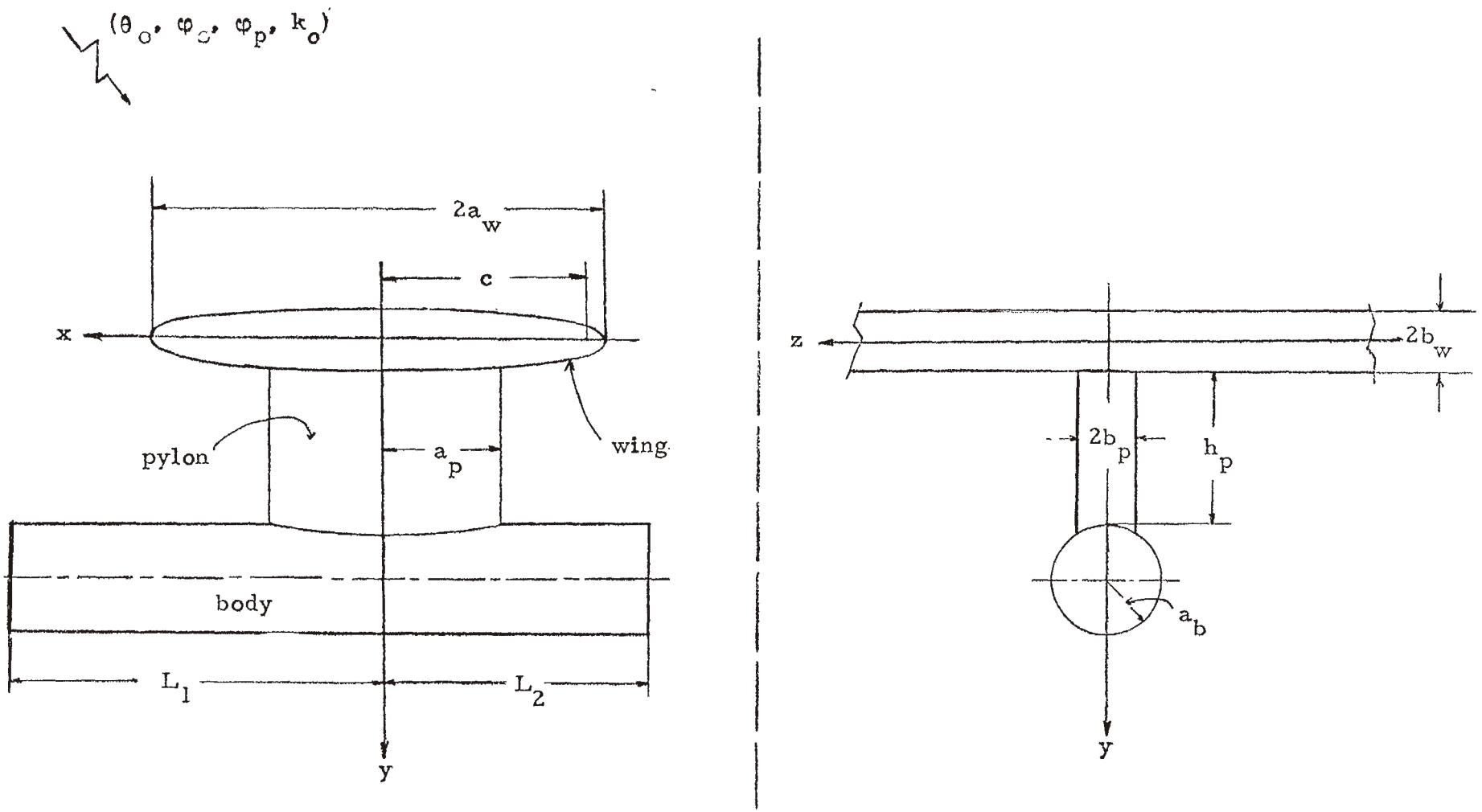

Figure 1: Geometry of wing (modeled as an infinite elliptical cylinder) and hanging structures.

The kernel in (1) can be written as

$$\underline{\underline{K}}(\underline{r},\underline{r}_o) = \underline{\underline{K}}_o(\underline{r},\underline{r}_o) + \underline{\underline{K}}_1(\underline{r},\underline{r}_o) \tag{4}$$

$$\underline{\underline{K}}_o(\underline{r},\underline{r}_o) = \hat{n}(\underline{r}) \times [\nabla G_o(\underline{r},\underline{r}_o) \times \underline{\underline{I}}] \tag{5}$$

$$\underline{\underline{K}}_1(\underline{r},\underline{r}_o) = \hat{n}(\underline{r}) \times [\nabla \times \underline{\underline{G}}_{1s}(\underline{r},\underline{r}_o)] \tag{6}$$

where G_o is the free-space Green's function

$$G_o = \frac{\exp[ik_o|\underline{r} - \underline{r}_o|]}{4\pi|\underline{r} - \underline{r}_o|} \tag{7}$$

$\underline{\underline{I}}$ is the unit dyadic, k_o is the free-space wavenumber and $\underline{\underline{G}}_{1s}(\underline{r},\underline{r}_o)$ is given by (154) of reference 1 ,

$$\underline{\underline{G}}_{1s}(r,r_o) = -\frac{i}{2\pi}\int_{C_n}\frac{dh}{k_o^2-h^2}\sum_{m=0}^{\infty}\Bigg\{(N_m^{(e)}(\lambda))^{-1}$$

$$\times\Big[C_m^{(e)}(\lambda,\xi_1^*)\underline{Me}_m^{(3)}(h,\underline{r})\underline{M}^{(3)}(-h,\underline{r}_o)$$

$$+ D_m^{(e)}(\lambda,\xi_1^*)\,\underline{Ne}_m^{(3)}(h,\underline{r})\underline{N}^{(3)}(-h,\underline{r}_o)\Big]$$

$$+\left(N_m^{(o)}(\lambda)\right)^{-1}\Big[C_m^{(o)}(\lambda,\xi_1^*)\underline{Mo}_m^{(3)}(h,\underline{r})\,\underline{Mo}_m^{(3)}(-h,\underline{r}_o)$$

$$+ D_m^{(o)}(\lambda,\xi_1^*)\,\underline{No}_m^{(3)}(h,\underline{r})\underline{No}_m^{(3)}(-h,\underline{r}_o)\Big]\Bigg\} \tag{8}$$

where

$$\underline{M}\alpha_m^{(3)}(n,\underline{r}) = \frac{e^{ihz}}{c\beta}\left[\hat{u}\,R\alpha_m^{(3)}(\lambda,\xi)S\alpha_m'(\lambda,n) - \hat{v}R\alpha_m^{(3)'}(\lambda,\xi)S\alpha_m(\lambda,n)\right] \tag{9}$$

$(\alpha = e, o)$

$$N\alpha_m^{(3)}(h,\underline{r}) = \frac{ihe^{ihz}}{k_o c\beta}\left[\hat{u}R\alpha_m^{(3)'}(\lambda,\xi)S\alpha_m(\lambda,\eta)+\hat{v}R\alpha_m^{(3)}(\lambda,\xi)S'\alpha_m(\lambda,\eta)\right]$$

$$+\frac{\lambda^2}{c^2k_o}e^{ihz}zR\alpha_m^{(3)}(\lambda,\xi)S\alpha_m(\lambda,\eta) \qquad (\alpha = e,o) \qquad (10)$$

$$\left.\begin{aligned}\lambda^2 &= c^2(k_o^2-h^2)\\ \hat{u} &= \beta^{-1}(a\hat{x}+b\hat{y})\\ \hat{v} &= \beta^{-1}(-b\hat{x}+a\hat{y})\end{aligned}\right\} \qquad (11)$$

The rest of the quantities in the above relationships are defined in reference 1 (Section V) and will not be given here because their specific form is not important to our symmetry considerations.

In reference 1 we considered the problem of finding the surface current density induced on the attached structures by an incident plane wave when the airplane wing is modeled as a perfectly conducting infinite elliptical cylinder. In this report we are still interested in the same problem, but we give numerical results for the surface current density for the case of a wing modeled as a perfectly conducting flat plate of infinite extent (fig. 2). For this reason we will present our symmetry arguments for both cases. The integral equation for the case of the flat plate has the form of (1) except that $\underline{H}_s(\underline{r})$ in (2) is the scattered magnetic field by the flat plate rather than by the infinite cylinder. (However, as we mentioned in the introduction, using $\underline{H}_s$ for the elliptical cylinder is a better approximation.) Also $\underline{\underline{K}}_1$ in (6) now has the form

$$\underline{\underline{K}}_1 = -\hat{n} \times \left[\nabla G_o(\underline{r},\underline{r}_{oi}) \times \underline{\underline{R}}\right] \qquad (12)$$

where G_o is given by (7),

$$\underline{\underline{R}} = \underline{\underline{I}} - 2\hat{y}\,\hat{y} \qquad (13)$$

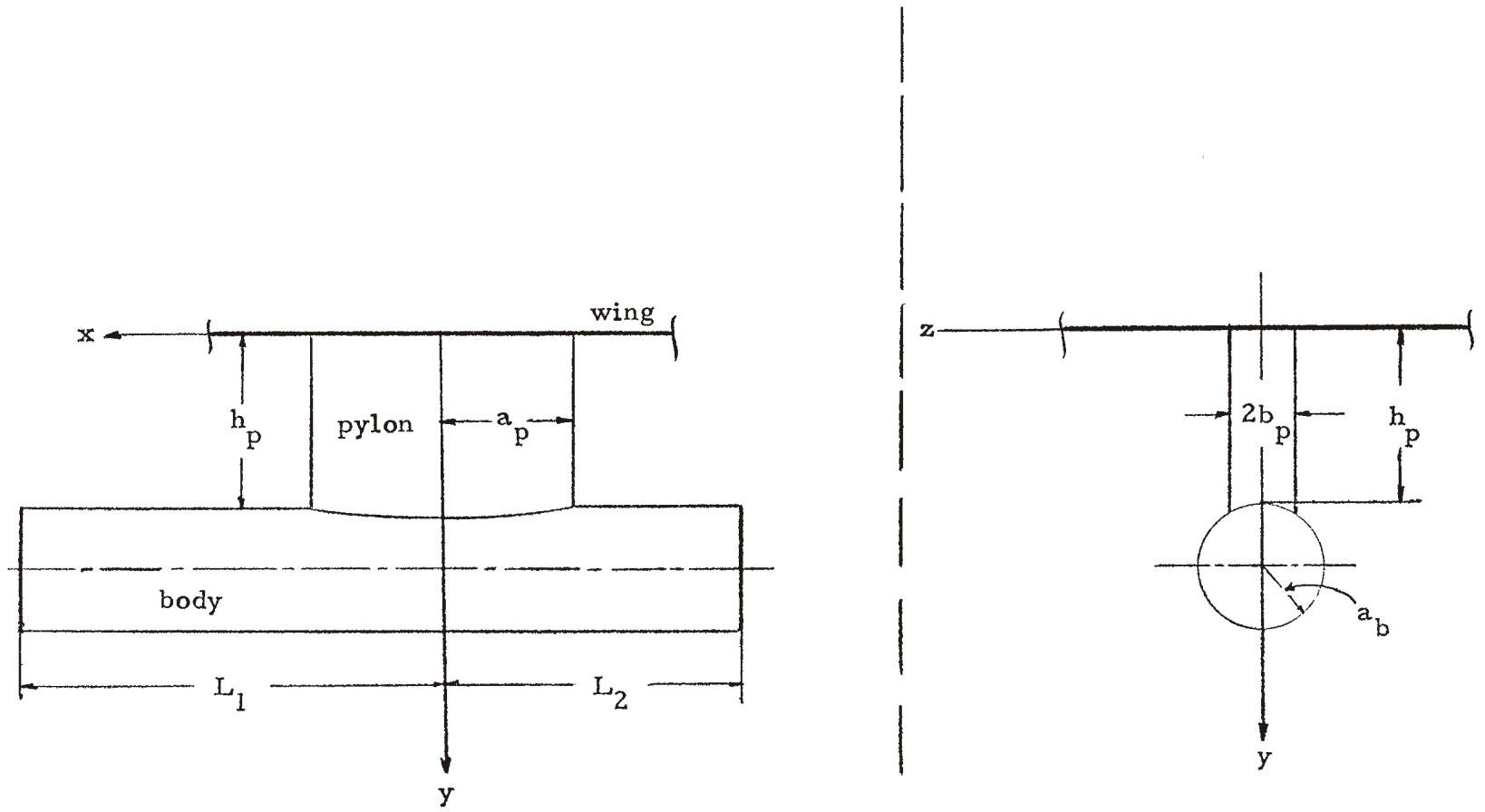

Figure 2: Geometry of wing (modeled as a flat plate) and hanging structures.

is the reflection operator on the xz plane and

$$\underline{r}_{oi} = \underline{\underline{R}} \cdot \underline{r}_o \tag{14}$$

The coordinate vectors $\underline{r}_o$ and $\underline{r}_{oi}$ correspond to a point P and its image (with respect to the xz plane) respectively.

Before proceeding with our analysis we refer the reader to reference 4 for an earlier application of symmetry considerations for electromagnetic field interaction problems. We start with a general perfectly conducting body possessing a plane of symmetry xy (fig. 3). The $z<o$ half is the negative side and the $z>o$ half the positive side. We write (1) for points on both sides

$$f(\Omega)\,\underline{J}(r^+) = \underline{J}_T(\underline{r}^+) + \int_{S^+} \underline{\underline{K}}(\underline{r}^+, \underline{r}_o{}^+) \cdot \underline{J}(\underline{r}_o{}^+) dS_o{}^+ + \int_{S^-} \underline{\underline{K}}(\underline{r}^+, \underline{r}_o{}^-) \cdot \underline{J}(\underline{r}_o{}^-) dS_o{}^- \tag{15}$$

$$f(\Omega)\,\underline{J}(\underline{r}^-) = \underline{J}_T(\underline{r}^-) + \int_{S} \underline{\underline{K}}(\underline{r}^-, \underline{r}_o{}^+) \cdot \underline{J}(\underline{r}_o{}^+) dS_o{}^+ + \int_{S^-} \underline{\underline{K}}(\underline{r}^-, \underline{r}_o{}^-) \cdot \underline{J}(\underline{r}_o{}^-) dS_o{}^- \tag{16}$$

We choose r^+ and r^- such that (fig. 3)

$$\left.\begin{aligned} &\underline{r}^+ = \underline{\underline{R}}_1 \cdot r^-, \; r^- = \underline{\underline{R}}_1 \cdot \underline{r}^+ \\ &\underline{\underline{R}}_1 = \underline{\underline{I}} - 2\hat{z}\,\hat{z} \end{aligned}\right\} \tag{17}$$

$\underline{\underline{R}}_1$ is the reflection operator on the xy plane and is such that

$$\underline{\underline{R}}_1 \cdot \underline{\underline{R}}_1 = \underline{\underline{I}} \tag{18}$$

Also notice that for symmetric points about the xy plane the surface elements have equal areas i. e. $dS_o{}^- = dS_o{}^+ = dS_o$. Next we define

$$\underline{\underline{R}}_1 \cdot \underline{J}(\underline{r}^-) = \underline{\underline{R}}_1 \cdot \underline{J}(\underline{\underline{R}}_1 \cdot \underline{r}^+) \equiv \underline{J}^*(\underline{r}^+) \tag{19}$$

4. Baum, C. E., "Interaction of electromagnetic fields with an object which has an electromagnetic symmetry plane," AFWL Interaction Notes, Note 63, March 1971.

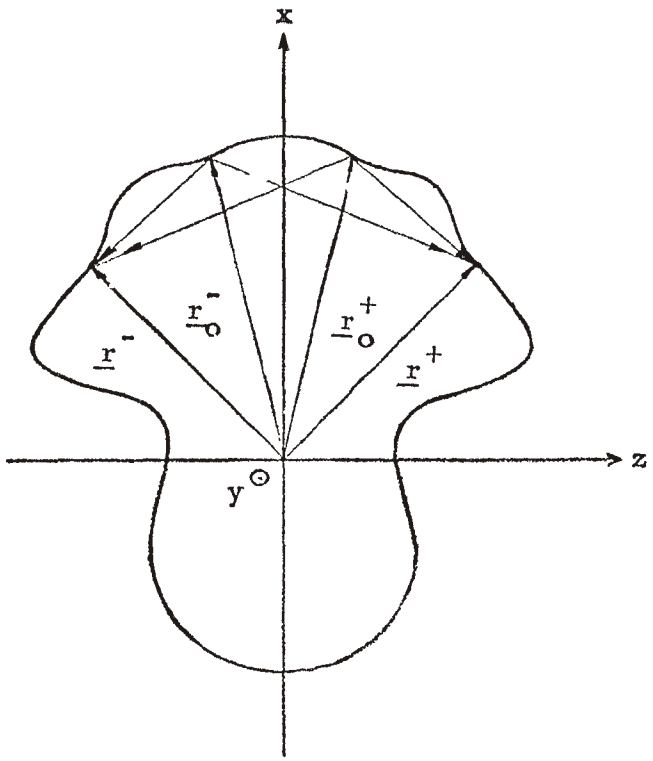

Figure 3: Geometry of a general body with an xy plane of symmetry.

$$\underline{\underline{K}}(\underline{r}^+, \underline{r}_o^-) = \underline{\underline{K}}(\underline{r}^+, \underline{\underline{R}}_1 \cdot \underline{r}_o^+) \equiv \underline{\underline{K}}^*(\underline{r}^+, \underline{r}_o^+) \tag{20}$$

$$\underline{\underline{K}}(\underline{r}^-, \underline{r}_o^-) = \underline{\underline{K}}(\underline{\underline{R}}_1 \cdot \underline{r}^+, \underline{\underline{R}}_1 \cdot \underline{r}_o^+) \equiv \underline{\underline{K}}^{**}(\underline{r}^+, \underline{r}_o^+)$$

If we now scalar multiply (16) by $\underline{\underline{R}}_1$ and take (18), (19) and (20) into account we obtain

$$f(\Omega)\underline{J}^*(\underline{r}^+) = \underline{J}_T{}^*(\underline{r}^+) + \int_{S^+} \underline{\underline{R}}_1 \cdot \underline{\underline{K}}(\underline{r}^-, \underline{r}_o^+) \cdot \underline{J}(\underline{r}_o^+)\, dS_o$$

$$+ \int_{S^+} \underline{\underline{R}}_1 \cdot \underline{\underline{K}}^{**}(\underline{r}^+, \underline{r}_o^+) \cdot \underline{\underline{R}}_1 \cdot \underline{J}^*(\underline{r}_o^+) dS_o \tag{21}$$

where

$$J_T{}^*(\underline{r}^+) \equiv \underline{\underline{R}}_1 \cdot \underline{J}_T(\underline{r}^-) \tag{22}$$

Notice that the second surface integral is now evaluated on S^+. The reason is that all the functions in the integrand can be thought of as functions of $\underline{r}_o^+$ and consequently we can perform the integral over S^+ because of the pointwise symmetry between S^+ and S^-.

Using (18) and (19) we can rewrite (15) as

$$f(\Omega)\, \underline{J}(\underline{r}^+) = \underline{J}_T(\underline{r}^+) + \int_{S^+} \underline{\underline{K}}(\underline{r}^+, \underline{r}_o^+) \cdot \underline{J}(\underline{r}_o^+)\, dS_o + \int_{S^+} \underline{\underline{K}}^*(\underline{r}^+, \underline{r}_o^+) \cdot \underline{\underline{R}}_1 \cdot \underline{J}^*(\underline{r}_o^+) dS_o \tag{23}$$

We will shortly prove that

$$\underline{\underline{R}}_1 \cdot \underline{\underline{K}}(\underline{r}^-, \underline{r}_o^+) = \underline{\underline{K}}(\underline{r}^+, \underline{r}_o^-) \cdot \underline{\underline{R}}_1 \tag{24a}$$

$$\underline{\underline{R}}_1 \cdot \underline{\underline{K}}(\underline{r}^-, \underline{r}_o^-) \cdot \underline{\underline{R}}_1 = \underline{\underline{K}}(\underline{r}^+, \underline{r}_o^+) \tag{24b}$$

or

$$\underline{\underline{R}}_1 \cdot \underline{\underline{K}}(\underline{r}^-, \underline{r}_o^+) = \underline{\underline{K}}^*(\underline{r}^+, \underline{r}_o^+) \cdot \underline{\underline{R}}_1 \equiv \underline{\underline{K}}^{(o)}(\underline{r}^+, \underline{r}_o^+) \tag{24c}$$

$$\underline{\underline{R}}_1 \cdot \underline{\underline{K}}^{**}(\underline{r}^+, \underline{r}_o^+) \cdot \underline{\underline{R}}_1 = \underline{\underline{K}}(\underline{r}^+, \underline{r}_o^+) \tag{24d}$$

With the aid of these relationships, (21) and (23) can be rewritten as

$$f(\Omega)\, \underline{J}(\underline{r}^+) = \underline{J}_T(\underline{r}^+) + \int_{S^+} \underline{\underline{K}}(\underline{r}^+, \underline{r}_o^+) \cdot \underline{J}(\underline{r}_o^+) dS_o + \int_{S^+} \underline{\underline{K}}^{(o)}(\underline{r}^+, \underline{r}_o^+) \cdot \underline{J}^*(\underline{r}_o^+) dS_o \tag{25}$$

$$f(\Omega)\, \underline{J}^*(\underline{r}^+) = \underline{J}_T{}^*(\underline{r}^+) + \int_{S^+} \underline{\underline{K}}^{(o)}(\underline{r}^+, \underline{r}_o^+) \cdot \underline{J}(\underline{r}_o^+) dS_o + \int_{S^+} \underline{\underline{K}}(\underline{r}^+, \underline{r}_o^+) \cdot \underline{J}^*(\underline{r}^+) dS_o \tag{26}$$

From (25) and (26) we now obtain

$$f(\Omega)\left[\underline{J}(\underline{r}^+) + \underline{J}^*(\underline{r}^+)\right] = J_T(\underline{r}^+) + J_T{}^*(\underline{r}^+)$$

$$+ \int_{S^+} \left[\underline{\underline{K}}(\underline{r}^+, \underline{r}_o^+) + \underline{\underline{K}}^{(o)}(\underline{r}^+, \underline{r}_o^+)\right] \cdot \left[\underline{J}(\underline{r}_o^+) + \underline{J}^*(\underline{r}_o^+)\right] dS_o \tag{27}$$

$$f(\Omega)\left[\underline{J}(\underline{r}^+) - \underline{J}^*(\underline{r}^+)\right] = \underline{J}_T(\underline{r}^+) - \underline{J}_T(\underline{r}^-)$$

$$+ \int_{S^+} \left[\underline{\underline{K}}(\underline{r}^+, \underline{r}_o^+) - \underline{\underline{K}}^{(o)}(\underline{r}^+, \underline{r}_o^+)\right] \cdot \left[\underline{J}(\underline{r}_o^+) - \underline{J}^*(\underline{r}_o^+)\right] dS_o \tag{28}$$

We now define

$$\underline{J}^+(\underline{r}^+) \equiv \frac{1}{2}\left[\underline{J}(\underline{r}^+) + \underline{J}^*(\underline{r}^+)\right] \tag{29a}$$

$$\underline{J}^-(\underline{r}^+) \equiv \frac{1}{2}\left[\underline{J}(\underline{r}^+) - \underline{J}^*(\underline{r}^+)\right] \tag{29b}$$

$$\underline{\underline{K}}^{+}(\underline{r}^{+},\underline{r}_{o}^{+}) \equiv \underline{\underline{K}}(\underline{r}^{+},\underline{r}_{o}^{+}) + \underline{\underline{K}}^{(o)}(\underline{r}^{+},\underline{r}_{o}^{+}) \tag{30a}$$

$$\underline{\underline{K}}^{-}(\underline{r}^{+},\underline{r}_{o}^{+}) \equiv \underline{\underline{K}}(\underline{r}^{+},\underline{r}_{o}^{+}) - \underline{\underline{K}}^{(o)}(\underline{r}^{+},\underline{r}_{o}^{+}) \tag{30b}$$

$$\underline{J}_{T}^{+}(\underline{r}^{+}) \equiv \frac{1}{2}\left[\underline{J}_{T}(\underline{r}^{+}) + \underline{J}_{T}^{*}(\underline{r}^{+})\right] \tag{31a}$$

$$\underline{J}_{T}^{-}(\underline{r}^{+}) \equiv \frac{1}{2}\left[\underline{J}_{T}(\underline{r}^{+}) - \underline{J}_{T}^{*}(\underline{r}^{+})\right] \tag{31b}$$

and use these definitions to cast (27) and (28) into the form

$$f(\Omega)\underline{J}^{+}(\underline{r}^{+}) = \underline{J}_{T}^{+}(\underline{r}^{+}) + \int_{S^{+}} \underline{\underline{K}}^{+}(\underline{r}^{+},\underline{r}_{o}^{+}) \cdot \underline{J}^{+}(\underline{r}_{o}^{+})dS_{o} \tag{32}$$

$$f(\Omega)\,\underline{J}^{-}(\underline{r}^{+}) = \underline{J}_{T}^{-}(\underline{r}^{+}) + \int_{S^{+}} \underline{\underline{K}}^{-}(\underline{r}^{+},\underline{r}_{o}^{+}) \cdot \underline{J}^{-}(\underline{r}_{o}^{+})dS_{o} \tag{33}$$

The advantage of having to solve (32) and (33) rather than (1) is the following. Our integral equations must be cast into a matrix equation form in order to numerically calculate the current density at the centers of zones into which we have divided our body. If the number of zones for the whole body is N then solving (1) would require the inversion of a $2N \times 2N$ matrix ($\underline{J}$ has two curvilinear components on the surface). The solution of (32) or (33) requires N/2 zones and consequently the inversion of a $2(\frac{N}{2}) \times 2(\frac{N}{2})$ matrix for each case. To obtain the current density at points on both sides of the body we must solve (32) as well as (33) and use (29) and (19) to solve for $\underline{J}(\underline{r}^{+})$ and $\underline{J}(\underline{r}^{-})$. Recalling that the inversion of a $M \times M$ matrix requires computer time proportional to M^3 we understand that solving (1) would coorespond to a time proportional to $(2N)^3$ whereas solving (32) and (33) would correspond to a time proportional to $2(2\frac{N}{2})^3 = \frac{1}{4}(2N)^3$. Thus we save a factor of four in computer time for matrix inversion which is rather significant.

Next we show that the symmetry relationships (24)a and (24)b are valid. Recall that

$$\underline{\underline{K}}(\underline{r}, \underline{r}_o) = \underline{\underline{K}}_o(\underline{r}, \underline{r}_o) + \underline{\underline{K}}_1(\underline{r}, \underline{r}_o) \tag{4}$$

where K_o is associated with the free-space Green's function G_o and $\underline{\underline{K}}_1$ depends on the manner we model the wing. We will show the validity of (24)a and (24)b for $\underline{\underline{K}}_o$ and $\underline{\underline{K}}_1$ separately. We start with $\underline{\underline{K}}_o$. Equations (24)a and (24)b can be rewritten as

$$\underline{\underline{R}}_1 \cdot \underline{\underline{K}}_o(\underline{r}^-, \underline{r}_o^+) = \underline{\underline{K}}_o(\underline{r}^+, \underline{r}_o^-) \cdot \underline{\underline{R}}_1 \tag{34)a}$$

$$\underline{\underline{R}}_1 \cdot \underline{\underline{K}}_o(\underline{r}^-, \underline{r}_o^-) \cdot \underline{\underline{R}}_1 = \underline{\underline{K}}(\underline{r}^+, \underline{r}_o^+) \tag{34)b}$$

From (5) and (7) we recall that

$$\underline{\underline{K}}_o(\underline{r}, \underline{r}_o) = \hat{\underline{n}}(\underline{r}) \times \left[\nabla G_o(\underline{r}, \underline{r}_o) \times \underline{\underline{I}}\right] \tag{5}$$

$$G_o(\underline{r}, \underline{r}_o) = \frac{\exp[iko\,|r-r_o|]}{4\pi\,|r-r_o|} \tag{7}$$

Thus

$$\nabla G_o(r, r_o) = \frac{\underline{R}}{R} \frac{d}{dR} \frac{\exp(ikR)}{4\pi R}$$

$$= \hat{\underline{R}}(ik_o - \frac{1}{R})\, G_o = \hat{\underline{R}}\, F(R) \tag{35)a}$$

where

$$\hat{\underline{R}} \equiv \frac{\underline{R}}{R}$$

$$\underline{R} \equiv \underline{r}-\underline{r}_o, \quad R \equiv |\,\underline{R}\,| \tag{35)b}$$

$$F(R) \equiv ik_o - \frac{1}{R}$$

and

$$\hat{n} \times \left[\hat{\underline{R}} \times \underline{\underline{I}}\right] = \hat{R}\hat{n} - (\hat{R} \cdot \hat{n})\,\underline{\underline{I}} \tag{36}$$

Next we introduce the following definitions (fig. 3)

$$\hat{R}(\underline{r}^+, \underline{r}_o^+) \equiv \underline{R}_{xy} + \underline{R}_z \tag{37a}$$

$$\hat{R}(\underline{r}^-, \underline{r}_o^-) = \underline{R}_{xy} - \underline{R}_z \tag{37b}$$

$$\hat{R}(\underline{r}^-, \underline{r}_o^+) \equiv \underline{Q}_{xy} + \underline{Q}_z \tag{37c}$$

$$\hat{R}(\underline{r}^+, \underline{r}_o^-) = \underline{Q}_{xy} - \underline{Q}_z \tag{37d}$$

$$\hat{n}(\underline{r}) \equiv \underline{n}_{xy}(\underline{r}) + \underline{n}_z(\underline{r}) \tag{38a}$$

$$\hat{n}(\underline{r}^+) = \underline{n}_{xy}(\underline{r}^+) + \underline{n}_z(\underline{r}^+) = \underline{n}_{xy} + \underline{n}_z \tag{38b}$$

$$\hat{n}(\underline{r}^-) = \underline{n}_{xy}(\underline{r}^+) - \underline{n}_z(\underline{r}^+) = \underline{n}_{xy} - \underline{n}_z \tag{38c}$$

Equation (37)b is derivable from (37)a, (37)d from (37)c and (38)c from (38)b with the aid of figure 3.

Using (7) and (35) through (38) we have

$$\underline{\underline{K}}_o(\underline{r}^+, \underline{r}^-) \cdot \underline{R}_1 = F(R)\left[(\underline{Q}_{xy} - \underline{Q}_z)(\underline{n}_{xy} + \underline{n}_z) - (\underline{Q}_{xy} - \underline{Q}_z) \cdot (\underline{n}_{xy} + \underline{n}_z)\underline{\underline{I}}\right] \cdot \underline{\underline{R}}_1$$

$$F(R)\left[(\underline{Q}_{xy} - \underline{Q}_z)(\underline{n}_{xy} - \underline{n}_z) - (\underline{n}_{xy} \cdot \underline{Q}_{xy} - \underline{n}_z \cdot \underline{Q}_z)\,\underline{\underline{R}}_1\right] \tag{39}$$

$$\underline{R}_1 \cdot \underline{\underline{K}}_o(\underline{r}^-, \underline{r}_o^+) = F(R)\,\underline{R}_1 \cdot \left[(\underline{Q}_{xy} + \underline{Q}_z)(\underline{n}_{xy} - \underline{n}_z) - (\underline{Q}_{xy} + \underline{Q}_z) \cdot (\underline{n}_{xy} - \underline{n}_z)\,\underline{\underline{I}}\right]$$

$$\left[F(R)\,(\underline{Q}_{xy} - \underline{Q}_z)(\underline{n}_{xy} - \underline{n}_z) - (\underline{n}_{xy} \cdot \underline{Q}_{xy} - \underline{n}_z \cdot \underline{Q}_z)\,\underline{R}_1\right] \tag{40}$$

We can see that (39) and (40) are identical and (34)a is true. We can show the validity of (34)b in a similar manner. Next we show the truth of (24)a and (24)b for $\underline{\underline{K}}_1$ given by (12)

$$\underline{\underline{K}}_1(\underline{r},\underline{r}_o) = F(R)\left[\hat{\underline{R}}(\hat{\underline{n}}\cdot\underline{\underline{R}}) - (\hat{\underline{R}}\cdot\hat{\underline{n}})\,\underline{\underline{R}}\right] \tag{41}$$

The reflection operator $\underline{\underline{R}}$ is given by (13)

$$\underline{\underline{R}} = \underline{\underline{I}} - 2\hat{\nu}\,\hat{\nu} \tag{13}$$

and should not be confused with $\underline{R} = \underline{r} - \underline{r}_o$.

Again we calculate $\underline{\underline{K}}_1(\underline{r}^+,\underline{r}_o^-)\cdot\underline{\underline{R}}_1$ and $\underline{\underline{R}}_1\cdot\underline{\underline{K}}_1(\underline{r}^-,\underline{r}_o^+)$ with the aid of (41), (13), (37), and (38).

$$\begin{aligned}\underline{\underline{K}}_1(\underline{r}^+,\underline{r}_o^-)\cdot\underline{\underline{R}}_1 &= F(R)\Big[(\underline{Q}_{xy}-\underline{Q}_z)(\underline{n}_{xy}+\underline{n}_z)\cdot\underline{\underline{R}}\\ &\quad -(\underline{Q}_{xy}-\underline{Q}_z)\cdot(\underline{n}_{xy}+\underline{n}_z)\,\underline{\underline{R}}\Big]\cdot\underline{\underline{R}}_1\\ &= F(R)\Big[(\underline{Q}_{xy}-\underline{Q}_z)(\underline{n}_x-\underline{n}_y-\underline{n}_z)\\ &\quad -(\underline{Q}_{xy}\cdot\underline{n}_{xy}-\underline{Q}_z\cdot\underline{n}_z)(\underline{\underline{R}}\cdot\underline{\underline{R}}_1)\Big]\end{aligned} \tag{42}$$

$$\begin{aligned}\underline{\underline{R}}_1\cdot\underline{\underline{K}}_1(\underline{r}^-,\underline{r}_o^+) &= F(R)\,\underline{\underline{R}}_1\Big[(\underline{Q}_{xy}+\underline{Q}_z)(\underline{n}_{xy}-\underline{n}_z)\cdot\underline{\underline{R}}\\ &\quad -(\underline{Q}_{xy}+\underline{Q}_z)\cdot(\underline{n}_{xy}-\underline{n}_z)\,\underline{\underline{R}}\Big]\\ &= F(R)\Big[(\underline{Q}_{xy}-\underline{Q}_z)(\underline{n}_x-\underline{n}_y-\underline{n}_z)\\ &\quad -(\underline{Q}_{xy}\cdot\underline{n}_{xy}-\underline{Q}_z\cdot\underline{n}_z)(\underline{\underline{R}}_1\cdot\underline{\underline{R}})\Big]\end{aligned} \tag{43}$$

where

$$\underline{n}_{xy}(\underline{r}) = \underline{n}_x(\underline{r}) + \underline{n}_y(\underline{r}) \tag{44}$$

Noticing that

$$\underline{\underline{R}} \cdot \underline{\underline{R}} = \underline{\underline{I}} - 2\hat{y}\,\hat{y} - 2\hat{z}\,\hat{z}$$

$$\underline{\underline{R}}_1 \cdot \underline{\underline{R}} = \underline{\underline{I}} - 2\hat{z}\,\hat{z} - 2\hat{y}\,\hat{y}$$

we understand that (42) and (43) are identical and (24)a is true. Equation (24)b can be shown to be valid in a similar manner.

Finally, we show that (24)a and (24)b are true for $\underline{\underline{K}}_1$ given by (6). First we calculate $\nabla \times \underline{\underline{G}}_{1s}$ by recalling that (ref. 1 , (164) and (165))

$$\left.\begin{aligned} \nabla \times \underline{M}\alpha_m^{(3)} &= k_o \underline{N}\alpha_m^{(3)} \\ \nabla \times \underline{N}\alpha_m^{(3)} &= k_o \underline{M}\alpha_m^{(3)} \end{aligned}\right\} \tag{45}$$

Thus,

$$\nabla \times \underline{\underline{G}}_{1s} = -\frac{iko}{2\pi}\int_{C_h} \frac{dh}{k_o^2 - h^2} \sum_{m=0}^{\infty} \sum_{\alpha=e,o} (N_m^{(\alpha)}(\lambda))^{-1}$$

$$\left[C_m^{(\alpha)}(\lambda, \varepsilon_1^*)\, \underline{N}\alpha_m^{(3)}(h, \underline{r})\underline{M}\alpha_m^{(3)}(h, \underline{r}_o) + D_m^{(\alpha)}(\lambda, \varepsilon_1^*)\underline{M}\alpha_m^{(3)}(h, \underline{r})\underline{N}^{(3)}(-h, \underline{r}_o)\right] \tag{46}$$

Next we rewrite (9) and (10) as

$$\underline{M}\alpha_m^{(3)}(h, \underline{r}) \equiv e^{ihz}\underline{M}\alpha_m^{(3)^1}(h, \underline{r}_T) \tag{47}$$

$$\underline{N}\alpha_m^{(3)}(h, \underline{r}) \equiv e^{ihz}\underline{N}\alpha_m^{(3)^1}(h, \underline{r}_T) \tag{48}$$

and define

$$(N_m^{(\alpha)}(\lambda))^{-1} C_m^{(\alpha)}(\lambda, \xi_1^*) \equiv C\alpha_m \tag{49a}$$

$$(N_m^{(\alpha)}(\lambda))^{-1} D_m^{(\alpha)}(\lambda, \xi_1^*) \equiv D\alpha_m \tag{49b}$$

The definitions of $\underline{M}\alpha_m^{(3)^1}$ and $\underline{N}\alpha_m^{(3)^1}$ are obvious and $\underline{r}_T$ is a transverse coordinate vector

$$\underline{r}_T = x\hat{x} + y\hat{y} \tag{50}$$

We also decompose $\underline{N}\alpha_m^{(3)^1}$ into longitudinal and transverse components in the form ($\underline{M}\alpha_m^{(3)^1}$ is purely transverse)

$$\underline{N}\alpha_m^{(3)^1}(h, \underline{r}_T) \equiv \underline{N}\alpha_{mT}(h, \underline{r}_T) + \underline{N}\alpha_{mz}(h, \underline{r}_T) \tag{51}$$

$$\underline{N}\alpha_{mT} = \frac{ih}{k_o c\beta}\left[\hat{u} S\alpha_m(\lambda, \eta) \frac{\partial}{\partial \xi} R\alpha_m^{(3)}(\lambda, \xi) + \hat{v} R\alpha_m^{(3)}(\lambda, \xi) \frac{\partial}{\partial \eta} S\alpha_m(\lambda, \eta)\right] \tag{52}$$

$$\underline{N}\alpha_{mz} = \frac{\lambda^2}{c^2 k_o} \hat{z} R\alpha_m^{(3)}(\lambda, \xi) S\alpha_m(\lambda, \eta) \tag{53}$$

With the above definitions, (46) can be rewritten as

$$\nabla \times \underline{\underline{G}}_{1s} = -\frac{iko}{2\pi} \int_{C_h} \frac{e^{ih(z-z_o} dh}{k_o^2 - h^2} \sum_{m=0}^{\infty} \sum_{\alpha=e,o} \Bigg\{ \Big[C\alpha_m \Big[\underline{N}\alpha_{mT}(h, \underline{r}_T) \underline{M}\alpha_m^{(3)^1}(h, \underline{r}_{oT}) + \underline{N}\alpha_{mz}(h, \underline{r}_T) \underline{M}\alpha_m^{(3)^1}(h, \underline{r}_{oT}) \Big] + D\alpha_m \Big[\underline{M}\alpha_m^{(3)^1}(h, \underline{r}_T) \underline{N}\alpha_{mT}(h, \underline{r}_{oT}) + \underline{M}\alpha_m^{(3)^1}(h, \underline{r}_T) \underline{N}\alpha_{mz}(h, \underline{r}_{oT}) \Big] \Bigg\} \tag{54}$$

As it was explained in reference 1 the contour C_h should be taken as the one in figure 4 and with this understanding we can rewrite (54) as

$$\nabla \times \underline{\underline{G}}_{1s} = \int_{-\infty}^{\infty} e^{ihq} \underline{\underline{f}}_1(h)dh + \int_{-\infty}^{\infty} e^{ihq} \underline{\underline{f}}_2(h)\, dh \tag{55}$$

where $q = z - z_o$ and the definitions of $\underline{\underline{f}}_1$ and $\underline{\underline{f}}_2$ are

$$\underline{\underline{f}}_1 = -\frac{ik_o}{2\pi} \frac{1}{k_o^2 - h^2} \sum_{m=0}^{\infty}{}' \sum_{\alpha=e,o} \Big[C\sigma_m \underline{N}\sigma_{mT}(h, \underline{r}_T) \underline{M}\sigma_m^{(3)1}(h, \underline{r}_{oT})$$

$$+ D\sigma_m \underline{M}\sigma_m^{(3)1}(h, \underline{r}_T) \underline{N}\sigma_{mT}(h, \underline{r}_{oT}) \Big]$$

$$\underline{\underline{f}}_2 = -\frac{ik_o}{2\pi} \frac{1}{k_o^2 - h^2} 2 \sum_{m=0}^{\infty} \sum_{\alpha=e,o} \Big[C\sigma_m \underline{N}\sigma_{mz}(h, \underline{r}_T) \underline{M}\sigma_m^{(3)1}(h, \underline{r}_{oT})$$

$$+ D\sigma_m \underline{M}\sigma_m^{(3)1}(h, \underline{r}_T) \underline{N}\sigma_{mz}(h, \underline{r}_{oT}) \Big]$$

Assume now that $z < z_o$ i.e. $q = -|q|$. By making a change of variable $h \rightarrow -h$, the first integral can be rewritten as

$$I_1 = \int_{-\infty}^{\infty} e^{ih|q|} \underline{\underline{f}}_1(h)\, dh = \int_{-\infty}^{\infty} e^{ih|q|} \underline{\underline{f}}_1(-h)\, dh \qquad q < 0$$

From (9) through (11) and (51) through (53) we can see that $\underline{\underline{f}}_1(h)$ is an odd function of h whereas $\underline{\underline{f}}_2(h)$ is an even function of h. Thus

$$I_1 = -\int_{-\infty}^{\infty} e^{ih|q|} \underline{\underline{f}}_1(h)\, dh \qquad q < 0$$

The true contour C_h includes two bumps as shown in figure 4, but because of their position we still have $\underline{\underline{f}}_1(-h) = -\underline{\underline{f}}_1(h)$). When $q > 0$ we have $q = |q|$ and

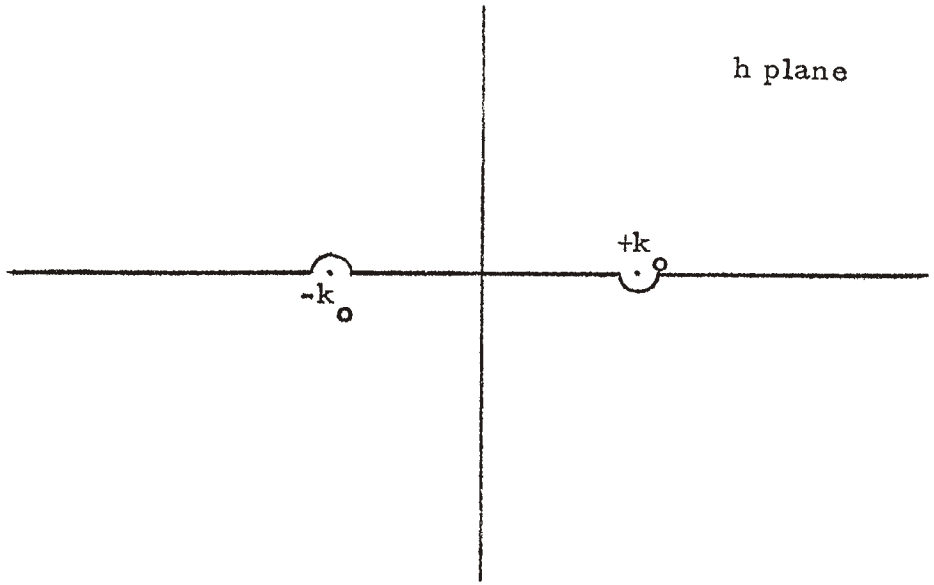

Figure 4: Integration Contour C_h

$$I_1 = \int_{-\infty}^{\infty} e^{ih|q|} \underline{f}_1(h)\, dh \qquad q > 0$$

Thus

$$I_1 = \frac{z-z_o}{|z-z_o|} \int_{-\infty}^{\infty} e^{ih|z-z_o|} \underline{f}_1(h)\, dh \tag{56}$$

When $z = z_o$, $I_1 = 0$ and we can define a symbol $\epsilon(z, z_o)$ such that

$$\left.\begin{aligned} \epsilon(z, z_o) &= 1 && z > z_o \\ &= -1 && z < z_o \\ &= 0 && z = z_o \end{aligned}\right\} \tag{57}$$

Following the same procedure we can show that

$$I_2 = \int_{-\infty}^{\infty} e^{ih|z-z_o|} \underline{f}_2(h)\, dh \tag{58}$$

for any q and (54) becomes

$$\begin{aligned} \nabla \times \underline{\underline{G}}_{1s} = -\frac{ik_o}{2\pi} \int_{-\infty}^{\infty} \frac{e^{ih|z-z_o|}\, dh}{k_o^2 - h^2} \sum_{m=0}^{\infty} \sum_{\alpha=e,o} \Big\{ & C\alpha_m \\ & \Big[\epsilon(z, z_o) \underline{N}\alpha_{mT}(h, \underline{r}_T) \underline{M}\alpha_m^{(3)1}(h, \underline{r}_{oT}) \\ & + \underline{N}\alpha_{mz}(h, \underline{r}_T) \underline{M}\alpha_m^{(3)1}(h, \underline{r}_{oT}) \Big] \\ & + D\alpha_m \Big[\epsilon(z, z_o) \underline{M}\alpha_m^{(3)1}(h, \underline{r}_T) \underline{N}\alpha_{mT}(h, \underline{r}_{oT}) + \underline{M}\alpha_m^{(3)1}(h, r_T) N\alpha_{mz}(h, r_{oT}) \Big] \Big\} \end{aligned} \tag{59}$$

We are now in a position to show the validity of (24)a and (24)b. We start with (24)a by first recalling $\underline{\underline{K}}_1$

$$\underline{\underline{K}}_1(\underline{r},\underline{r}_o) = \hat{n}(\underline{r}) \times \left[\nabla \times \underline{\underline{G}}_{1s}\right] \tag{6}$$

From (24)a we see that the argument of $\underline{\underline{K}}_1$ involves the pairs $\underline{r}^-, \underline{r}_o^+$, $\underline{r}^+, \underline{r}_o^-$. From figure 3 we see that

$$z^- - z_o^+ < 0, \quad z^+ - z_o^- > 0$$

$$|z^- - z_o^+| = |z^+ - z_o^-|$$

Thus the proof of (24)a depends on the quantities inside the angular brackets in (59) and we should prove (24)a for $\underline{\underline{K}}_1^{\,1}(\underline{r},\underline{r}_o)$ defined by

$$\underline{\underline{K}}_1^{\,1}(\underline{r},\underline{r}_o) = \hat{n}(\underline{r}) \times \left[\nabla \times \underline{\underline{G}}_{1s}^{1}\right] \tag{60a}$$

where $\nabla \times \underline{\underline{G}}_{1s}^{1}$ is given by

$$\nabla \times \underline{\underline{G}}_{1s}^{1} = C\left[\epsilon(z,z_o)\underline{N}_T(\underline{r}_T)\underline{M}(\underline{r}_{oT}) + \underline{N}_z(r_T)\underline{M}(r_{oT})\right]$$

$$+ D\left[\epsilon(z,z)\underline{M}(\underline{r}_T)\underline{N}_T(\underline{r}_{oT}) + \underline{M}(\underline{r}_T)\underline{N}_z(\underline{r}_{oT})\right] \tag{60b}$$

Notice that we have simplified the notation in (60)b to avoid unnecessary writing. Now we calculate

$$\underline{\underline{K}}_1^{\,1}(\underline{r}^+,\underline{r}_o^-) \cdot \underline{\underline{R}}_1 = \Big\{C\left[\epsilon(z^+,z_o^-)(\underline{n}_{xy}+\underline{n}_z)\times \underline{N}_T(\underline{r}_T^+)\,\underline{M}(\underline{r}_{oT}^-)\right.$$

$$\left. + (\underline{n}_{xy}+\underline{n}_z)\times \underline{N}_z(\underline{r}_T^+)\underline{M}(\underline{r}_{oT}^-)\right]$$

$$+ D\left[\epsilon(z^+,z_o^-)(\underline{n}_{xy}+\underline{n}_z)\times \underline{M}(\underline{r}_T^+)\,\underline{N}_T(\underline{r}_{oT}^-)\right.$$

$$\left. + (\underline{n}_{xy}+\underline{n}_z)\times \underline{M}(\underline{r}_T^+)\,\underline{N}_z(\underline{r}_{oT}^-)\right]\Big\} \cdot \underline{\underline{R}}_1$$

$$= C\left[(\underline{n}_{xy}+\underline{n}_z) \times \underline{N}_T(\underline{r}_T)\underline{M}(\underline{r}_{oT})\right.$$

$$\left. + \underline{n}_{xy} \times \underline{N}_z(\underline{r}_T)\underline{M}(\underline{r}_{oT})\right]$$

$$+ D\left[(\underline{n}_{xy}+\underline{n}_z) \times \underline{M}(\underline{r}_T)\underline{N}_T(\underline{r}_{oT})\right.$$

$$\left. - (\underline{n}_{xy}+\underline{n}_z) \times \underline{M}(\underline{r}_T)\underline{N}_z(\underline{r}_{oT})\right] \qquad (61)$$

where we have taken into account that: $\epsilon(z^+, z_o^-) = 1$, $\underline{r}_T^+ = \underline{r}_T^- = \underline{r}_T$, $\underline{r}_{oT}^+ = \underline{r}_{oT}^- = \underline{r}_{oT}$, $\underline{M}$ is a transverse vector lying in the xy plane and $\underline{\underline{R}}_1$ is given by (17). Next we calculate

$$\underline{\underline{R}}_1 \cdot \underline{\underline{K}}_1(\underline{r}^-, \underline{r}_o^+) = C\underline{\underline{R}}_1 \cdot \left\{\left[\epsilon(z^-, z_o^+)(\underline{n}_{xy}-\underline{n}_z) \times \underline{N}_T(\underline{r}_T)\underline{M}(\underline{r}_{oT})\right.\right.$$

$$\left. + (\underline{n}_{xy}-\underline{n}_z) \times \underline{N}_z(\underline{r}_T)\underline{M}(\underline{r}_{oT})\right]$$

$$+ D\left[\epsilon(z^-, z_o^+)(\underline{n}_{xy}-\underline{n}_z) \times \underline{M}(\underline{r}_T)\underline{N}_T(\underline{r}_{oT})\right.$$

$$\left.\left. + (\underline{n}_{xy}-\underline{n}_z) \times \underline{M}(\underline{r}_T)\underline{N}_z(\underline{r}_{oT})\right]\right\}$$

$$= C\left\{-\underline{\underline{R}}_1 \cdot \left[\underline{n}_{xy} \times \underline{N}_T(\underline{r}_T)-\underline{n}_z \times \underline{N}_T(\underline{r}_T)\right]\underline{M}(\underline{r}_{oT})\right.$$

$$+ \underline{\underline{R}}_1 \cdot \left[\underline{n}_{xy} \times \underline{N}_z(\underline{r}_T)\right]\underline{M}(\underline{r}_{oT})$$

$$+ D\left\{-\underline{\underline{R}}_1 \cdot \left[\underline{n}_{xy} \times \underline{M}(\underline{r}_T)-\underline{n}_z \times \underline{M}(\underline{r}_T)\right]\underline{N}_T(\underline{r}_{oT})\right.$$

$$\left.\left. + \underline{\underline{R}}_1 \cdot \left[\underline{n}_{xy} \times \underline{M}(\underline{r}_T) - \underline{n}_z \times \underline{M}(\underline{r}_T)\right]\underline{N}_z(\underline{r}_{oT})\right\}\right. \qquad (62)$$

We now observe that $\underline{n}_{xy} \times \underline{N}_T(\underline{r}_T)$ and $\underline{n}_{xy} \times \underline{M}(\underline{r}_T)$ are vectors in the z direction whereas $\underline{n}_z \times \underline{N}_T$ and $\underline{n}_z \times \underline{M}$ are vectors in the transverse direction. Noting that $\underline{\underline{R}}_1 \cdot$ leaves a transverse vector unaffected but changes the sign of a vector parallel to the z-axis, (62) can be rewritten as

$$\underline{\underline{R}}_1 \cdot \underline{\underline{K}}_1(\underline{r}^-, \underline{r}_o^+) = C\Big\{\Big[\underline{n}_{xy} \times \underline{N}_T(\underline{r}_T) + \underline{n}_z \times \underline{N}_T(\underline{r}_T)\Big]\underline{M}(\underline{r}_{oT})$$
$$\Big[\underline{n}_{xy} \times \underline{N}_z(\underline{r}_T)\Big]\underline{M}(\underline{r}_{oT})\Big\}$$
$$+ D\Big\{\Big[\underline{n}_{xy} \times \underline{M}(\underline{r}_T) + \underline{n}_z \times \underline{M}(\underline{r}_T)\Big]\underline{N}_T(\underline{r}_{oT})$$
$$-\Big[\underline{n}_{xy} \times \underline{M}(\underline{r}_T) + \underline{n}_z \times \underline{M}(\underline{r}_T)\Big]\underline{N}_z(\underline{r}_{oT})\Big\} \qquad (63)$$

We thus see that (61) and (63) are identical and (24)a has been shown to be true. The validity of (24)b is shown in a similar manner.

We conclude that the symmetry relationships (24)a and (24)b are true for K corresponding to a wing modeled either as a perfectly conducting infinite elliptical cylinder or a perfectly conducting infinite plate and consequently integral equations (32) and (33) are valid.

SECTION III

INTEGRAL EQUATION FOR CURRENT COMPONENTS

In order to solve (32) and (33) we decompose the vector current densities $\underline{J}^+$ and $\underline{J}^-$ into their components along two orthogonal surface tangential directions defined by the unit vectors $\hat{s}$ and $\hat{t}$ such that (fig. 5)

$$\hat{s} \times \hat{t} = \hat{n} \tag{64}$$

where $\hat{n}$ is the outward unit normal on the surface,

$$\underline{J}^+(\underline{r}) = J_s^+(\underline{r})\,\hat{s} + J_t^+(\underline{r})\,\hat{t} \tag{65a}$$

$$\underline{J}^-(\underline{r}) = J_s^-(\underline{r})\,\hat{s} + J_t^-(\underline{r})\,\hat{t} \tag{65b}$$

For reasons that will become apparent shortly we define

$$\underline{\underline{K}}^+(\underline{r},\underline{r}_o) = \hat{n}(\underline{r}) \times \underline{\underline{D}}^+(\underline{r},\underline{r}_o) \tag{66a}$$

$$\underline{\underline{K}}^-(\underline{r},\underline{r}_o) = \hat{n}(\underline{r}) \times \underline{\underline{D}}^-(\underline{r},\underline{r}_o) \tag{66b}$$

and use (64) through (66) to rewrite (32) and (33) in component form

$$f(\Omega)\,J_s^\alpha(\underline{r}) = J_{Ts}^\alpha(\underline{r}) - \int_S dS_o \left\{ [\hat{t}\cdot\underline{\underline{D}}^\alpha(\underline{r},\underline{r}_o)\cdot\hat{s}_o]\,J_s^\alpha(\underline{r}_o) + [\hat{t}\cdot\underline{\underline{D}}^\alpha(\underline{r},\underline{r}_o)\cdot\hat{t}_o]\,J_t^\alpha(\underline{r}_o) \right\} \tag{67}$$

$$f(\Omega)\,J_t^\alpha(\underline{r}) = J_{Tt}^\alpha(\underline{r}) + \int_S dS_o \left\{ [\hat{s}\cdot\underline{\underline{D}}^\alpha(\underline{r},\underline{r}_o)\cdot\hat{s}_o]\,J_s^\alpha(\underline{r}_o) + [\hat{s}\cdot\underline{\underline{D}}^\alpha(\underline{r},\underline{r}_o)\cdot\hat{t}_o]\,J_t^\alpha(\underline{r}_o) \right\} \tag{68}$$

where $\underline{r}, \underline{r}_o$ are position vectors of points on S^+ (which is now denoted by S) and α stands for + or -.

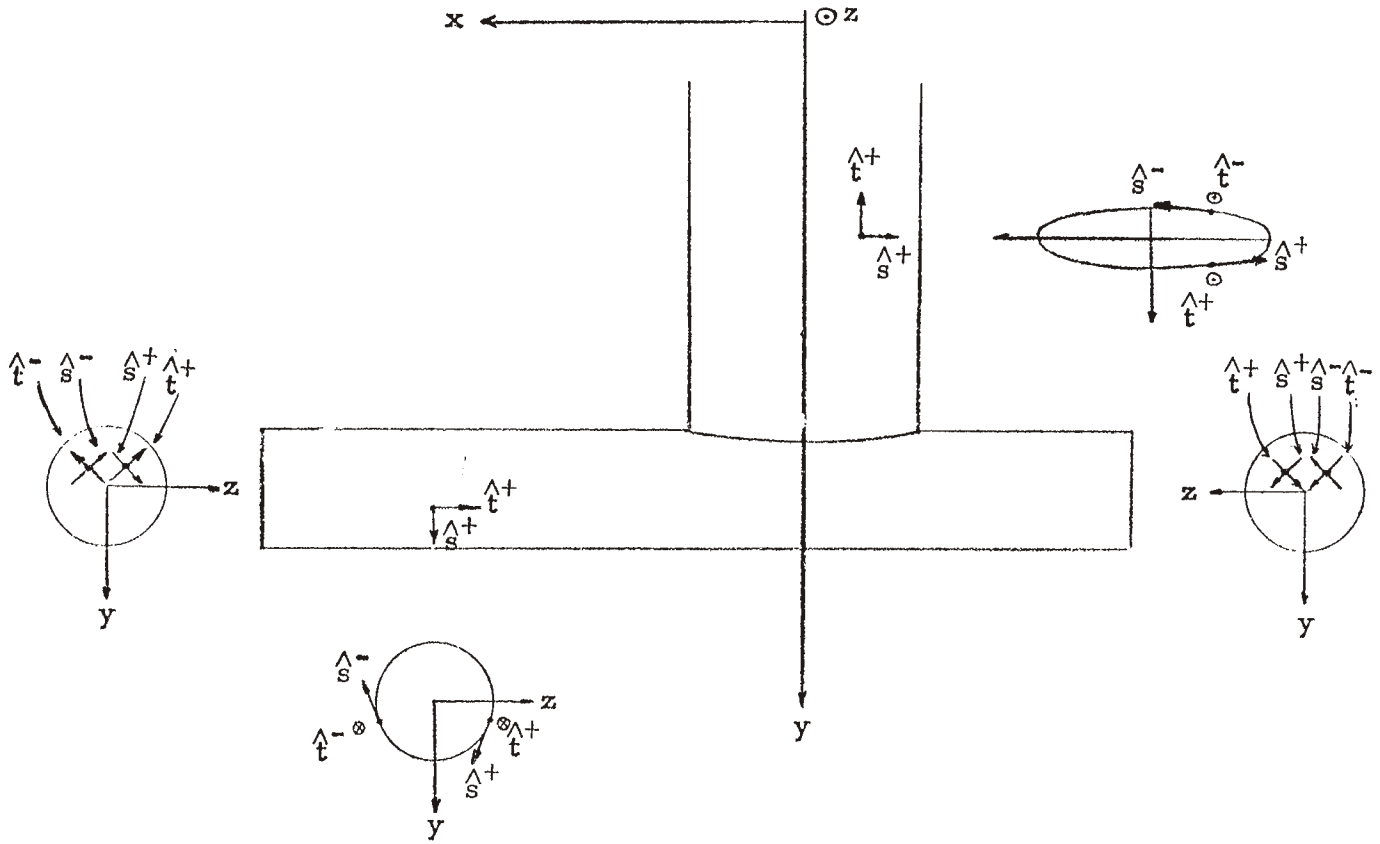

Figure 5: The unit vectors $\hat{t}$ and $\hat{s}$ on front ($z>0$) and back ($z<0$) surfaces of the attached structure

Next we calculate $\underline{J}_T^{\alpha}(\underline{r})$ and $\underline{\underline{D}}^{\alpha}(\underline{r}, \underline{r}_o)$ for a wing modeled as an infinite elliptical cylinder and also as an infinite plate.

From (66), (30), (24) and (20) we have

$$\underline{\underline{D}}^{+}(\underline{r}^{+}, \underline{r}_o^{+}) = \underline{\underline{D}}(\underline{r}^{+}, \underline{r}_o^{+}) + \underline{\underline{D}}(\underline{r}^{+}, \underline{r}_o^{-}) \cdot \underline{\underline{R}}_1 \tag{69}$$

$$\underline{\underline{D}}^{-}(\underline{r}^{+}, \underline{r}_o^{+}) = \underline{\underline{D}}(\underline{r}^{+}, \underline{r}_o^{+}) - \underline{\underline{D}}(\underline{r}^{+}, \underline{r}_o^{-}) \cdot \underline{\underline{R}}_1 \tag{70}$$

where $\underline{\underline{R}}_1$ is given by (17), $\underline{\underline{D}}$ from

$$\underline{\underline{D}}(\underline{r}, \underline{r}_o) = \nabla G_o(\underline{r}, \underline{r}_o) \times \underline{\underline{I}} + \nabla \times \underline{\underline{G}}_{1s} \tag{71}$$

and $\nabla \times \underline{\underline{G}}_{1s}$ is given by (46) for the infinite elliptical cylinder and by

$$\nabla \times \underline{\underline{G}}_{1s} = -\nabla G_o(\underline{r}, \underline{r}_{oi}) \times \underline{\underline{R}} \tag{72}$$

for the infinite plate (see (12)).

The position vector $\underline{r}_o^{-}$ is equal to $\underline{\underline{R}}_1 \cdot \underline{r}_o^{+}$ and has the same x and y coordinates as $\underline{r}_o^{+}$ but opposite z coordinates, i.e.

$$\underline{r}_o^{+} = (x_o, y_o, z_o)$$

$$\underline{r}_o^{-} = \underline{\underline{R}}_1 \cdot \underline{r}_o^{+} = (x_o, y_o, -z_o)$$

To calculate the components of $\underline{\underline{D}}$ in the $\hat{t}$ and $\hat{s}$ directions we use (69) and (70). For example,

$$\hat{t} \cdot \underline{\underline{D}}^{+}(\underline{r}^{+}, \underline{r}_o^{+}) \cdot \hat{s}_o = \hat{t} \cdot \underline{\underline{D}}(\underline{r}^{+}, \underline{r}_o^{-}) \cdot \hat{s}_o + \hat{t} \cdot \underline{\underline{D}}(\underline{r}^{+}, \underline{r}_o^{-}) \cdot \underline{\underline{R}}_1 \cdot \hat{s}_o \tag{73}$$

The reflection operator $\underline{\underline{R}}_1$ acts on $\hat{s}_o$ and transforms it into a unit vector such that

$$\underline{\underline{R}}_1 \cdot \hat{s}_o = (s_{ox}, s_{oy}, -s_{oz})$$

where

$$\hat{s}_o = (s_{ox}, s_{oy}, s_{oz})$$

For the case of the infinite plate, (73) can be simplified by using (71) and (72). For example

$$\hat{t} \cdot \underline{\underline{D}}^+(\underline{r}^+, \underline{r}_o^+) \cdot \hat{s}_o = \hat{t} \cdot \Big\{ [\nabla G_o(\underline{r}^+, \underline{r}_o^+) \times \underline{\underline{I}}] - [\nabla G_o(\underline{r}^+, \underline{r}_{oi}^+) \times \underline{\underline{R}}] + [[\nabla G_o(\underline{r}^+, \underline{r}_o^-) \times \underline{\underline{I}}] - [\nabla G_o(\underline{r}^+, \underline{r}_{oi}^-) \times \underline{\underline{R}}]] \cdot \underline{\underline{R}}_1 \Big\} \cdot \hat{s}_o \qquad (74)$$

and

$$\left.\begin{aligned}
\hat{t} \cdot [\nabla G_o \times \underline{\underline{I}}] \cdot \hat{s}_o &= \hat{t} \cdot [\nabla G_o \times \hat{s}_o] = -[\hat{t} \times \hat{s}_o] \cdot \nabla G_o(\underline{r}^+, \underline{r}_o^+) \\
\hat{t} \cdot [\nabla G_o \times \underline{\underline{R}}] \cdot \hat{s}_o &= \hat{t} \cdot [\nabla G_o \times (\underline{\underline{R}} \cdot \hat{s}_o)] = -[\hat{t} \times (\underline{\underline{R}} \cdot \hat{s}_o)] \cdot \nabla G_o(\underline{r}^+, \underline{r}_{oi}^+) \\
\hat{t} \cdot [\nabla G_o \times \underline{\underline{I}}] \cdot \underline{\underline{R}}_1 \cdot \hat{s}_o &= -[\hat{t} \times (\underline{\underline{R}}_1 \cdot \hat{s}_o)] \cdot \nabla G_o(\underline{r}^+, \underline{r}_o^-) \\
\hat{t} \cdot [\nabla G_o \times \underline{\underline{R}}] \cdot \underline{\underline{R}}_1 \cdot \hat{s}_o &= -[\hat{t} \times (\underline{\underline{R}} \cdot \underline{\underline{R}}_1 \cdot \hat{s}_o)] \cdot \nabla G_o(\underline{r}^+, \underline{r}_o^-)
\end{aligned}\right\} \qquad (75)a$$

$$\left.\begin{aligned}
\hat{s}_o &= (s_{ox}, s_{oy}, s_{oz}) \\
\underline{\underline{R}} \cdot \hat{s}_o &= (s_{ox}, -s_{oy}, s_{oz}) \\
\underline{\underline{R}}_1 \hat{s}_o &= (s_{ox}, s_{oy}, -s_{oz}) \\
\underline{\underline{R}} \cdot \underline{\underline{R}}_1 \cdot \hat{s}_o &= (s_{ox}, -s_{oy}, -s_{oz})
\end{aligned}\right\} \qquad (75)b$$

For the case of the infinite elliptical cylinder we can see from (46) that we have dyads of the form $\underline{NM}$, $\underline{MN}$ and $\underline{NM} \cdot \underline{R}_1$, $\underline{MN} \cdot \underline{R}_1$ and the calculation of (69) or (71) is straightforward.

Next, we calculate the "incident" current densities $\underline{J}_T^{\alpha}$. From (31), (22) and (2) we understand that

$$\underline{J}_T^+(\underline{r}^+) = \tfrac{1}{2}\left\{\hat{n}(\underline{r}^+) \times \underline{H}_T(\underline{r}^+) + \underline{\underline{R}}_1 \cdot [\hat{n}(\underline{r}^-) \times \underline{H}_T(\underline{r}^-)]\right\} \tag{76}a$$

$$\underline{J}_T^-(\underline{r}^+) = \tfrac{1}{2}\left\{\hat{n}(\underline{r}^+) \times \underline{H}_T(\underline{r}^+) - \underline{\underline{R}}_1 \cdot [\hat{n}(\underline{r}^-) \times \underline{H}_T(\underline{r}^-)]\right\} \tag{76}b$$

To simplify (76) we recall (38)c and the second term in (76) can be written as

$$\begin{aligned}
\underline{\underline{R}}_1 \cdot [\hat{n}(\underline{r}^-) \times \underline{H}_T(\underline{r}^-)] &= \underline{\underline{R}}_1 \cdot \left\{[\hat{n}_{xy}(\underline{r}^+) - \hat{n}_z(\underline{r}^+)] \times [\underline{H}_{Txy}(\underline{r}^-) + \underline{H}_z(\underline{r}^-)]\right\} \\
&= \underline{\underline{R}}_1 \cdot [\hat{n}_{xy}(\underline{r}^+) \times \underline{H}_{Txy}(\underline{r}^-) + \hat{n}_{xy}(\underline{r}^+) \times \underline{H}_z(\underline{r}^-) - \hat{n}_z(\underline{r}^+) \times \underline{H}_{Txy}(\underline{r}^-)] \\
&= -\hat{n}_{xy}(\underline{r}^+) \times \underline{H}_{Txy}(\underline{r}^-) + \hat{n}_{xy}(\underline{r}^+) \times \underline{H}_z(\underline{r}^-) - \hat{n}_z(\underline{r}^+) \times \underline{H}_{Txy}(\underline{r}^-) \\
&= -\hat{n}(\underline{r}^+) \times \underline{H}_{Txy}(\underline{r}^-) + \hat{n}_{xy}(\underline{r}^+) \times \underline{H}_z(\underline{r}^-) \\
&= -\hat{n}(\underline{r}^+) \times [\underline{H}_{Txy}(\underline{r}^-) - \underline{H}_z(\underline{r}^-)] \\
&= -\hat{n}(\underline{r}^+) \times \underline{\underline{R}}_1 \cdot \underline{H}_T(\underline{r}^-)
\end{aligned}$$

and (76)a can be used to obtain

$$J_{Ts}^+(\underline{r}^+) = -\tfrac{1}{2}\hat{t} \cdot [\underline{H}_T(\underline{r}^+) - \underline{\underline{R}}_1 \cdot \underline{H}_T(\underline{r}^-)] \tag{77}a$$

$$J_{Tt}^+(\underline{r}^+) = \tfrac{1}{2}\hat{s} \cdot [\underline{H}_T(\underline{r}^+) - \underline{\underline{R}}_1 \cdot \underline{H}_T(\underline{r}^-)] \tag{77}b$$

$$J_{Ts}^-(\underline{r}^+) = -\tfrac{1}{2}\hat{t} \cdot [\underline{H}_T(\underline{r}^+) + \underline{\underline{R}}_1 \cdot \underline{H}_T(\underline{r}^-)] \tag{78}a$$

$$J_{Tt}^-(\underline{r}^+) = \tfrac{1}{2}\hat{s} \cdot [\underline{H}_T(\underline{r}^+) + \underline{\underline{R}}_1 \cdot \underline{H}_T(\underline{r}^-)] \tag{78}b$$

The "incident" field $\underline{H}_T(\underline{r})$ is given by (108) of reference 1 for the case of an infinite elliptical cylinder, or in the case of a flat plate by

$$\underline{H}_T(\underline{r}) = \underline{H}_i(\underline{r}) + \underline{H}_{sc}(\underline{r}) = \underline{H}_o e^{i\underline{k} \cdot \underline{r}} + \underline{\underline{R}} \cdot \underline{H}_o e^{i\underline{\underline{R}} \cdot \underline{k} \cdot \underline{r}} \tag{79}$$

where $\underline{\underline{R}}$ is given by (13). (Equation (79) evaluated at $\underline{r} = 0$ gives a magnetic field in the xz plane, i.e. the normal component of the magnetic field at points on the plate is zero as it should be.)

Assume now that we have solved (67) and (68) and wish to calculate the true surface current density components J_t and J_s at any point on a given surface, i.e. on both the positive ($z > 0$) and negative ($z < 0$) sides. From (29) and (19) we obtain

$$\underline{J}(\underline{r}^+) = \underline{J}^+(\underline{r}^+) + \underline{J}^-(\underline{r}^+) \tag{80a}$$

$$\underline{\underline{R}}_1 \cdot \underline{J}(\underline{r}^-) = \underline{J}^+(\underline{r}^+) - \underline{J}^-(\underline{r}^+) \tag{80b}$$

From (80)a it is straightforward to obtain the components of the current density $\underline{J}$ on the positive side. From (80)b we find

$$\underline{J}(\underline{r}^-) = \underline{\underline{R}}_1 \left[\underline{J}^+(\underline{r}^+) - \underline{J}^-(\underline{r}^+)\right] \tag{81}$$

We can now write

$$\underline{J}^+(\underline{r}^+) - \underline{J}^-(\underline{r}^+) = \left\{\left[\underline{J}^+(\underline{r}^+) - \underline{J}^-(\underline{r}^+)\right] \cdot s^+\right\} \hat{s}^+ + \left\{\left[\underline{J}^+(\underline{r}^+) - \underline{J}^-(\underline{r}^+)\right] \cdot \hat{t}^+\right\} \hat{t}^+ \tag{82}$$

and

$$J_t(\underline{r}^-) = \hat{t}^- \underline{\underline{R}}_1 \cdot \hat{s}^+ [J_s^+(\underline{r}^+) - J_s^-(\underline{r}^+)] + \hat{t}^- \cdot \underline{\underline{R}}_1 \cdot \hat{t}^+ [J_t^+(\underline{r}^+) - J_t^-(\underline{r}^+] \tag{83a}$$

$$J_s(\underline{r}^-) = \hat{s}^- \cdot \underline{\underline{R}}_1 \cdot \hat{s}^+ [J_s^+(\underline{r}^+) - J_s^-(\underline{r}^+)] + \hat{s}^- \cdot \underline{\underline{R}}_1 \cdot \hat{t}^+ [J_t^+(\underline{r}^+) - J_t^-(\underline{r}^+)] \tag{83b}$$

To simplify the above equations we consider the case of the pylon and body separately. We start with the pylon surface. From figure 5 where the orientations of $\hat{s}$ and $\hat{t}$ are depicted we see that

$$\hat{t}^+ = \hat{t}^- = -\hat{y}$$

$$s_x^+ = -s_x^-$$

$$s_z^+ = s_z^-$$

$$s_y^+ = s_y^- = 0$$

and consequently

$$\hat{t}^- \cdot \underline{\underline{R}}_1 \cdot \hat{s}^+ = 0$$

$$\hat{t}^- \cdot \underline{\underline{R}}_1 \cdot \hat{t}^+ = 1$$

$$\hat{s}^- \cdot \underline{\underline{R}}_1 \cdot \hat{s}^+ = -1$$

$$\hat{s}^- \cdot \underline{\underline{R}}_1 \cdot \hat{t}^+ = 0$$

In view of the previous relationships, (83) give

$$J_t(\underline{r}^-) = J_t^+(\underline{r}^+) - J_t^-(\underline{r}^+) \qquad (84)a$$

$$J_s(\underline{r}^-) = -[J_s^+(\underline{r}^+) - J_s^+(\underline{r}^+)] \qquad (84)b$$

whereas from (80)a

$$J_t(\underline{r}^+) = J_t^+(\underline{r}^+) + J_t^-(\underline{r}^+) \qquad (85)a$$

$$J_s(\underline{r}^+) = J_s^+(\underline{r}^+) + J_s^-(\underline{r}^+) \qquad (85)b$$

To derive the corresponding relationships for the body we refer to figure 5 from which we obtain

$$\left.\begin{aligned} \hat{t}^+ &= \hat{t}^- = -\hat{x} \\ s_y^+ &= -s_y^- \\ s_z^+ &= s_z^- \\ s_x^+ &= s_x^- = 0 \end{aligned}\right\} \text{Cylindrical Surface}$$

$$\left.\begin{aligned} t_y^+ &= t_y^- \\ t_z^+ &= -t_z^- \\ t_x^+ &= t_x^- = 0 \\ s_y^+ &= -s_y^- \\ s_z^+ &= s_z^- \\ s_x^+ &= s_x^- = 0 \end{aligned}\right\} \text{End Caps}$$

One can easily see that for both the cylindrical surface and the end caps we have

$$\hat{t}^- \cdot \underline{\underline{R}}_1 \cdot \hat{s}^+ = 0$$
$$\hat{t}^- \cdot \underline{\underline{R}}_1 \cdot \hat{t}^+ = 1$$
$$\hat{s}^- \cdot \underline{\underline{R}}_1 \cdot \hat{s}^+ = -1$$
$$\hat{s}^- \cdot \underline{\underline{R}}_1 \cdot \hat{t}^+ = 0$$

and (84), (85) are true for the body as well as for the pylon.

We conclude this Section by repeating that (84) and (85) give the surface current density components J_t and J_s at any point on the pylon or body in terms of J_t^+, J_s^+ and J_t^-, J_s^- evaluated only on the positive ($z > 0$) side of the structure under consideration.

SECTION IV

MATRIX EQUATION

In this section we cast (67) and (68) into a matrix equation in order to numerically solve for the two surface components of $\underline{J}^+$ and $\underline{J}^-$ at the centers of zones on the positive ($z > 0$) side of the pylon and body. The components of the real surface current density $\underline{J}$ at any point can be obtained with the aid of (84) and (85). As we explained in Section III, the centers of all zones have been chosen away from surface intersections, and consequently, according to (3), $f(\Omega) = \frac{1}{2}$ since $\Omega = 2\pi$.

In matrix form (67) and (68) can be written as

$$-[J_T^\alpha] = [\tau^\alpha]\,[J^\alpha] \qquad (\alpha = +, -) \tag{86a}$$

or

$$S_i^\alpha = \sum_{j=1}^{2N_F} \tau_{ij}^\alpha\, J_j^\alpha \qquad i, j = 1, 2, \cdots, 2N_F \tag{86b}$$

where N_F is the total number of zones on the entire structure (pylon and body), and

$$J_\ell^\alpha = J_s^\alpha, \quad S_\ell^\alpha = -J_{Ts}^\alpha \qquad 1 \le \ell \le N_F \tag{87a}$$

$$J_\ell^\alpha = J_t^\alpha, \quad S_\ell^\alpha = -J_{Tt}^\alpha \qquad N_F + 1 \le \ell \le 2N_F \tag{87b}$$

$$[\tau^\alpha] = \begin{bmatrix} [A^\alpha] & [B^\alpha] \\ [C^\alpha] & [D^\alpha] \end{bmatrix} \tag{88}$$

To determine the above submatrices we notice that the current density components will be calculated at the centers of the zones and also that the interaction between zones involves a more detailed division, that is a

division of each zone into a number of subzones. To calculate the integrals in (67) and (68) numerically we assume that the current is constant over a zone and equal to its value at the center of the zone. This allows us to factor the current out of the integral and write the remaining surface integral as a sum over the subzones of the zone. (We have chosen nine subzones as we explain in Appendix A.) In what follows we will describe the interaction of any two zones by the interaction between their respective subzones. In the course of determining the accuracy of this procedure we established that it was necessary to consider such detail interaction for adjacent zones only. Even so it is only the free-space part of the Green's dyadic that should be rendered to such detailed treatment because of the existing singularity, whereas the scattered part is free of singularity with the exception of points near the wing-pylon intersection. For this reason the interaction between adjacent zones in the vicinity of the wing-pylon intersection involves subzone interaction for the entire Green's function. Special care should be taken for interaction within a zone and this point is examined in detail later in this section. Thus A, B, C and D can be defined as follows ($i \neq j$)

$$\left.\begin{aligned}
A_{ij}^{\alpha} &= -\sum_{k=0}^{8} \hat{t}_i \cdot \underline{\underline{D}}^{\alpha}(\underline{r}_i, \underline{r}_{jk}) \cdot \hat{s}_{jk} \Delta S_{jk} \\
B_{ij}^{\alpha} &= -\sum_{k=0}^{8} \hat{t}_i \cdot \underline{\underline{D}}^{\alpha}(\underline{r}_i, \underline{r}_{jk}) \cdot \hat{t}_{jk} \Delta S_{jk} \\
C_{ij}^{\alpha} &= \sum_{k=0}^{8} \hat{s}_i \cdot \underline{\underline{D}}^{\alpha}(\underline{r}_i, \underline{r}_{jk}) \cdot \hat{s}_{jk} \Delta S_{jk} \\
D_{ij}^{\alpha} &= \sum_{k=0}^{8} \hat{s}_i \cdot \underline{\underline{D}}^{\alpha}(\underline{r}_i, \underline{r}_{jk}) \cdot \hat{t}_{jk} \Delta S_{jk}
\end{aligned}\right\} \quad 1 \leq i, j \leq N_F, \; i \neq j \qquad (89)$$

and

$$
\left.
\begin{aligned}
\tau_{ij} &= A^{\alpha}_{ij} && 1 \le i,j \le N_F \\
&= B^{\alpha}_{i,j-N_F} && 1 \le i \le N_F,\ N_F+1 \le j \le 2N_F \\
&= C^{\alpha}_{i-N_F,j} && N_F+1 \le i \le 2N_F,\ 1 \le j \le N_F \\
&= D^{\alpha}_{i-N_F,j-N_F} && N_F+1 \le i,j \le 2N_F
\end{aligned}
\right\} \qquad (90)
$$

As we mentioned earlier, summation over the subzones is necessary for adjacent zones only, i.e. for i and j non-adjacent

$$A^{\alpha}_{ij} = -\hat{t}_i \cdot \underline{\underline{D}}^{\alpha}(\underline{r}_i, \underline{r}_j) \cdot \hat{s}_j \Delta S_j$$

However for generality in the rest of this section we will use the detailed subzone interaction for any two zones. In the above relationships, $\hat{s}_i$, $\hat{t}_i$, $\underline{r}_i$ are the $\hat{s},\hat{t}$ and position vectors at the center of the ith zone, $\hat{s}_{jk}$, $\hat{t}_{jk}$, $\underline{r}_{jk}$ are the $\hat{s},\hat{t}$ and position vectors at the center of the kth subzone of the jth zone, ΔS_{jk} is the area of the (jk)th subzone and $\underline{\underline{D}}^{+}$, $\underline{\underline{D}}^{-}$ are given by (69) and (70) respectively. The areas of subzones and coordinates of the centers of zones and subzones and also the numbering scheme of zones and subzones are given in Appendix A.

When i = j it is obvious from (32) and (33) that a term $\frac{1}{2}\delta_{ij}$ should be included, due to the well-known delta-function singularity of the kernel of the integral equation as the observation point approaches the surface. As it was mentioned in reference 1, the above singularity is integrable as long as both the observation and integration points lie on the surface. From the numerical point of view this integrable singularity should be treated carefully in order to secure sufficient accuracy of the numerical results. At this point we should recall that the singularity under consideration is due to the free-space part of the Green's function and consequently it is only the terms involving G_o that should be treated separately. (Notice that because of (4), (5) and (6) the treatment of the singularity is independent of the particular form of the Green's function, that is independent of the manner we model the wing.) To be more specific it is only the free-space

part of the $\underline{\underline{D}}(\underline{r}^+, \underline{r}_o^+)$ terms in (69) or (70) that will be treated differently because none of the other terms involves a singularity. This part has the form

$$\underline{\underline{D}}_o(\underline{r}, \underline{r}_o) = \nabla G_o(\underline{r}, \underline{r}_o) \times \underline{\underline{I}} \tag{91}$$

and we should first calculate its components along the t and s directions as indicated in (89). To that effect we rewrite $\underline{\underline{D}}_o$ as

$$\begin{pmatrix} \hat{t} \\ \hat{s} \end{pmatrix} \cdot \underline{\underline{D}}_o(\underline{r}, \underline{r}_o) \cdot \begin{pmatrix} \hat{t}_o \\ \hat{s}_o \end{pmatrix} = \begin{pmatrix} \hat{t} \\ \hat{s} \end{pmatrix} \cdot \left[\underline{\underline{D}}_o^{(1)}(\underline{r}, \underline{r}_o) + \underline{\underline{D}}_o^{(2)}(\underline{r}, \underline{r}_o) \right] \cdot \begin{pmatrix} \hat{t}_o \\ \hat{s}_o \end{pmatrix} \tag{92}$$

The first term on the right-hand side is chosen free of singularity and the second term can be integrated analytically to a simpler form. In performing the integration we assume, as before, that the current components do not change over a zone and from (67), (68) we have integrals of the form

$$I = \int_s ds_o \begin{pmatrix} \hat{t} \\ \hat{s} \end{pmatrix} \cdot \underline{\underline{D}}^{(2)}(\underline{r}, \underline{r}_o) \cdot \begin{pmatrix} \hat{t}_o \\ \hat{s}_o \end{pmatrix} \tag{93}$$

These integrals have been evaluated in Appendix B. The results in this Appendix show that

a) for all zones the self-contribution to B_{ii}^{α} is zero,
b) for all zones on the end caps all self-contributions are zero,
c) for all zones on the pylon and body, except near surface intersections, the self-contribution to C_{ii}^{α} is also zero.

Thus, we can complete the list of submatrix elements by writing

$$\left.\begin{aligned} A_{ii}^{\alpha} &= -\sum_{k=0}^{8} \hat{t}_i \cdot \underline{\underline{D}}^{\alpha *}(\underline{r}_i, \underline{r}_{ik}) \cdot \hat{s}_{ik} \Delta S_{ik} + Z_{ii}^{A} - \tfrac{1}{2} \\ B_{ii}^{\alpha} &= -\sum_{k=0}^{8} \hat{t}_i \cdot \underline{\underline{D}}^{\alpha *}(\underline{r}_i, \underline{r}_{ik}) \cdot \hat{t}_{ik} \Delta S_{ik} \qquad \text{(cont.)} \end{aligned}\right\} \quad 1 \le i \le N_F \tag{94}$$

$$C_{ii}^{\alpha} = \sum_{k=0}^{8} \hat{s}_i \cdot \underline{\underline{D}}^{\alpha *}(\underline{r}_i, \underline{r}_{ik}) \cdot \hat{s}_{ik} \Delta S_{ik} + Z_{ii}^{C}$$

$$D_{ii}^{\alpha} = \sum_{k=0}^{8} \hat{s}_i \cdot \underline{\underline{D}}^{\alpha *}(\underline{r}_i, \underline{r}_{ik}) \cdot \hat{t}_{ik} \Delta S_{ik} + Z_{ii}^{D} - \tfrac{1}{2} \qquad 1 \le i \le N_F \qquad (94)$$

where

$$\underline{\underline{D}}^{\alpha *} \equiv \underline{\underline{D}}^{\alpha} - \underline{\underline{D}}_o^{(2)}$$

and Z are terms defined in Appendix B. We can collect (89) and (94) under a single mantle by writing

$$A_{ij}^{\alpha} = - \sum_{k=0}^{8} \hat{t}_i \cdot \underline{\underline{\tilde{D}}}^{\alpha}(\underline{r}_i, \underline{r}_{jk}) \cdot \hat{s}_{jk} \Delta S_{jk} + (Z_{ii}^{A} - \tfrac{1}{2}) \delta_{ij}$$

$$B_{ij}^{\alpha} = - \sum_{k=0}^{8} \hat{t}_i \cdot \underline{\underline{\tilde{D}}}^{\alpha}(\underline{r}_i, \underline{r}_{jk}) \cdot \hat{t}_{jk} \Delta S_{jk}$$

$$C_{ij}^{\alpha} = \sum_{k=0}^{8} \hat{s}_i \cdot \underline{\underline{\tilde{D}}}^{\alpha}(\underline{r}_i, \underline{r}_{jk}) \cdot \hat{s}_{jk} \Delta S_{jk} + \delta_{ij} Z_{ii}^{C}$$

$$D_{ij}^{\alpha} = \sum_{k=0}^{8} \hat{s}_i \cdot \underline{\underline{\tilde{D}}}^{\alpha}(\underline{r}_i, \underline{r}_{jk}) \cdot \hat{t}_{jk} \Delta S_{jk} + (Z_{ii}^{D} - \tfrac{1}{2}) \delta_{ij} \qquad 1 \le i, j \le N_F \qquad (95)a$$

where

$$\underline{\underline{\tilde{D}}}^{\alpha}(\underline{r}_i, \underline{r}_{jk}) = \underline{\underline{D}}^{\alpha}(\underline{r}_i, \underline{r}_{jk}) - \delta_{ij} \underline{\underline{D}}_o^{(2)}(\underline{r}_i, \underline{r}_{jk}) \qquad (95)b$$

Before we proceed to give detailed expressions for the elements of the submatrices we first present the "incident" terms S_{ℓ}^{α} in an expanded form. To accomplish this we assume that the true incident field has the form given by (100) and (101) in reference 1

$$\underline{E}_i = \alpha \underline{E}^{(1)} + \beta \underline{E}^{(2)} \tag{96a}$$

$$\underline{H}_i = \alpha \underline{H}^{(1)} + \beta \underline{H}^{(2)} \tag{96b}$$

$$\left.\begin{aligned}
\underline{E}^{(1)} &= -\sin\theta_o(\cos\varphi_o\cos\theta_o\hat{x} + \sin\varphi_o\cos\theta_o\hat{y} - \sin\theta_o\hat{z})\, e^{ik_o\hat{k}\cdot\underline{r}} \\
\underline{E}^{(2)} &= -\frac{1}{Y}\sin\theta_o(\sin\varphi_o\hat{x} - \cos\varphi_o\hat{y})\, e^{ik_o\hat{k}\cdot\underline{r}} \\
\underline{H}^{(1)} &= -Y\sin\theta_o(\sin\varphi_o\hat{x} - \cos\varphi_o\hat{y})\, e^{ik_o\hat{k}\cdot\underline{r}} \\
\underline{H}^{(2)} &= \sin\theta_o(\cos\varphi_o\cos\theta_o\hat{x} + \sin\varphi_o\cos\theta_o\hat{y} - \sin\theta_o\hat{z})\, e^{ik_o\hat{k}\cdot\underline{r}} \\
\alpha &= \frac{E_o\cos\varphi_p}{\sin\theta_o} \\
\beta &= \frac{E_o\, y\sin\varphi_p}{\sin\theta_o} \\
k &= \frac{k_o}{k_o}
\end{aligned}\right\} \tag{97}$$

E_o is the magnitude of the incident electric field, Y the free-space admittance and $\varphi_o, \theta_o, \varphi_p$ are relevant angles defined in figure 6 . In order to calculate S_ℓ^α we recall (87), (77) and (78) and notice that $\underline{\underline{R}}_1$ acting on $\underline{H}_T(\underline{r}^-)$ changes the sign of the z-component and that the components of $\underline{H}_T$ at $\underline{r}^-$ can be calculated with the aid of $\underline{H}_T$ at $\underline{r}^+$ by changing z to -z. The "total" magnetic field $\underline{H}_T$ for the case of a wing modeled by an infinite elliptical cylinder is given by (108) through (112) of reference 1 and for the case of the flat plate $\underline{H}_T$ is given by (79). From these expressions we observe that the z-dependence $\exp(-ik_o z\cos\theta_o)$ factors out for both the incident and scattered parts and the source term S_ℓ^α can be written as

$$\begin{aligned}
S_\ell^+ = &-i\sin(2k_o z_\ell\cos\theta_o)[t_{\ell x}H_{Tx}(x_\ell, y_\ell) + t_{\ell y}H_{Ty}(x_\ell, y_\ell)] \\
&+ \cos(2k_o z_\ell\cos\theta_o)\, t_{\ell z}H_{Tz}(x_\ell, y_\ell) \quad 1 \le \ell \le N_F
\end{aligned} \tag{98a}$$

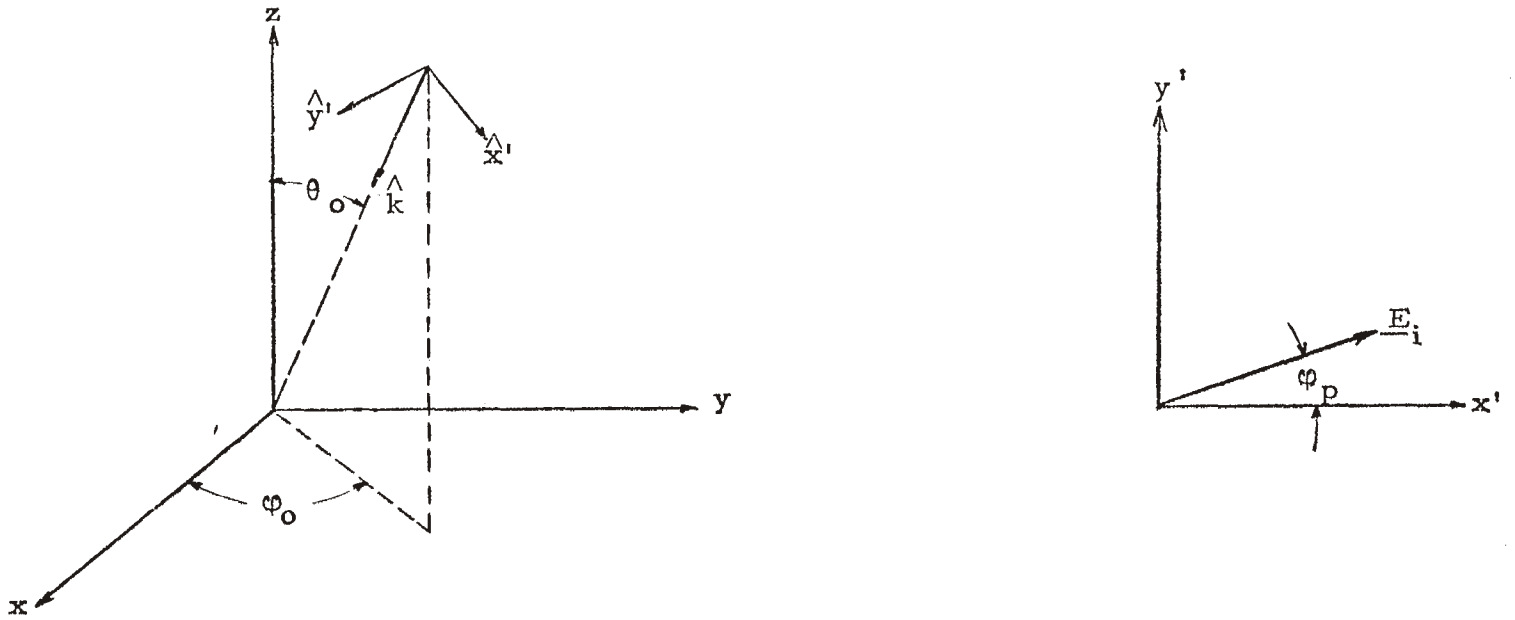

Figure 6: Incident plane wave description.

$$S_\ell^+ = i \sin(2k_o z_\ell \cos\theta_o)[s_{\ell x} H_{Tx}(x_\ell, y_\ell) + s_{\ell y} H_{Ty}(x_\ell, y_\ell)]$$
$$- \cos(2k_o z_\ell \cos\theta_o)\, s_{\ell z} H_{Tz}(x_\ell, y_\ell) \quad N_p + 1 \le \ell \le 2N_F \qquad (98)b$$

$$S_\ell^- = \cos(2k_o z_\ell \cos\theta_o)[t_{\ell x} H_{Tx}(x_\ell, y_\ell) + t_{\ell y} H_{Ty}(x_\ell, y_\ell)]$$
$$- i \sin(2k_o z_\ell \cos\theta_o)\, t_{\ell z} H_{Tz}(x_\ell, y_\ell)] \quad 1 \le \ell \le N_F \qquad (99)a$$

$$S_\ell^- = -\cos(2k_o z_\ell \cos\theta_o)[s_{\ell x} H_{Tx}(x_\ell, y_\ell) + s_{\ell y} H_{Ty}(x_\ell, y_\ell)]$$
$$+ i \sin(2k_o z_\ell \cos\theta_o)\, s_{\ell z} H_{Tz}(x_\ell, y_\ell) \quad N_F + 1 \le \ell \le 2N_F \qquad (99)b$$

where $\underline{H}_T(x_\ell, y_\ell)$ is the x, y dependence of $\underline{H}_T(\underline{r})$.

For the case of the <u>infinite elliptical cylinder</u>

$$H_{Tx}(x_\ell, y_\ell) = (\sin\varphi_p \cos\varphi_o \cos\theta_o - \cos\varphi_p \sin\varphi_o)\, e^{-i\psi_\ell}$$
$$- \frac{i}{(q')^{\frac{1}{2}}\beta_\ell}\Big\{\sin\varphi_p \cos\theta_o [a_\ell S_4(q', \xi_\ell, \eta_\ell) - b_\ell S_5(q', \xi_\ell, \eta_\ell)]$$
$$- \cos\varphi_p [a_\ell S_2(q', \xi_\ell, \eta_\ell) - b_\ell S_3(q', \xi_\ell, \eta_\ell)]\Big\} \qquad (100)a$$

$$H_{Ty}(x_\ell, y_\ell) = (\sin\varphi_p \cos\varphi_o \cos\theta_o + \cos\varphi_p \cos\varphi_o)\, e^{-i\psi_\ell}$$
$$- \frac{i}{(q')^{\frac{1}{2}}\beta_\ell}\Big\{\sin\varphi_p \cos\theta_o [b_\ell S_4(q', \xi_\ell, \eta_\ell) - a_\ell S_5(q', \xi_\ell, \eta_\ell)]$$
$$+ \cos\varphi_p [b_\ell S_2(q', \xi_\ell, \eta_\ell) - a_\ell S_3(q', \xi_\ell, \eta_\ell)]\Big\} \qquad (100)b$$

$$H_{Tz}(x_\ell, y_\ell) = -\sin\varphi_p \sin\theta_o\, e^{-i\psi_\ell} + 2\sin\varphi_p \sin\theta_o\, S_1(q', \xi_\ell, \eta_\ell) \qquad (100)c$$

$$\left.\begin{aligned} \psi_\ell &= k_o(\cos\varphi_o \sin\theta_o x_\ell + \sin\varphi_o \sin\theta_o y_\ell) \\ q' &= \frac{k_o^2}{4}\sin^2\theta_o \end{aligned}\right\} \qquad (101)$$

$$\left.\begin{aligned} a_\ell &= \frac{\sinh\xi_\ell \cos\eta_\ell}{\beta_\ell} \\ b_\ell &= \frac{\cosh\xi_\ell \sin\eta_\ell}{\beta_\ell} \\ \beta_\ell &= (\cosh^2\xi_\ell - \cos^2\eta_\ell)^{\frac{1}{2}} \end{aligned}\right\} \qquad (102)$$

The elliptical coordinates ξ, η are related to x, y through

$$x = c \cosh\xi \cos\eta$$

$$y = c \sinh\xi \sin\eta$$

where c is the semifocal length equal to $(a^2 - b^2)^{\frac{1}{2}}$. More on the definition of the elliptical coordinates can be found in reference 1. The S_i's ($i = 1, 2, \cdots, 5$) are defined in terms of Mathieu functions and are given by (125) and (135) through (138) in reference 1 . For the case of the <u>flat plate</u> the expressions for $\underline{H}_T(x_\ell, y_\ell)$ are considerably simpler,

$$H_{Tx}(x_\ell, y_\ell) = 2(\sin\varphi_o \cos\varphi_o \cos\theta_o - \cos\varphi_p \sin\varphi_o)\, e^{-i\Phi_\ell} \cos\varphi_\ell \qquad (103)a$$

$$H_{Ty}(x_\ell, y_\ell) = -2i(\sin\varphi_p \cos\varphi_o \cos\theta_o + \cos\varphi_p \cos\varphi_o)\, e^{-i\Phi_\ell} \sin\varphi_\ell \qquad (103)b$$

$$H_{Tz}(x_\ell, y_\ell) = -2 \sin\varphi_p \sin\theta_o \cos\varphi_p\, e^{-i\Phi_\ell} \qquad (103)c$$

$$\left.\begin{aligned} \Phi_\ell &= k_o x_\ell \cos\varphi_o \sin\theta_o \\ \varphi_\ell &= k_o y_\ell \sin\varphi_o \sin\theta_o \end{aligned}\right\} \qquad (104)$$

Next we calculate the A, B, C, D elements by considering the t, s components of $\underline{\underline{\tilde{D}}}^\alpha$ in detail. At this point we should be reminded that $\underline{\underline{\tilde{D}}}^\alpha$ where $\alpha = +$, or $-$, is given by (69) or (70) and that $\underline{\underline{D}}$ is given by (71). The $\underline{\underline{D}}_o^{(2)}$ appearing in (95)b is defined in (92) and was calculated in Appendix B

((B-14)). We start by calculating the t, s components of $\underline{\underline{D}}_o(\underline{r}_i, \underline{r}_{jk})$ $- \underline{\underline{D}}_o^{(2)}(\underline{r}_i, \underline{r}_{jk})$ in terms of the cartesian components of the quantities involved

$$- \hat{t}_i \cdot [\underline{\underline{D}}_o(\underline{r}_i, \underline{r}_{jk}) - \underline{\underline{D}}_o^{(2)}(\underline{r}_i, \underline{r}_{jk})] \cdot \hat{s}_{jk} = - P_{ijk}[R_{ijky}(t_{ix}s_{jkz} - t_{iz}s_{jkx})$$

$$+ R_{ijkz}(t_{iy}s_{jkx} - t_{ix}s_{jky}) + R_{ijkx}(t_{iz}s_{jky} - t_{iy}s_{jkz})] \qquad (105)a$$

$$- \hat{t}_i \cdot [\underline{\underline{D}}_o(\underline{r}_i, \underline{r}_{jk}) - \underline{\underline{D}}_o^{(2)}(\underline{r}_i, \underline{r}_{jk})] \cdot \hat{t}_{jk} = - P_{ijk}[R_{ijky}(t_{ix}t_{jkz} - t_{iz}t_{jkx})$$

$$+ R_{ijkx}(t_{iy}t_{jkx} - t_{ix}t_{jky}) + R_{ijkx}(t_{iz}t_{jky} - t_{iy}t_{jkz})] \qquad (105)b$$

$$\hat{s}_i \cdot [\underline{\underline{D}}_o(\underline{r}_i, \underline{r}_{jk}) - \underline{\underline{D}}_o^{(2)}(\underline{r}_i, \underline{r}_{jk})] \cdot \hat{s}_{jk} = P_{ijk}[R_{ijky}(s_{ix}s_{jkz} - s_{iz}s_{jkx})$$

$$+ R_{ijkz}(s_{iy}s_{jkx} - s_{ix}s_{jky}) + R_{ijkx}(s_{iz}s_{jky} - s_{iy}s_{jkz})] \qquad (105)c$$

$$\hat{s}_i \cdot [\underline{\underline{D}}_o(\underline{r}_i, \underline{r}_{jk}) - \underline{\underline{D}}_o^{(2)}(\underline{r}_i, \underline{r}_{jk})] \cdot \hat{t}_{jk} = P_{ijk}[R_{ijky}(s_{ix}t_{jkz} - s_{iz}t_{jkx})$$

$$+ R_{ijkz}(s_{iy}t_{jkx} - s_{ix}t_{jky}) + R_{ijkx}(s_{iz}t_{jky} - s_{iy}t_{jkz})] \qquad (105)d$$

where

$$P_{ijk} = [(ik_oR_{ijk} - 1)e^{ik_oR_{ijk}} + 1]\,(1/4\pi R_{ijk}^3) \qquad (106)$$

$$R_{ijk} = |\underline{R}_{ijk}| = [(x_i - x_{jk})^2 + (y_i - y_{jk})^2 + (z_i - z_{jk})^2]^{\frac{1}{2}} \qquad (107)$$

$$\underline{R}_{ijk} = (x_i - x_{jk})\,\hat{x} + (y_i - y_{jk})\,\hat{y} + (z_i - z_{jk})\hat{z} \qquad (108)$$

and $\hat{t}, \hat{s}$ have the following cartesian components

Pylon

$$\left.\begin{aligned} &t_x = 0, \quad t_y = -1, \quad t_z = 0 \\ &s_x = - za_p^2(a_p^4z^2 + b_p^4x^2)^{-\frac{1}{2}}, \quad s_y = 0, \quad s_z = xb_p^2(a_p^4z^2 + b_p^4x^2)^{-\frac{1}{2}} \end{aligned}\right\} \qquad (109)$$

Body (Cylindrical Surface)

$$\left.\begin{aligned} & t_x = -1, \quad t_y = 0, \quad t_z = 0 \\ & s_x = 0, \quad s_y = z[(y-\ell)^2 + z^2]^{-\frac{1}{2}} \quad s_z = (\ell - y)[(y-\ell)^2 + z^2]^{-\frac{1}{2}} \\ & \ell = b_w + h_p + a_b \end{aligned}\right\} \tag{110}$$

Body (End Caps)

$$x > 0 \begin{cases} t_x = 0, \quad t_y = (y-\ell)[(y-\ell)^2 + z^2]^{-\frac{1}{2}}, \quad t_z = z[(y-\ell)^2 + z^2]^{-\frac{1}{2}} \\ s_x = 0, \quad s_y = z[(y-\ell)^2 + z^2]^{-\frac{1}{2}}, \quad s_z = (\ell - y)[(y-\ell)^2 + z^2]^{-\frac{1}{2}} \end{cases} \tag{111}$$

$$x < 0 \begin{cases} t_x = 0, \quad t_y = (\ell - y)[(y-\ell)^2 + z^2]^{-\frac{1}{2}}, \quad t_z = -z[(y-\ell)^2 + z^2]^{-\frac{1}{2}} \\ s_x = 0, \quad s_y = z[(y-\ell)^2 + z^2]^{-\frac{1}{2}}, \quad s_z = (\ell - y)[(y-\ell)^2 + z^2]^{-\frac{1}{2}} \end{cases} \tag{112}$$

$$\ell = b_w + h_p + a_b$$

The next calculation involves the z-reflected free space contribution in (69) or (70), i.e.

$$\underline{\underline{D}}_o(R_1) \equiv \underline{\underline{D}}_o(\underline{r}^+, \underline{r}_o^-) \cdot \underline{\underline{R}}_1 = [\nabla G_o(\underline{r}^+, \underline{r}_o^-) \times \underline{\underline{I}}] \cdot \underline{\underline{R}}_1 \tag{113}$$

where $\underline{r} = \underline{r}_i$, $\underline{r}_o^- = \underline{r}_{jk}^- = \underline{\underline{R}}_1 \cdot \underline{r}_{jk}^+ = \underline{\underline{R}}_1 \cdot \underline{r}_o^+$, $\underline{r}_{jk}^+ = \underline{r}_{jk}$ and $\underline{\underline{R}}_1$ is defined by (17). To derive the t, s components of $\underline{\underline{D}}_o(R_1)$ we recall the third equation in (75)a, (75)b and (105) to arrive at the following expressions

$$-\hat{t}_i \cdot \underline{\underline{D}}_o(R_1) \cdot \hat{s}_{jk} = -P_{ijk}^{(z)}[-R_{ijky}^{(z)}(t_{ix}s_{jkz} + t_{iz}s_{jkx}) + R_{ijkz}^{(z)}(t_{iy}s_{jkx} - t_{ix}s_{jky}) + R_{ijkx}^{(z)}(t_{iy}s_{jkz} + t_{iz}s_{jky})] \tag{114}a$$

$$-\hat{t}_i \cdot \underline{\underline{D}}_o(R_1) \cdot \hat{t}_{jk} = - P^{(z)}_{ijk}[-R^{(z)}_{ijky}(t_{ix}t_{jkz} + t_{iz}t_{jkx})$$

$$+R^{(z)}_{ijkz}(t_{iy}t_{jkx} - t_{ix}t_{jky}) + R^{(z)}_{ijkx}(t_{iz}t_{jky} + t_{iy}t_{jkz})] \qquad (114)b$$

$$\hat{s}_i \cdot \underline{\underline{D}}_o(R_1) \cdot \hat{s}_{jk} = P^{(z)}_{ijk}[-R^{(z)}_{ijky}(s_{ix}s_{jkz} + s_{iz}s_{jkx})$$

$$+R^{(z)}_{ijkz}(s_{iy}s_{jkx} - s_{ix}s_{jky}) + R^{(z)}_{ijkx}(s_{iz}s_{jky} + s_{iy}s_{jkz})] \qquad (114)c$$

$$\hat{s}_i \cdot \underline{\underline{D}}_o(R_1) \cdot \hat{t}_{jk} = P^{(z)}_{ijk}[-R^{(z)}_{ijky}(s_{ix}t_{jkz} + s_{iz}t_{jkx})$$

$$+R^{(z)}_{ijkz}(s_{iy}t_{jkx} - s_{ix}t_{jky}) + R^{(z)}_{ijkx}(s_{iz}t_{jky} + s_{iy}t_{jkz})] \qquad (114)d$$

where

$$P^{(z)}_{ijk} = (ik_o R^{(z)}_{ijk} - 1)\, e^{ik_o R^{(z)}_{ijk}} (1/4\pi)[R^{(z)}_{ijk}]^{-3} \qquad (115)$$

$$R^{(z)}_{ijk} = |\underline{R}^{(z)}_{ijk}| = [(x_i - x_{jk})^2 + (y_i - y_{jk})^2 + (z_i + z_{jk})^2]^{\frac{1}{2}} \qquad (116)$$

$$\underline{R}^{(z)}_{ijk} = (x_i - x_{jk})\hat{x} + (y_i - y_{jk})\hat{y} + (z_i + z_{jk})\hat{z} \qquad (117)$$

To complete the calculation of the t, s components of $\underline{\underline{\tilde{D}}}^{\alpha}_o(\underline{r}_i, \underline{r}_{jk})$ in (95)a we should now refer to the specific manner we model the wing. Thus for an infinite elliptical wing we consider $\nabla \times \underline{\underline{G}}_{is}(\underline{r}^+, \underline{r}^+_o)$ and $\nabla \times \underline{\underline{G}}_{is}(\underline{r}^+, \underline{r}^-_o) \cdot \underline{\underline{R}}_1$, where $\underline{\underline{D}}_1 = \nabla \times \underline{\underline{G}}_{is}$ is given by (46) or more specifically by (167) in reference [1]. In order to derive the expressions for the t, s components of $\underline{\underline{D}}_1$ we start with

$$-\hat{t}_i \cdot \underline{\underline{D}}_1(\underline{r}_i, \underline{r}_{jk}) \cdot \hat{s}_{jk} = -(t_{ix}D_{ix,jkx}s_{jkx} + t_{ix}D_{ix,jky}s_{jky} + t_{ix}D_{ix,jkz}s_{jkz}$$

$$+ t_{iy}D_{iy,jkx}s_{jkx} + t_{iy}D_{iy,jky}s_{jky} + t_{iy}D_{iy,jkz}s_{ikz}$$

$$+ t_{iz}D_{iz,jkx}s_{jkx} + t_{iz}D_{iz,jky}s_{jky} \qquad (118)$$

where

$$D_{ix,jkx} = (2\pi\beta_i\beta_{jk})^{-1}[a_i a_{jk} K_1(i,jk) + a_i b_{jk} K_2(i,jk) - b_i a_{jk} K_3(i,jk) - b_i b_{jk} K_4(i,jk)] \quad (119)$$

$$D_{ix,jky} = (2\pi\beta_i\beta_{jk})^{-1}[a_i b_{jk} K_1(i,jk) - a_i a_{jk} K_2(i,jk) - b_i b_{jk} K_3(i,jk) + b_i a_{jk} K_4(i,jk)] \quad (120)$$

$$D_{ix,jkz} = -i(2\pi c\beta_i)^{-1}[a_i K_7(i,jk) + b_i K_8(i,jk)] \quad (121)$$

$$D_{iy,jkx} = (2\pi\beta_i\beta_{jk})^{-1}[b_i a_{jk} K_1(i,jk) + b_i b_{jk} K_2(i,jk) + a_i a_{jk} K_3(i,jk) + a_i b_{jk} K_4(i,jk)] \quad (122)$$

$$D_{iy,jky} = (2\pi\beta_i\beta_{jk})^{-1}[b_i b_{jk} K_1(i,jk) - b_i a_{jk} K_2(i,jk) + a_i b_{jk} K_3(i,jk) - a_i a_{jk} K_4(i,jk)] \quad (123)$$

$$D_{iy,jkz} = -i(2\pi c\beta_i)^{-1}[b_i K_7(i,jk) - a_i K_8(i,jk)] \quad (124)$$

$$D_{iz,jkx} = -i(2\pi c\beta_{jk})^{-1}[a_{jk} K_5(i,jk) + b_{jk} K_6(i,jk)] \quad (125)$$

$$D_{iz,jky} = -i(2\pi c\beta_{jk})^{-1}[b_{jk} K_5(i,jk) - a_{jk} K_6(i,jk)] \quad (126)$$

where K_1 through K_8 are given by (198)-(201) and (341)-(344) in reference 1 and a, b, β by (184) through (186) in the same reference.

The evaluation of the rest of the t, s components of $\underline{\underline{D}}_1$ is similar to (118) provided we make the correct replacements for the unit vectors $\hat{t}, \hat{s}$.

Next we calculate the t, s components of

$$\underline{\underline{D}}_1(R_1) \equiv (\nabla \times \underline{\underline{G}}_{is}(\underline{r}^+, \underline{r}_o^-)] \cdot \underline{\underline{R}}_1 \tag{127}$$

If we recall that $\underline{r}_o^- = \underline{\underline{R}}_1 \cdot \underline{r}_o^+$, $\underline{r}^+ = \underline{r} = \underline{r}_i$, $\underline{r}_o^+ = \underline{r}_o = \underline{r}_{jk}$ and that $\nabla \times \underline{\underline{G}}_{is}$ is given by (46) we understand that the t, s components of $\underline{\underline{D}}_1(R_1)$ have the same form as (118) provided we account for the changes due to the action of the reflection operator $\underline{\underline{R}}_1$. In that respect the third of (75)b is helpful. Then

$$\begin{aligned} -\hat{t}_i \cdot \underline{\underline{D}}_1(\underline{r}_i, \underline{\underline{R}}_1 \cdot \underline{r}_{jk})(\underline{\underline{R}}_1 \cdot \hat{s}_{jk}) = &- (t_{ix} D^{(z)}_{ix,jkx} s_{jkx} + t_{ix} D^{(z)}_{ix,jky} s_{jky} \\ &- t_{ix} D^{(z)}_{iy,jkz} s_{jkz} + t_{iz} D^{(z)}_{iz,jkx} s_{jkx} + t_{iy} D^{(z)}_{iy,jky} s_{jky} \\ &- t_{iy} D^{(z)}_{iy,jkz} s_{jkz} + t_{iz} D^{(z)}_{iz,jkx} s_{jkx} + t_{iz} D^{(z)}_{iz,jky} s_{jky}) \end{aligned} \tag{128}$$

where $\underline{\underline{D}}^{(z)}$ is the same as $\underline{\underline{D}}_1$ except that we have replaced z_{jk} in the argument of $\underline{\underline{D}}_1$ by $-z_{jk}$.

The calculation of the remaining t, s components of $\underline{\underline{D}}_1(N)$ is similar provided we allow for the correct replacement of the unit vectors $\hat{t}$ and $\hat{s}$.

Finally we consider the alternate model of the wing as an <u>infinite flat plate</u> and proceed to calculate the t, s elements of $\nabla \times \underline{\underline{G}}_{is}(\underline{r}^+, \underline{r}_o^+)$ and $[\nabla \times \underline{\underline{G}}_{is}(\underline{r}^+, \underline{r}_o^-)] \cdot \underline{\underline{R}}_1$ where $\nabla \times \underline{\underline{G}}_{is}(\underline{r}^+, \underline{r}_o^+)$ is given by (72)

$$\nabla \times \underline{\underline{G}}_{is}(\underline{r}^+, \underline{r}_o^+) = - \nabla G_o(\underline{r}^+, \underline{r}_{oi}^+) \times \underline{\underline{R}} \tag{129}$$

and $\underline{r}_{oi}^+ = \underline{\underline{R}} \cdot \underline{r}_o^+$, $\underline{\underline{R}} = \underline{\underline{I}} - 2\hat{y}\hat{y}$. If we recall (75)a and (75)b we can arrive at the following expressions

$$\begin{aligned} -\hat{t}_i \cdot [- \nabla G_o(\underline{r}^+, \underline{r}_{oi}^+) \times \underline{\underline{R}}] \cdot \hat{s}_{jk} = &- P^{(y)}_{ijk} [- R^{(y)}_{ijky}(t_{ix} s_{jkz} - t_{iz} s_{jkx}) \\ &+ R^{(y)}_{ijkz}(t_{iy} s_{jkx} + t_{ix} s_{jky}) - R^{(y)}_{ijkx}(t_{iz} s_{jky} + t_{iy} s_{jkz})] \end{aligned} \tag{130}$$

where

$$P_{ijk}^{(y)} = (ik_o R_{ijk}^{(y)} - 1)\, e^{ik_o R_{ijk}^{(y)}} (1/4\pi)[R_{ijk}^{(y)}]^{-3} \tag{131}$$

$$R_{ijk}^{(y)} = |\underline{R}_{ijk}^{(y)}| = [(x_i - x_{jk})^2 + (y_i + y_{jk})^2 + (z_i - z_{jk})^2]^{\frac{1}{2}} \tag{132}$$

$$\underline{R}_{ijk}^{(y)} = (x_i - x_{jk})\hat{x} + (y_i + y_{jk})\hat{y} + (z_k - z_{jk})\hat{z} \tag{133}$$

To calculate the remaining t, s components of $-\nabla G_o(\underline{r}^+, \underline{r}_{oi}^+) \times \underline{\underline{R}}$ we use (130) allowing for the correct replacements of the unit vectors $\hat{t}, \hat{s}$.

The last calculation involves the .t, s component of

$$[\nabla \times \underline{\underline{G}}_{is}(\underline{r}^+, \underline{r}_o^-)] \cdot \underline{\underline{R}}_1 = [-\nabla G_o(\underline{r}^+, \underline{r}_{oi}^-) \times \underline{\underline{R}}] \cdot \underline{\underline{R}}_1 \tag{134}$$

With the aid of (75)a and (75)b we can arrive at the following expression

$$-\hat{t}_i[-\nabla G_o(\underline{r}^+, \underline{r}_{oi}^-) \times \underline{\underline{R}}] \cdot \underline{\underline{R}}_1 \cdot s_{jk} = -P_{ijk}^{(yz)}[-R_{ijky}^{(yz)}(t_{ix}s_{jkz} + t_{iz}s_{jkx})$$

$$+ R_{ijkz}^{(yz)}(t_{iy}s_{jkx} + t_{ix}s_{jky}) - R_{ijkx}(t_{iz}s_{jky} - t_{iy}s_{jkz})] \tag{135}$$

where

$$P_{ijk}^{(yz)} = (ik_o R_{ijk}^{(yz)} - 1)\, e^{ik_o R_{ijk}^{(yz)}} (1/4\pi)[R_{ijk}^{(yz)}]^{-3} \tag{136}$$

$$R_{ijk}^{(yz)} = |\underline{R}_{ijk}^{(yz)} = [(x_i - x_{jk})^2 + (y_i + y_{jk})^2 + (z_i + z_{jk})^2]^{\frac{1}{2}} \tag{137}$$

$$\underline{R}_{ijk}^{(yz)} = (x_i - x_{jk})\hat{x} + (y_i + y_{jk})\hat{y} + (z_i + z_{jk})\hat{z} \tag{138}$$

The derivation of the remaining t, s components of $[-\nabla G_o(\underline{r}^+, \underline{r}_{oi}^-) \times \underline{\underline{R}}] \cdot \underline{\underline{R}}_1$ is similar and is given by (135) provided we make the correct replacements for the unit vectors $\hat{t}, \hat{s}$.

Thus we have completed the derivation of the t, s components of $\underline{\underline{\tilde{D}}}^{\alpha}$ in (95)a for both wing models, i. e. the infinite elliptical cylinder and

the infinite flat plate. The matrix equation (87) can now be inverted in order to calculate the t and s components of $\underline{J}^+$ and $\underline{J}^-$. The components of the real surface current density $\underline{J}$ at any point can be obtained with the aid of (84) and (85).

We now present symmetry relations that could be used to reduce the number of matrix elements that need to be calculated. They are particularly useful in reducing computer time when the elliptic cylinder model of the wing is used. In this note we are interested in obtaining numerical results only for the flat plate model of the wing and for that reason as well as time limitations we have note programmed these relations. For completeness we present the following symmetry relations.

$$\left.\begin{aligned} A_{i^*,j^*} &= A_{i,j} \\ B_{i^*,j^*} &= -B_{i,j} \\ C_{i^*,j^*} &= -C_{i,j} \\ D_{i^*,j^*} &= D_{i,j} \end{aligned}\right\} \quad \text{Pylon}$$

where i^*, j^* refer to zones symmetric (with respect to $x = 0$) to i, j respectively, i. e.

$$m^* = \left\{2\left[\frac{m}{N_p}\right]^* + 1\right\} N_p + m - 1, \quad m = i, j$$

Further matrix element symmetries exist if $L_1 = L_2$, however, then we could do considerably more than just reduce the number of matrix elements that must be calculated. This is so because we would have an additional plane of symmetry (yz plane) and we could further reduce the size of the matrix that must be inverted by supplying the analysis contained in Section II.

Finally the following remarks are in order. In debugging the program that solves (86) we first considered a familiar problem, that is the interaction of a perfectly conducting circular cylinder with an incident plane electromagnetic wave. Thus the wing and the pylon were removed and the hole left over at the pylon-body intersection was properly filled out by correcting the areas and coordinates of zones and subzones. The Green's function also had to be modified, that is we deleted the scattered part corresponding to the presence of the wing. The symmetry considerations were still true and valuable and were left unchanged. Thus our debugging had endowed us with the very interesting problem of calculating the current density components on the surface of a perfectly conducting cylinder illuminated by a plane wave. The ensuing calculations and comparisons to known results were interesting and important enough to be published as a forthcoming Interaction Note.

SECTION V

CALCULATION OF INTERIOR CABLE CURRENTS AND VOLTAGES

In this section we consider a cable or cable bundle to be running coaxial with the axis of our circular cylindrical portion of the attached structure. This analysis is also appropriate for the modification of our program where the circular cylinder is situated in free space. The geometry describing the orientation of the cable and the aperture exposing the cable is depicted in figure 7 . The parameters defined by this figure are a, ζ, φ_w, and φ_a^k with only φ_a^k requiring further definition. This is the angle as indicated measured to the geometric center of the k^{th} aperture. The other coordinate needed to locate this aperture is x_a^k where x is the Cartesian coordinate defined in figure 1 . For our purposes we require two additional parameters to characterize the aperture, the electric polarizability α_e^k and the magnetic polarizability α_m^k. We are now in a position to use the results of reference 5 to represent the EMP excited aperture as the equivalent two port depicted in figure 8 . The equivalent voltage and current sources are given by

$$V_{eq}^k = ik_o \alpha_m^k D^k J_t(x_a^k, \varphi_a^k) \tag{139}$$

and

$$I_{eq}^k = \frac{\alpha_e^k D^k}{Z_c} \nabla_s \cdot \underline{J}(x_a^k, \varphi_a^k) \tag{140}$$

where $\nabla_s \cdot$ is the surface divergence and

$$Z_c = \left(\frac{Z_o}{2\pi}\right) \operatorname{arccosh}\left[\frac{a_b^2 + a^2 - \zeta^2}{2a_b a}\right] \tag{141}$$

$$D^k = \frac{Z_o}{2\pi a_b} \frac{(1-\beta^2)^{\frac{1}{2}}}{1-\beta\cos(\varphi_w - \varphi_a^k)} \tag{142}$$

5. Latham, R. W., "Small holes in cable shields," AFWL Interaction Notes, Note 118, September 1972.

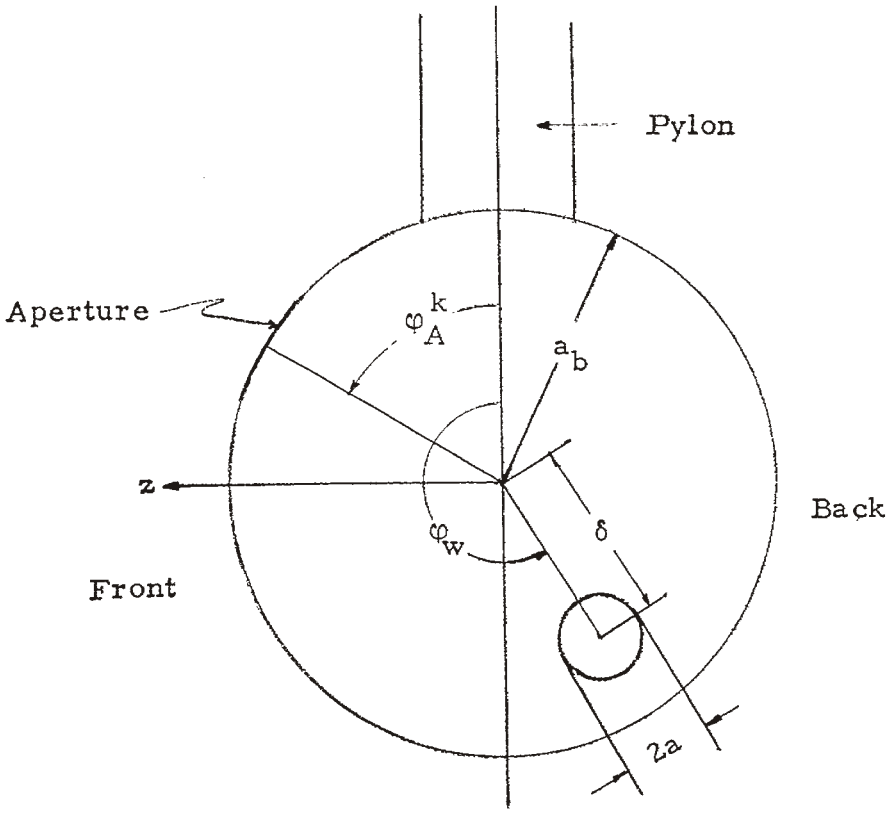

Figure 7: Internal cable geometry

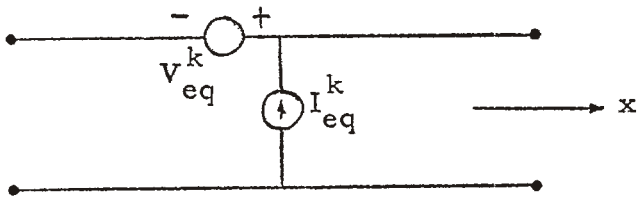

Figure 8: Two port equivalent circuit for the k^{th} excited aperture

$$\beta = \frac{2\zeta a_b}{a_b^2 - a^2 + \zeta^2} \tag{143}$$

In reference 5 the equivalent voltage and current source two port is due to an aperture in an infinite cylinder. In this note we assume that the same two port source can be inserted between the equivalent transmission lines associated with our finite cylinder as depicted in figure 9 . The internal terminating impedances Z_R and Z_L must be specified as input parameters and the characteristic impedance of the line is given in reference 5. The solution of the transmission line problem depicted in figure 9 for a single two port source is well known and depends on whether the position on the cable, where the voltage and currents are to be calculated, is associated with a coordinate x_c that is either larger or smaller than x_a^k. Using the principle of superposition, the solution for many apertures is

$$V(x_c) = \sum_{k=1}^{N_L} \epsilon(x_c, x_{aL}^k) \frac{Z_c}{Z_c + Z_{TL}^k} \frac{e^{ik_o(x_c - x_{aL}^k)} - \rho_R e^{ik_o[2(L_1 - x_{aL}^k) - (x_c - x_{aL}^k)]}}{1 - \rho_{oL}^k \rho_R e^{2ik_o(L_1 - x_{aL}^k)}} V_{TL}^k$$

$$+ \sum_{k=1}^{N_R} \epsilon(x_c, x_{aR}^k) \frac{Z_c}{Z_c + Z_{TR}^k} \frac{e^{ik_o(x_{aR}^k - x_c)} - \rho_L e^{ik_o[2(L_2 + x_{aR}^k) - (x_{aR}^k - x_c)]}}{1 - \rho_{oR}^k \rho_L e^{2ik_o(L_2 + x_{aR}^k)}} V_{TR}^k \tag{144}$$

$$I(x_c) = \sum_{k=1}^{N_L} \epsilon(x_c, x_{aL}^k) \frac{1}{Z_c + Z_{TL}^k} \frac{e^{ik_o(x_c - x_{aL}^k)} + \rho_R e^{ik_o[2(L_1 - x_{aL}^k) - (x_c - x_{aL}^k)]}}{1 - \rho_{oL}^k \rho_R e^{2ik_o(L_1 - x_{aL}^k)}} V_{TL}^k$$

$$+ \sum_{k=1}^{N_R} \epsilon(x_c, x_{aR}^k) \frac{1}{Z_c + Z_{TR}^k} \frac{e^{ik_o(x_{aR}^k - x_c)} + \rho_L e^{ik_o[2(L_2 + x_{aR}^k) - (x_{aR}^k - x_c)]}}{1 - \rho_{oR}^k \rho_L e^{ik_o(L_2 + x_{aR}^k)}} V_{TR}^k \tag{145}$$

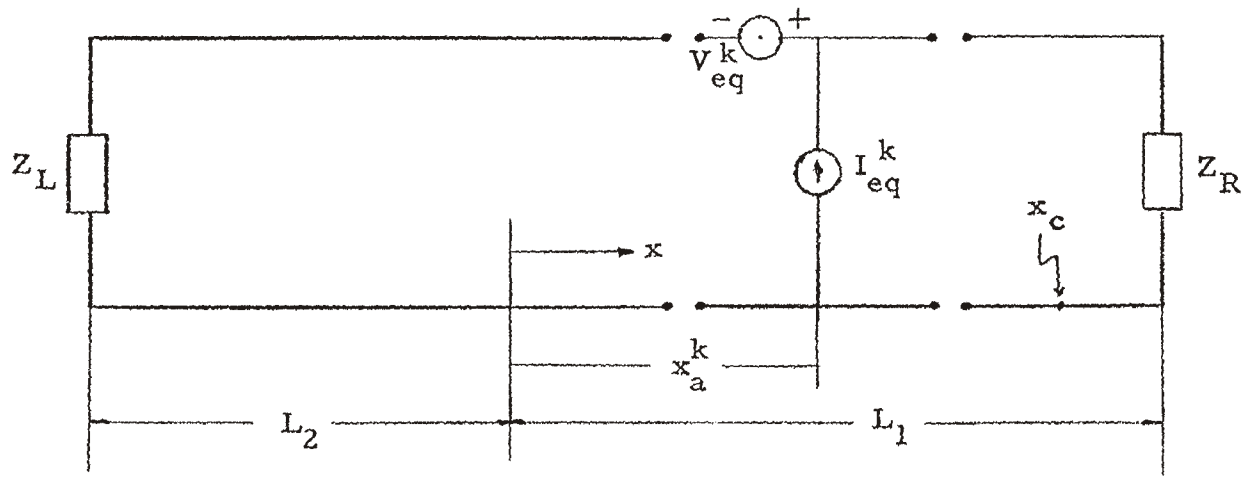

Figure 9: Total equivalent transmission line description of the internal coupling problem

where N_L and N_R are determined according to

$$x_c \geq x_{aL}^k \quad k = 1, \ldots, N_L$$

and

$$x_c \leq x_{aR}^k \quad k = 1, \ldots, N_R$$

The remaining quantities in (144) and (145) are given by

$$\epsilon(x_c, x_a^k) = \begin{cases} 1 & x_c \neq x_a^k \\ \frac{1}{2} & x_c = x_a^k \end{cases} \tag{146}$$

$$\rho_R = \frac{Z_c - Z_R}{Z_c + Z_R} \tag{147}$$

$$\rho_L = \frac{Z_c - Z_L}{Z_c + Z_L} \tag{148}$$

$$Z_{TL}^k = Z_c \frac{1 - \rho_L e^{2ik_o(L_2 + x_{aL}^k)}}{1 + \rho_L e^{2ik_o(L_2 + x_{aL}^k)}} \tag{149}$$

$$Z_{TR}^k = Z_c \frac{1 - \rho_R e^{2ik_o(L_1 - x_{aR}^k)}}{1 + \rho_R e^{2ik_o(L_1 - x_{aR}^k)}} \tag{150}$$

$$\rho_{oL}^k = \frac{Z_c - Z_{TL}^k}{Z_c + Z_{TL}^k} \tag{151}$$

$$\rho_{oR}^k = \frac{Z_c - Z_{TR}^k}{Z_c + Z_{TR}^k} \tag{152}$$

$$V_{TL}^{k} = V_{eq}^{k} + Z_{TL}^{k} I_{eq}^{k} \tag{153}$$

$$V_{TR}^{k} = Z_{TR}^{k} I_{eq}^{k} - V_{eq}^{k} \tag{154}$$

The relationship of the internal cable voltage and current given in (144) and (145) to the surface current densitites that are calculated in this note is through the equivalent source dependence as can be seen in (139) and (140). These quantities are evaluated at the point corresponding to the geometric center of the aperture (x_a^k, φ_a^k); however, for the calculation of these quantities the surface is assumed to be closed. In general, the center of an aperture will not correspond to the center of a zone where the two components of the surface current density are calculated. For this reason we use the four point interpolation procedure that will now be described. In general

$$J_t(x_a^k, \varphi_a^k) \equiv J_t^k = (1-p_k)(1-q_k)A_k^J + p_k(1-q_k)\, B_k^J + q_k(1-p_k)\, C_k^J + p_k q_k D_k^J \tag{155}$$

and

$$\nabla_s \cdot \underline{J}(x_a^k, \varphi_a^k) = (1-p_k)(1-q_k)A_k^Q + p_k(1-q_k)B_k^Q + q_k(1-p_k)C_k^Q + p_k q_k D_k^Q \tag{156}$$

where we have reduced the problem to specifying $p_k, q_k, A_k^{Q,J}, B_k^{Q,J}, C_k^{Q,J}$, and $D_k^{Q,J}$ as functions of x_a^k, φ_a^k, and the calculated components of the surface current densities at the determined center of appropriate neighboring zones.

We replace the dependence of these quantities on x_a^k with the equivalent and more convenient variable

$$\tau_k = L_1 - x_a^k$$

The resulting interpolation procedure is now summarized to the intent that a particular specification of τ_k and φ_a^k leads to the specification of all quantities appearing in (155) and (156). (The subsequent presentation involves the numbering scheme and dimensions of zones explained in detail in Appendix A.)

For

$$\frac{l_b^{(1)}}{2} \leq \tau_k \leq L_1 - \frac{l_b^{(1)}}{2} \tag{157}$$

we define

$$\beta_k = \left(\left[\frac{\tau_k}{l_b^{(1)}} \right]^* + \frac{1}{2} \right) l_b^{(1)} \tag{158}$$

where $l_b^{(1)}$ is the length of a body (circular cylinder) zone for $x \geq 0$ and $[x]^*$ is the largest integer smaller than x. If x is integer then $[x]^* = x-1$. Now we consider the cases $\beta_k \geq \tau_k$ and $\beta_k < \tau_k$. If

$\beta_k \geq \tau_k$, then

$$p_k = \frac{\beta_k - \tau_k}{l_b^{(1)}} \quad \text{and} \quad j_{Ak} = \left[\frac{\tau_k}{l_b^{(1)}} \right]^* + 1 + N_p N_h, \quad j_{Bk} = j_{Ak} - 1 \tag{159}$$

$\beta_k < \tau_k$, then

$$p_k = \frac{\beta_k + l_b^{(1)} - \tau_k}{l_b^{(1)}} \quad \text{and} \quad j_{Ak} = \left[\frac{\tau_k}{l_b^{(1)}} \right]^* + 2 + N_p N_h, \quad j_{Bk} = j_{Ak} - 1 \tag{160}$$

where N_p is the number of pylon zones along half the pylon circumference, N_h the number of zones along the pylon height and j_{Ak}, j_{Bk} will be used shortly.

For

$$L_1 - \frac{l_b^{(1)}}{2} < \tau_k \leq L_1 + \frac{l_b^{(2)}}{2} \tag{161}$$

$$p_k = \frac{L_1 + l_b^{(2)}/2 - \tau_k}{l_b^{(1)}/2 + l_b^{(2)}/2}, \quad j_{Ak} = N_b^{(1)} + 1 + N_p N_h, j_{Bk} = N_b^{(1)} + N_p N_h \tag{162}$$

where $l_b^{(2)}$ the length of a body zone for $x \leq 0$ and $N_b^{(1)}$ the number of longitudinal zones along the $x \geq 0$ portion of the body.

For

$$L_1 + \frac{l_b^{(2)}}{2} < \tau_k \leq L_1 + L_2 - \frac{l_b^{(2)}}{2}$$

define

$$\beta_k = L_1 + \left(\left[\frac{\tau_k - L_1}{l_b^{(2)}} \right]^* + \frac{1}{2} \right) l_b^{(2)}$$

and if

$\beta_k \geq \tau_k$, then

$$p_k = \frac{\beta_k - \tau_k}{l_b^{(2)}} \text{ and } j_{Ak} = N_b^{(1)} + \left[\frac{\tau_k - L_1}{l_b^{(1)}} \right]^* + 1 + N_p N_h, j_{Bk} = j_{Ak} - 1 \tag{165}$$

$\beta_k < \tau_k$, then

$$p_k = \frac{\beta_k + l_b^{(2)} - \tau_k}{l_b^{(2)}} \text{ and } j_{Ak} = N_b^{(1)} + \left[\frac{\tau_k - L_1}{l_b^{(1)}} \right]^* + 2 + N_p N_h, j_{Bk} = j_{Ak} - 1 \tag{166}$$

Next we consider the φ dependence. Thus for

$$0 < \varphi_\alpha^k \leq 3\pi/4 \tag{167}$$

$$\left.\begin{aligned}
&q_k = \frac{\varphi_\alpha^k - \pi/4}{\pi/2}, \quad A_k^J = J_{tF}(j_{Ak}), \quad B_k^J = J_{tF}(j_{Bk}) \\
&C_k^J = J_{tF}(j_{Ak} + N_b), \quad D_k^J = J_{tF}(j_{Bk} + N_b) \\
&A_k^Q = \frac{1}{a_b}\frac{\partial J_{sF}(j_{Ak})}{\partial \varphi} + \frac{\partial J_{tF}(j_{Ak})}{\partial \xi} \\
&B_k^Q = \frac{1}{a_b}\frac{\partial J_{sF}(j_{Bk})}{\partial \varphi} + \frac{\partial J_{tF}(j_{Bk})}{\partial \xi} \\
&C_k^Q = \frac{1}{a_b}\frac{\partial J_{sF}(j_{Ak}+N_b)}{\partial \varphi} + \frac{\partial J_{tF}(j_{Ak}+N_b)}{\partial \xi} \\
&D_k^Q = \frac{1}{a_b}\frac{\partial J_{sF}(j_{Bk}+N_b)}{\partial \varphi} + \frac{\partial J_{tF}(j_{Bk}+N_b)}{\partial \xi}
\end{aligned}\right\} \tag{168}$$

where $J_{tF}(j)$, $J_{sF}(j)$ are the t and s components of the surface current density evaluated at the center of the jth zone situated on the front $(F, z > 0)$ portion of the body, the partial derivatives are given in detail later and N_b is the number of longitudinal zones along the full length of the body. For

$$3\pi/4 < \varphi_\alpha^k < 5\pi/4 \tag{169}$$

$$\left.\begin{aligned}
&q_k = \frac{\varphi_\alpha^k - 3\pi/4}{\pi/2}, \quad A_k^J = J_{tF}(j_{Ak} + N_b), \quad B_k^J = J_{tF}(j_{Bk} + N_b) \\
&C_k^J = J_{tB}(j_{Ak} + N_b), \quad D_k^J = J_{tB}(j_{Bk} + N_b) \\
&A_k^Q = \frac{1}{a_b}\frac{\partial J_{sF}(j_{Ak}+N_b)}{\partial \varphi} + \frac{\partial J_{tF}(j_{Bk}+N_b)}{\partial \xi}
\end{aligned}\right\} \tag{170}$$

$$
\left.
\begin{aligned}
B_k^Q &= \frac{1}{a_b}\,\frac{\partial J_{sF}(j_{Bk}+N_b)}{\partial\varphi} + \frac{\partial J_{tF}(j_{Ak}+N_b)}{\partial\xi} \\
C_k^Q &= \frac{1}{a_b}\,\frac{\partial J_{sB}(j_{Ak}+N_b)}{\partial\varphi} + \frac{\partial J_{tB}(j_{Ak}+N_b)}{\partial\xi} \\
D_k^Q &= \frac{1}{a_b}\,\frac{\partial J_{sB}(j_{Bk}+N_b)}{\partial\varphi} + \frac{\partial J_{tB}(j_{Bk}+N_b)}{\partial\xi}
\end{aligned}
\right\} \qquad (170)
$$

where the index B stands for back i. e. the $z < 0$ portion of the body. For

$$5\pi/4 \le \varphi < 2\pi \qquad (171)$$

$$
\left.
\begin{aligned}
&q_k = \frac{7\pi/4 - \varphi_a^k}{\pi/2},\quad A_k^J = J_{tB}(j_{Ak}),\quad B_k^J = J_{tB}(j_{Bk}) \\
&C_k^J = J_{tB}(j_{Ak}+N_b),\quad D_k^J = J_{tB}(j_{Bk}+N_b) \\
&A_k^Q = \frac{1}{a_b}\,\frac{\partial J_{sB}(j_{Ak})}{\partial\varphi} + \frac{\partial J_{tB}(j_{Ak})}{\partial\xi} \\
&B_k^Q = \frac{1}{a_b}\,\frac{\partial J_{sB}(j_{Bk})}{\partial\varphi} + \frac{\partial J_{tB}(j_{Bk})}{\partial\xi} \\
&C_k^Q = \frac{1}{a_b}\,\frac{\partial J_{sB}(j_{Ak}+N_b)}{\partial\varphi} + \frac{\partial J_{tB}(j_{Bk}+N_b)}{\partial\xi} \\
&D_k^Q = \frac{1}{a_b}\,\frac{\partial J_{sB}(j_{Ak}+N_b)}{\partial\varphi} + \frac{\partial J_{tB}(j_{Bk}+N_b)}{\partial\xi}
\end{aligned}
\right\} \qquad (172)
$$

Finally we present explicit numerical expressions for the partial derivatives appearing in the previous relationships for the various zone locations. We start with the ξ-derivatives.

$$
\left.
\begin{aligned}
j &= N_p N_h + 1 \\
j &= N_p N_h + N_b + 1
\end{aligned}
\right\}
\frac{\partial J_{t(F,B)}^{(j)}}{\partial\xi} = \frac{J_{t(F,B)}^{(j+1)} - J_{t(F,B)}^{(j)}}{l_b^{(1)}} \qquad (173)
$$

$$\left.\begin{array}{l} j = N_p N_h + N_b \\ \\ j = N_p N_h + 2N_b \end{array}\right\} \frac{\partial J_{t(F,B)}^{(j)}}{\partial \xi} = \frac{J_{t(F,B)}^{(j)} - J_{t(F,B)}^{(j-1)}}{l_b^{(2)}} \qquad (174)$$

$$\left.\begin{array}{l} j = N_p N_h + N_b^{(1)} \\ \\ j = N_p N_h + N_b^{(1)} + N_b \end{array}\right\} \frac{\partial J_{t(F,B)}^{(j)}}{\partial \xi} = \frac{J_{t(F,B)}^{(j+1)} - J_{t(F,B)}^{(j-1)}}{(1/2)[3l_b^{(1)} + l_b^{(2)}]} \qquad (175)$$

$$\left.\begin{array}{l} j = N_p N_h + N_b^{(1)} + 1 \\ \\ j = N_p N_h + N_b^{(1)} + N_b + 1 \end{array}\right\} \frac{\partial J_{t(F,B)}^{(j)}}{\partial \xi} = \frac{J_{t(F,B)}^{(j+1)} - J_{t(F,B)}^{(j-1)}}{(1/2)[l_b^{(1)} + 3l_b^{(2)}]} \qquad (176)$$

$$\left.\begin{array}{l} N_p N_h + 2 \le j \le N_p N_h + N_b^{(1)} - 1 \\ \\ N_p N_h + 2 + N_b \le j \le N_p N_h + N_b + N_b^{(1)} - 1 \\ \\ \dfrac{\partial J_{t(F,B)}^{(j)}}{\partial \xi} = \dfrac{J_{t(F,B)}^{(j+1)} - J_{t(F,B)}^{(j-1)}}{2l_b^{(1)}} \end{array}\right\} \qquad (177)$$

$$\left.\begin{array}{l} N_p N_h + N_b^{(1)} + 2 \le j \le N_p N_h + N_b - 1 \\ \\ N_p N_h + N_b + N_b^{(1)} + 2 \le j \le N_p N_h + 2N_b - 1 \\ \\ \dfrac{\partial J_{t(F,B)}^{(j)}}{\partial \xi} = \dfrac{J_{t(F,B)}^{(j+1)} - J_{t(F,B)}^{(j-1)}}{2l_b^{(2)}} \end{array}\right\} \qquad (178)$$

The φ - derivatives are calculated as follows

$$\left.\begin{aligned} & N_p N_h + 1 \le j \le N_p N_h + N_b \\ & \frac{\partial J_{sF}(j)}{\partial \varphi} = \frac{J_{sF}(j+N_b) - J_{sF}(j)}{\pi/2} \\ & \frac{\partial J_{sB}(j)}{\partial \varphi} = \frac{J_{sB}(j) - J_{sB}(j+N_b)}{\pi/2} \end{aligned}\right\} \qquad (179)$$

$$\left.\begin{aligned} & N_p N_h + N_b + 1 \le j \le N_p N_h + 2N_b \\ & \frac{\partial J_{sF}(j)}{\partial \varphi} = \frac{J_{sB}(j) - J_{sF}(j-N_b)}{\pi} \\ & \frac{\partial J_{sB}(j)}{\partial \varphi} = \frac{J_{sB}(j-N_b) - J_{sF}(j)}{\pi} \end{aligned}\right\} \qquad (180)$$

APPENDIX A

In this Appendix we present the numbering scheme of zones (into which we divide the structure under consideration) and subzones (into which we divide each zone), and the necessary calculations to determine the dimensions, areas and coordinates of zones and subzones. Because of the symmetry considerations presented in Section II, we will only consider zones on surfaces corresponding to $z > 0$ (fig. 1).

The main requirement that must be satisfied in determining the size of a zone is that both components of the surface current density should be approximately constant over the zone. The zone size on the structure must satisfy both a geometry requirement and a wavelength requirement. The wavelength requirement depends somewhat on the accuracy desired and is accordingly 8 to 10 zones per wavelength. For the class of structures considered, geometry limited zoning is sufficiently dense so as to allow the calculation of all qualities for wavelengths that exhibit the major resonances of the structure as well as encompassing a significant portion of the EMP spectrum. We accomplish this without decreasing the wavelength beyond a value that would cause any geometry limited zone to be larger than a tenth of a wavelength. Specifically, the geometry zoning restrictions are that either dimension of a zone on the circular cylinder should be approximately equal to, or less than, the diameter of the cylinder and similarly, either dimension of a zone on the elliptic cylinder should be approximately equal to, or less than, the minor axis of the ellipse.

A separate consideration from the choice of the zone size is the choice of the number of subzones. This number is determined by the requirement that self and adjacent matrix elements are calculated accurately. It is actually the calculation of the adjacent matrix elements that imposes the most stringent requirement. This is the case because an analytical procedure, described in Appendix B, is used to calculate the self matrix elements and this procedure is insensitive to the subzoning.

By performing zoning and subzoning numerical experiments on a circular cylinder, we found that 9 subzones give sufficient accuracy. These experiments also eased our concern over the questionable approximation that the surface current densities were constant over zones adjacent to the edge formed by the end caps of the cylinder. We know that a component of the surface current density has an integrable singularity at the edge; however, our results were in good agreement with those presented by Sassman (ref. 2) for the total axial current even near the edge.

1. Numbering of Zones and Subzones

1.1 Pylon

As we mentioned earlier, geometrical considerations relevant to the zoning of the pylon surface require that the linear dimensions of a zone should be no larger than the minor axis $2b_p$ of the pylon elliptical cross section. Bearing this in mind, the longitudinal number of zones N_p (corresponding to half the circumference S_p of the elliptic cross section, and chosen as an even number for convenience) is

$$N_p = 2\left\{\left[\frac{S_p}{8b_p}\right]^* + 1\right\} \qquad (A\text{-}1)$$

where $[x]^*$ is the largest integer smaller than x. (If x integer, $[x]^* = x-1$.)

Similarly the number of zones N_h along the height of the pylon h_p is

$$N_h = \left[\frac{h_p}{2b_p}\right]^* + 1 \qquad (A\text{-}2)$$

To describe the location of a zone we will use one subscript, say i, i.e. i runs from 1 to N_pN_h (fig. 10). Each subzone can be characterized by two subscripts; one for the mother zone and the other for the subzone within the zone, i.e. i,k where i runs from 1 to N_pN_h and k from 0 to 8 (the zeroth subzone is the central one, fig. 10). However, a subzone can also be characterized by a single subscript, say $\alpha\,(1, 2, 3, \cdots, 9N_pN_h)$ and

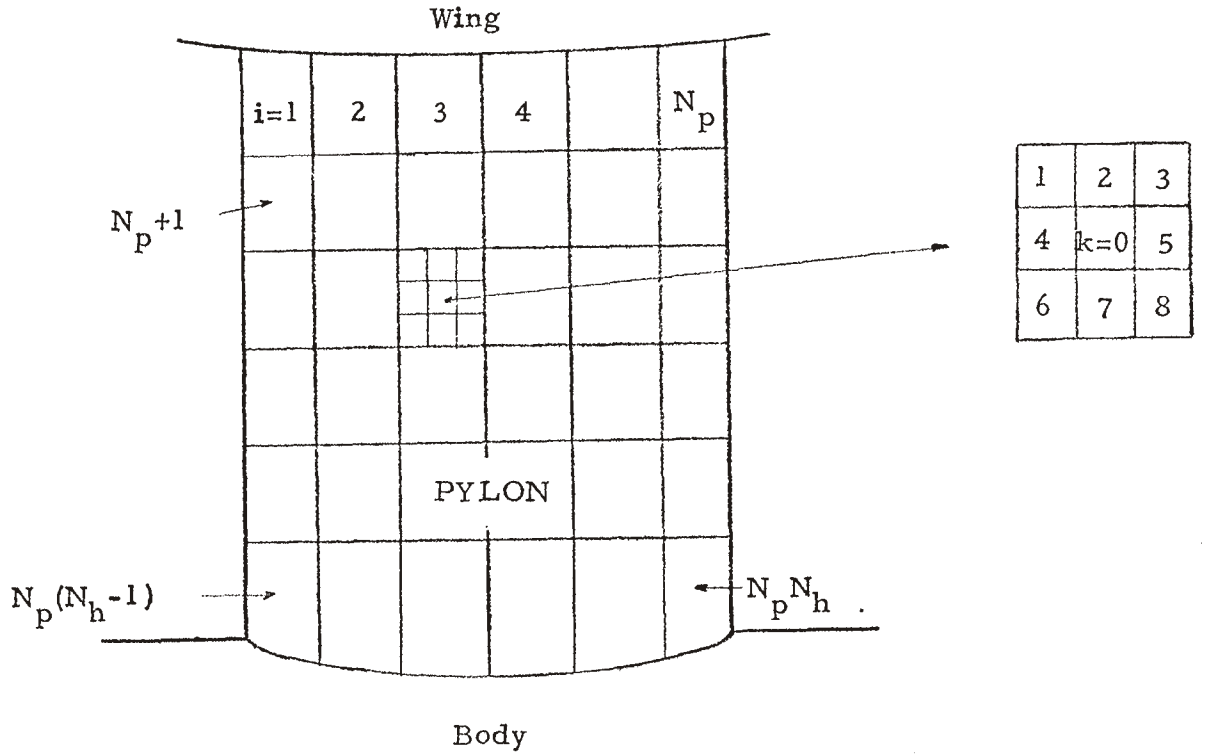

Figure 10: Numbering of zones on pylon.

the relationship between α and i,k is

$$\alpha(i,k=0) = 3N_p\left(2\left[\frac{i-1}{N_p}\right]^* + 1\right) + 3i - 1$$

$$\alpha(i,k=1) = \alpha(i,k=0) - 3N_p - 1$$

$$\alpha(i,k=2) = \alpha(i,k=0) - 3N_p$$

$$\alpha(i,k=3) = \alpha(i,k=0) - 3N_p + 1$$

$$\alpha(i,k=4) = \alpha(i,k=0) - 1$$

$$\alpha(i,k=5) = \alpha(i,k=0) + 1$$

$$\alpha(i,k=6) = \alpha(i,k=0) + 3N_p - 1$$

$$\alpha(i,k=7) = \alpha(i,k=0) + 3N_p$$

$$\alpha(i,k=8) = \alpha(i,k=0) + 3N_p + 1$$

As an example we choose $i = 50$, $N_p = 12$, $N_h > 5$ and the nine subzones are characterized by $\alpha = 436, 437, 438, 472, 473, 474, 508, 509, 510$ (fig.11).

1.2 Body (Cylindrical Surface)

Due to the asymmetry of the body with respect to the x-axis the number of longitudinal zones is different in the two sections, $x > 0$ and $x < 0$. Referring to figure 1 we have

$$N_b^{(1)} = \left[\frac{L_1}{2a_b}\right]^* + 1, \qquad x > 0 \tag{A-4}$$

$$N_b^{(2)} = \left[\frac{L_2}{2a_b}\right]^* + 1, \qquad x < 0 \tag{A-5}$$

Around the body we choose two zones ($z > 0$), each of length $(\pi/2)a_b$. Thus the total number of zones on (half) the cylindrical surface of the body is

$$2N_b = 2[N_b^{(1)} + N_b^{(2)}] \tag{A-6}$$

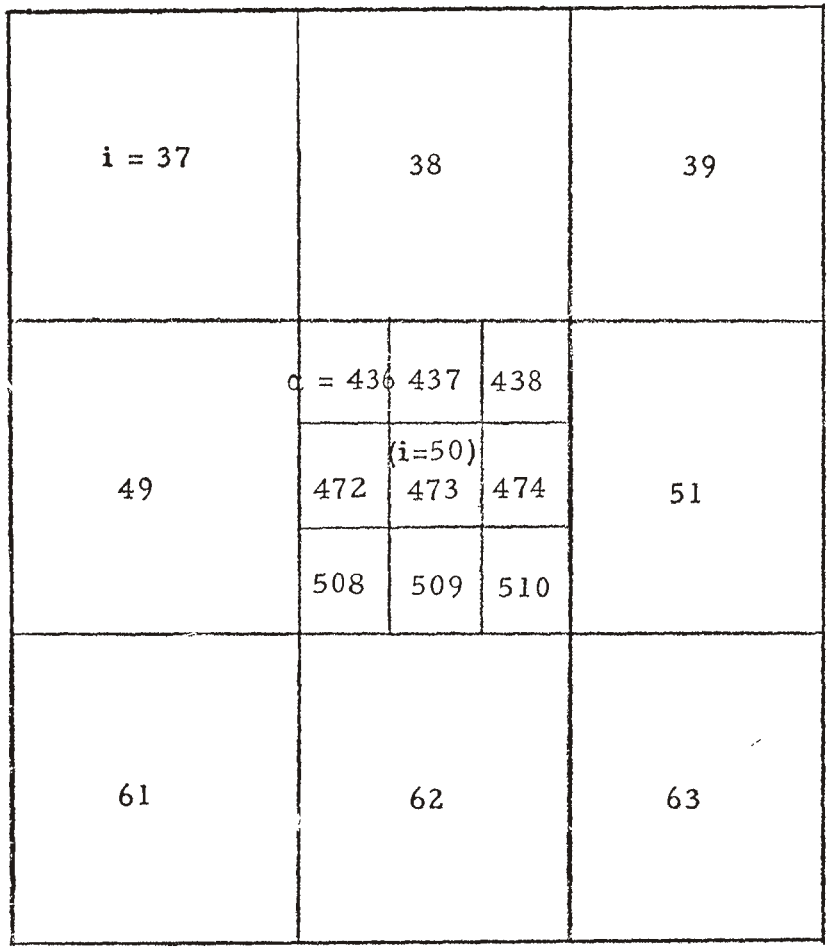

Figure 11: Numbering of subzones on pylon. Numbers correspond to $N_p = 12$ and $N_h > 5$.)

The numbering scheme of zones and subzones is similar to that on the pylon. A zone will be characterized by a subscript i ($N_pN_h+1, \cdots N_pN_h+2N_b$) and a subzone by two subscripts i,k (k = 0, 1, $\cdots$, 8) or by one subscript $\alpha^\dagger$ such that

$$\alpha^\dagger(i,k=0) = 3N_b\left\{2\left[\frac{i-N_pN_h-1}{N_b}\right]^* + 1\right\} + 3(i-N_pN_h) - 1 \qquad \text{(A-7)}$$

The relationship of $\alpha^\dagger(i,k)$ to $\alpha^\dagger(i,k=0)$ is the same as on the pylon (A-3) provided we replace N_p by N_b. Notice that the first subzone on the body corresponds to $\alpha^\dagger = 1$ whereas the first zone corresponds to $N_pN_h + 1$.

1.3 Body (End Caps)

Each cap is divided into two zones (z > 0) each of arc length $(\pi/2)a_b$. These four zones correspond to (fig.12)

$$\left.\begin{aligned} i &= N_{pb}+1 && x = L_1, && \theta < \pi/2 \\ &= N_{pb}+2 && x = L_1, && \theta > \pi/2 \\ &= N_{pb}+3 && x = -L_2, && \theta < \pi/2 \\ &= N_{pb}+4 && x = -L_2, && \theta > \pi/2 \end{aligned}\right\} \qquad \text{(A-8)}$$

where

$$N_{pb} = N_pN_h + 2N_b \qquad \text{(A-9)}$$

Each subzone will be divided into nine subzones characterized by two subscripts i,k (k = 0, 1, $\cdots$, 8). The arrangement of the subzones is shown in figure 13a.

2. Coordinates and Areas of Zones and Subzones Not Adjacent to Surface Intersections

2.1 Areas and Coordinates of Subzones

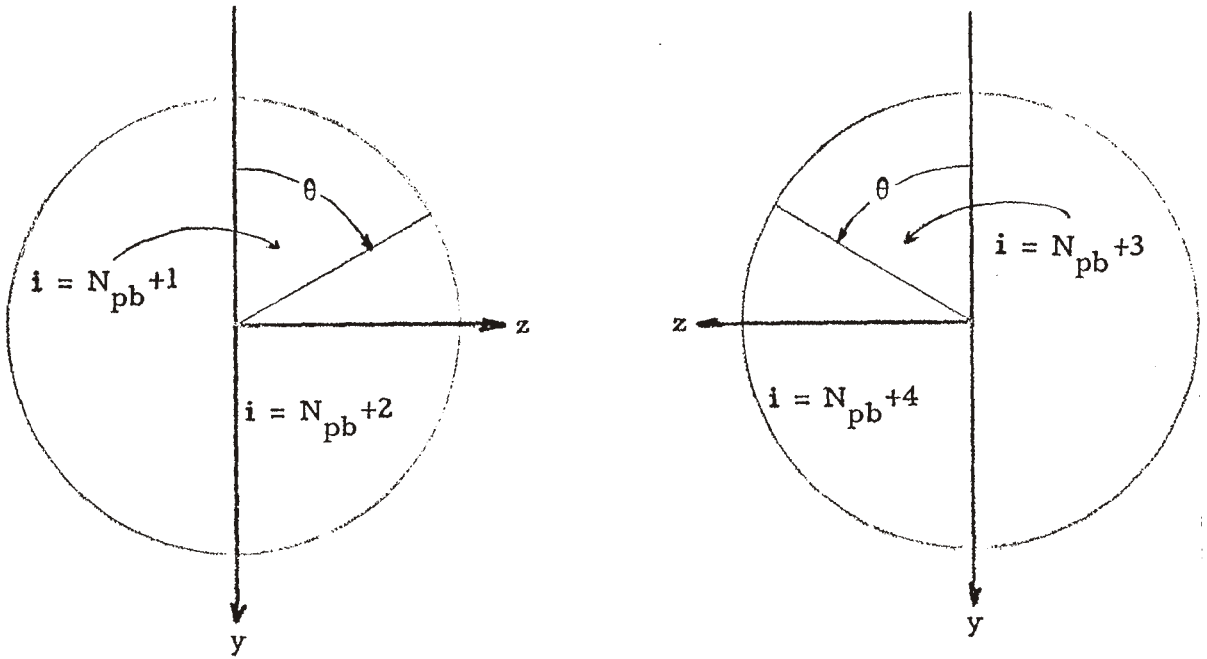

Figure 12: Numbering of zones on end caps.

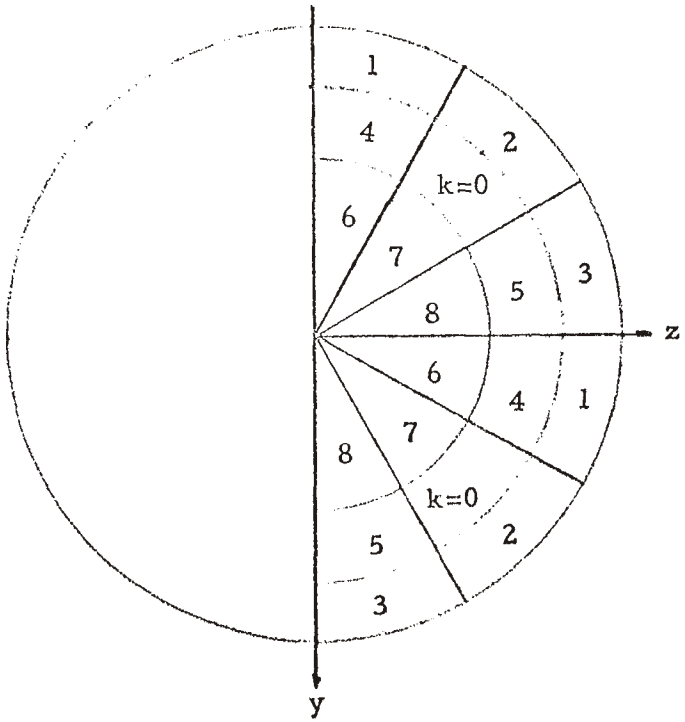

Figure 13a: Numbering of subzones on end caps.

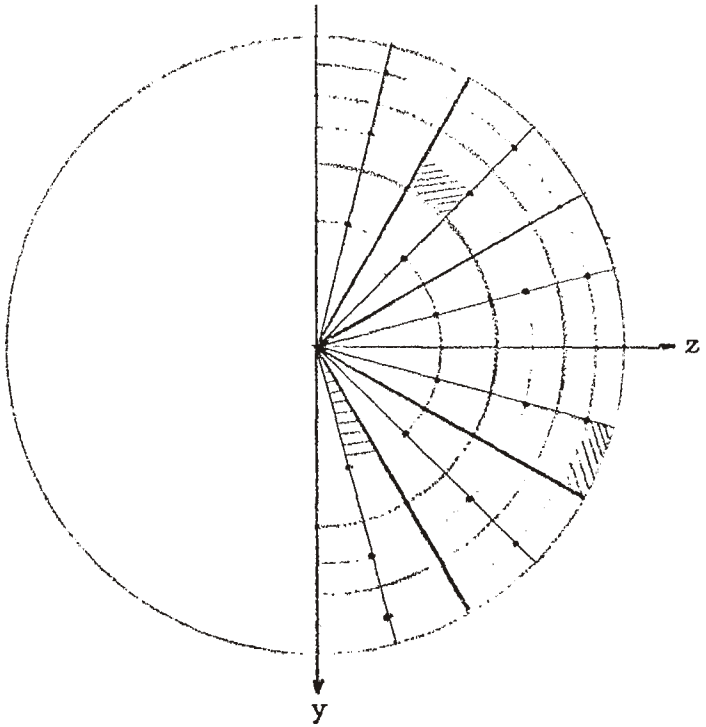

Figure 13b: Determination of centers of subzones on end caps. All subareas are equal (three of them are shown shaded).

2.1.1 Pylon

To determine the areas and coordinates at the center of a given subzone on the pylon we first define the linear dimensions of a zone. If we recall (A-1) and (A-2) we can write

$$\left.\begin{aligned} \ell_p &= \frac{S_p/2}{N_p} \\ \ell_h &= \frac{h_p}{N_h} \end{aligned}\right\} \qquad \text{(A-10)}$$

Consequently the linear dimensions of a subzone are $(1/3)\ell_p$, $(1/3)\ell_h$ and the corresponding area equal to $(1/9)\ell_p\ell_h$. The coordinates of the pylon subzones are given by

$$\left.\begin{aligned} &\alpha = 3N_p + 1, \cdots, 3N_p(3N_h - 1) \\ x_\alpha &= a_p \cos u \\ z_\alpha &= b_p \cos u \\ y_\alpha &= b_w + \frac{\ell_h}{6}\left\{2\left[\frac{\alpha-1}{3N_p}\right]^* + 1\right\} \end{aligned}\right\} \qquad \text{(A-11)}$$

where u is determined by

$$\frac{\ell_p}{6}\left\{2\left\{\alpha - \left[\frac{\alpha-1}{3N_p}\right]^* 3N_p\right\} - 1\right\} = \int_o^u (a_p^2 \sin^2 u + b_p^2 \cos^2 u)^{\frac{1}{2}}\, du \qquad \text{(A-12)}$$

Equations (A-11) and (A-12) can easily be understood with the aid of figures 14 and 15.

2.1.2 Body (Cylindrical Surface)

The longitudinal length of the body zones can be defined with the aid of (A-4) and (A-5)

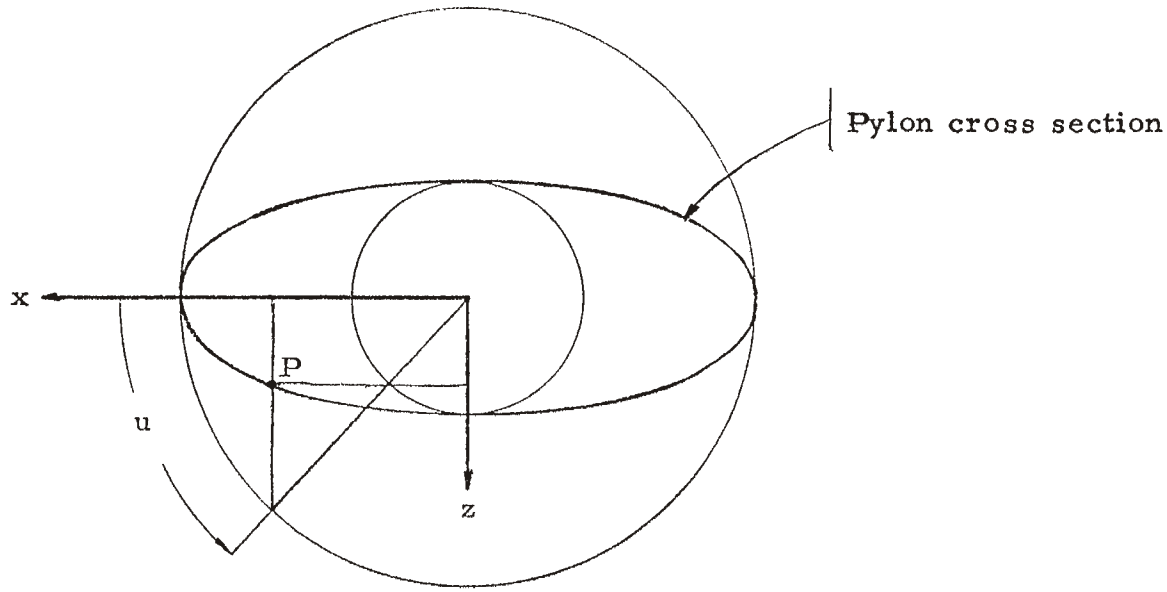

Figure 14: Cross section of pylon. Point P is the center of the αth subzone characterized by an azimuthal angle u.

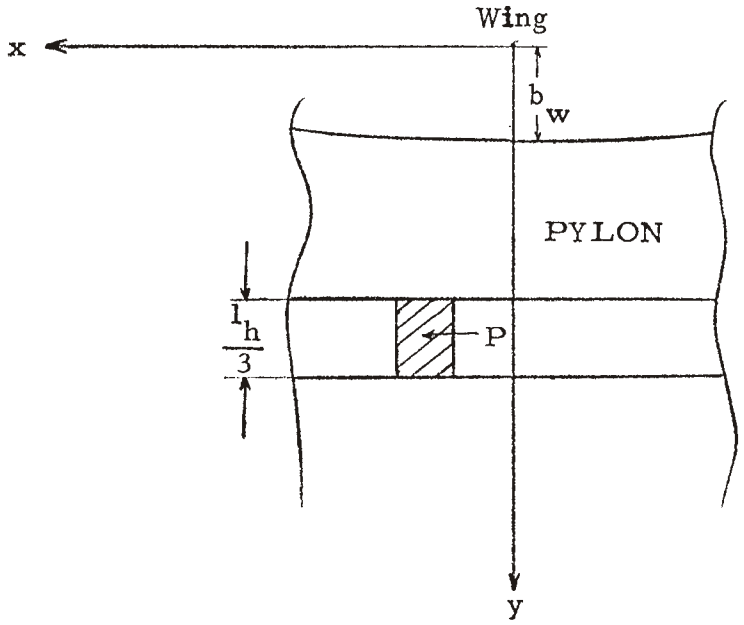

Figure 15: Calculation of the y coordinate of the center P of a pylon subzone not adjacent to surface intersections.

$$\left.\begin{aligned} \ell_b^{(1)} &= \frac{L_1}{N_b^{(1)}}, \quad x > 0 \\ \ell_b^{(2)} &= \frac{L_2}{N_b^{(2)}}, \quad x < 0 \end{aligned}\right\} \tag{A-13}$$

whereas the arc length of each zone is $(\pi/2)a_b$. Thus the corresponding lengths of a body subzone are $1/3\,\ell_b^{(1)}$ $(x > 0)$, $1/3\,\ell_b^{(2)}$ $(x < 0)$, $(\pi/6)a_b$ and the areas equal to $(\pi/18)\ell_b^{(1)}a_b$ $(x > 0)$ and $(\pi/18)\ell_b^{(2)}a_b$ $(x < 0)$. The coordinates at the center of a subzone for

$$\alpha^\dagger < A_1 \equiv \left[\frac{L_1 - a_p}{\ell_b^{(1)}/3}\right]^* + 1, \quad \alpha^\dagger > A_2 \equiv 3N_b^{(1)} + \left[\frac{a_p}{\ell_b^{(2)}/3}\right]^* + 1$$

are

$$x_{\alpha^\dagger} = L_1 - \left\{a^\dagger - \left[\frac{\alpha^\dagger - 1}{3N_b}\right] 3N_b\right\} \frac{\ell_b^{(1)}}{3} + \frac{\ell_b^{(1)}}{6}, \quad \alpha^\dagger - \left[\frac{a^\dagger}{3N_b}\right] 3N_b \le 3N_b^{(1)} \tag{A-14}$$

$$x_{\alpha^\dagger} = -\left\{\alpha^\dagger - \left[\frac{\alpha^\dagger - 1}{3N_b}\right] 3N_b - 3N_b^{(1)}\right\} \frac{\ell_b^{(2)}}{3} + \frac{\ell_b^{(2)}}{6}, \quad \alpha^\dagger - \left[\frac{\alpha^\dagger}{3N_b}\right] > 3N_b^{(1)}$$

$$\left.\begin{aligned} y_{\alpha^\dagger} &= b_w + h_p + a_b(1 - \cos \varphi_{\alpha^\dagger}) \\ z_{\alpha^\dagger} &= a_b \sin \varphi_{\alpha^\dagger} \end{aligned}\right\} \tag{A-15}$$

$$\varphi_{\alpha^\dagger} = \left\{2\left[\frac{\alpha^\dagger - 1}{3N_b}\right] + 1\right\} \frac{\pi}{12} \tag{A-16}$$

Equations (A-15) and (A-16) can easily be understood with the aid of figures 16 and 17.

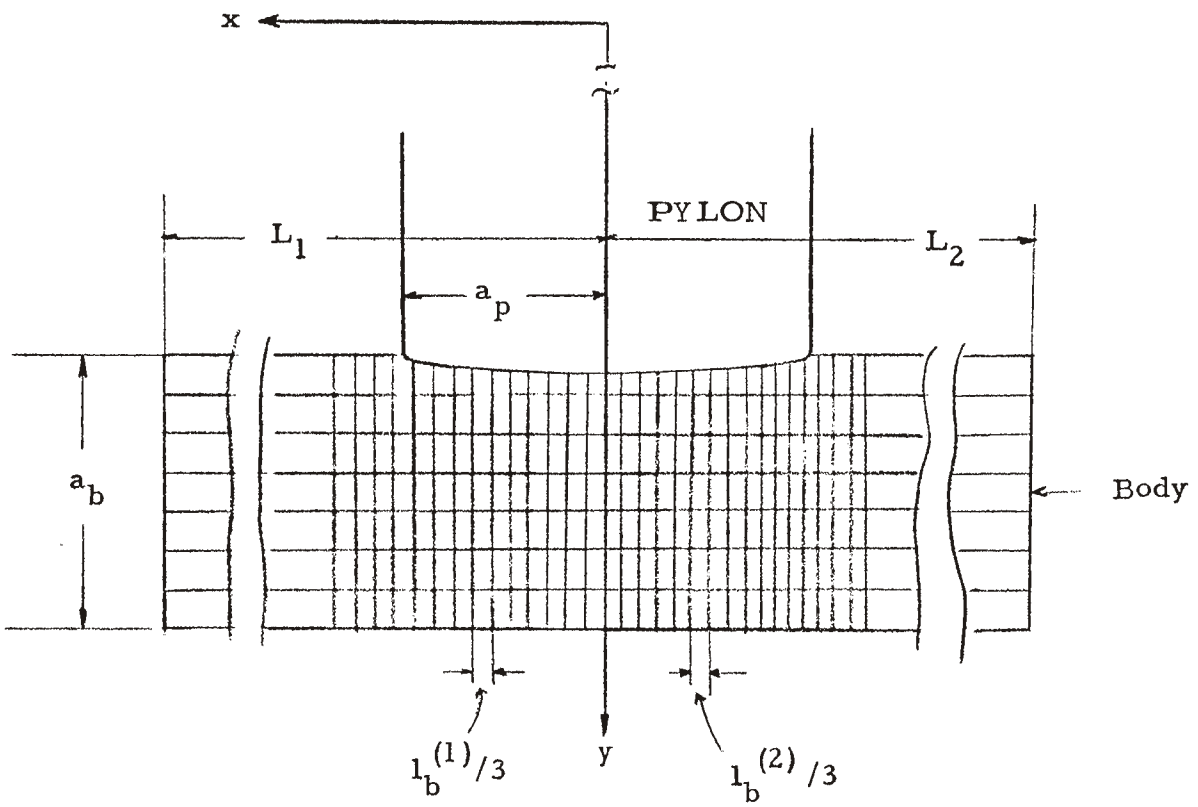

Figure 16: Geometry for the calculation the x coordinate of body subzones.

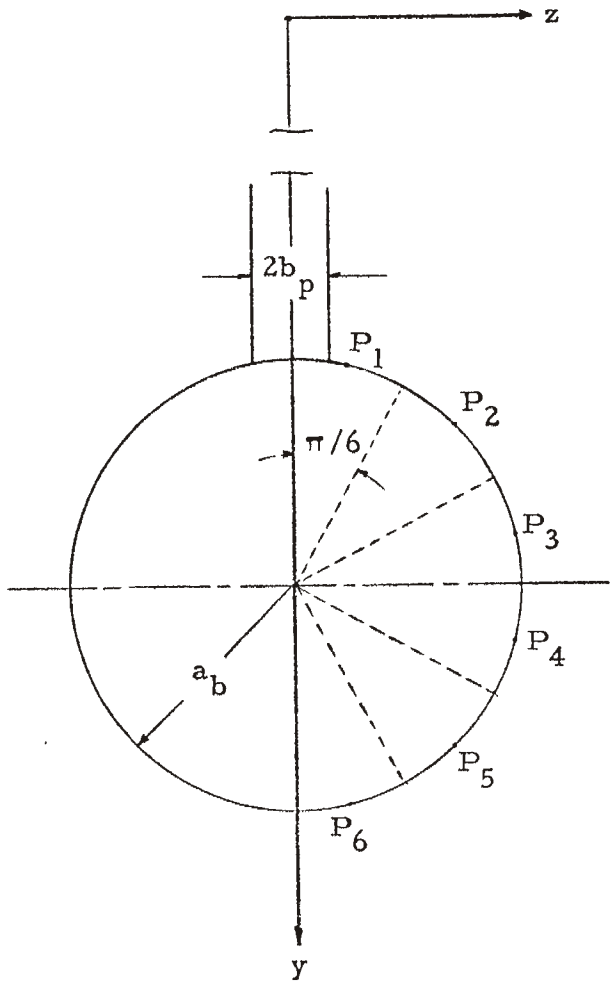

Figure 17: Geometry for the calculation of the y and z coordinates of the centers P_s (s = 1, 2, ..., 6) of body subzones not adjacent to the body-pylon intersection. (Scales of figures 16 and 17 are not the same).

2.1.3 Body (End Caps)

Each zone is divided into nine subzones of equal area ($=(\pi/36)a_b^2$) and the center of a subzone is defined as the common point of four segments of equal area as illustrated in figure 13b. The following results are obtained

$$\left.\begin{aligned} i &= N_{pb} + 1 \\ x &= L_1 \\ y &= b_w + h_p + a_b \left\{1 - \sqrt{\frac{5}{6}} \cos\left[\frac{\pi}{12}(2k-1)\right]\right\} \\ z &= \sqrt{\frac{5}{6}}\, a_b \sin\left[\frac{\pi}{12}(2k-1)\right] \end{aligned}\right\} \quad k = 1, 2, 3 \qquad \text{(A-17)}$$

$$\left.\begin{aligned} x &= L_1 \\ y &= b_w + h_p + a_b \left\{1 - \frac{1}{\sqrt{2}} \cos\left[\frac{\pi}{12}(2k-7)\right]\right\} \\ z &= \frac{a_b}{\sqrt{2}} \sin\left[\frac{\pi}{12}(2k-7)\right] \end{aligned}\right\} \quad k = 4, 5 \qquad \text{(A-18)}$$

$$\left.\begin{aligned} x &= L_1 \\ y &= b_w + h_p + a_b \left\{1 - \frac{1}{\sqrt{6}} \cos\left[\frac{\pi}{12}(2k-9)\right]\right\} \\ z &= \frac{a_b}{\sqrt{6}} \sin\left[\frac{\pi}{12}(2k-9)\right] \end{aligned}\right\} \quad k = 6, 7, 8 \qquad \text{(A-19)}$$

$$\left.\begin{aligned} x &= L_1 \\ y &= b_w + h_p + \frac{1}{2} a_b \\ z &= \frac{1}{2} a_b \end{aligned}\right\} \quad k = o \qquad \text{(A-20)}$$

$$i = N_{pb} + 2$$

The coordinates are the same as for $i = N_{pb} + 2$ except that the terms in the angular bracket for the y-coordinate add rather than subtract. For $k = 0$, $y = b_w + h_p + (3/2)\, a_b$.

$$i = N_{pb} + 3$$

The coordinates are the same as for $i = N_{pb} + 1$ except that $x = -L_2$.

$$i = N_{pb} + 4$$

The coordinates are the same as for $i = N_{pb} + 2$ except that $x = -L_2$.

2.2 Areas and Coordinates of Zones

2.2.1 Pylon

In view of (A-10) the area of a pylon zone is $\ell_p \ell_h$, whereas the coordinates at the center of the zone are the same as the coordinates at the center of the central subzone of the zone. They are given by (A-11) where α is equal to $\alpha(i, k = 0)$ and related to i according to (A-3).

2.2.2 Body (Cylindrical Surface)

The area of a body zone is equal to $(\pi/2)a_b \ell_b^{(1)}$ for $x > 0$ and $(\pi/2)a_b \ell_b^{(1)}$ for $x < 0$, whereas the coordinates at the center of the zone are given by (A-15) with $\alpha^\dagger$ equal to $\alpha^\dagger(i, k = 0)$ and related to i according to (A-7).

2.2.3 Body (End Caps)

The area of a zone is $(\pi/4)a_b^2$ and the coordinates at the center of the zone are given by

$$\left.\begin{aligned} x &= L_1 \\ y &= b_w + h_p + \tfrac{1}{2}a_b \\ z &= \tfrac{1}{2}a_b \end{aligned}\right\} \qquad i = N_p N_h + 1 \tag{A-21}$$

$$\left.\begin{aligned} x &= L_1 \\ y &= b_w + h_p + 3/2a_b \\ z &= \tfrac{1}{2}a_b \end{aligned}\right\} \qquad i = N_p N_h + 2 \tag{A-22}$$

$$\left.\begin{aligned} x &= -L_2 \\ y &= b_w + h_p + \tfrac{1}{2}a_b \\ z &= \tfrac{1}{2}a_b \end{aligned}\right\} \qquad i = N_p N_h + 3 \tag{A-23}$$

$$\left.\begin{aligned} x &= -L_2 \\ y &= b_w + h_p + 3/2a_b \\ z &= \tfrac{1}{2}a_b \end{aligned}\right\} \qquad i = N_p N_h + 4 \tag{A-24}$$

3. Coordinates and Areas of Zones and Subzones Adjacent to Surface Intersections

3.1 Coordinates and Areas of Subzones

3.1.1 Pylon

3.1.1.1 Wing-Pylon Intersection

The coordinates of the subzones adjacent to the wing-pylon intersection, i.e.

$$\alpha = 1, \cdots, 3N_p$$

are given by

$$\begin{aligned} x_\alpha &= a_p \cos u \\ z_\alpha &= b_p \sin u \\ y_\alpha &= \tfrac{1}{2}\left\{\frac{\ell_h}{3} + b_w\left[1 + \left(1 - \frac{x_\alpha^2}{a_w^2}\right)^{\frac{1}{2}}\right]\right\} \end{aligned} \tag{A-25}$$

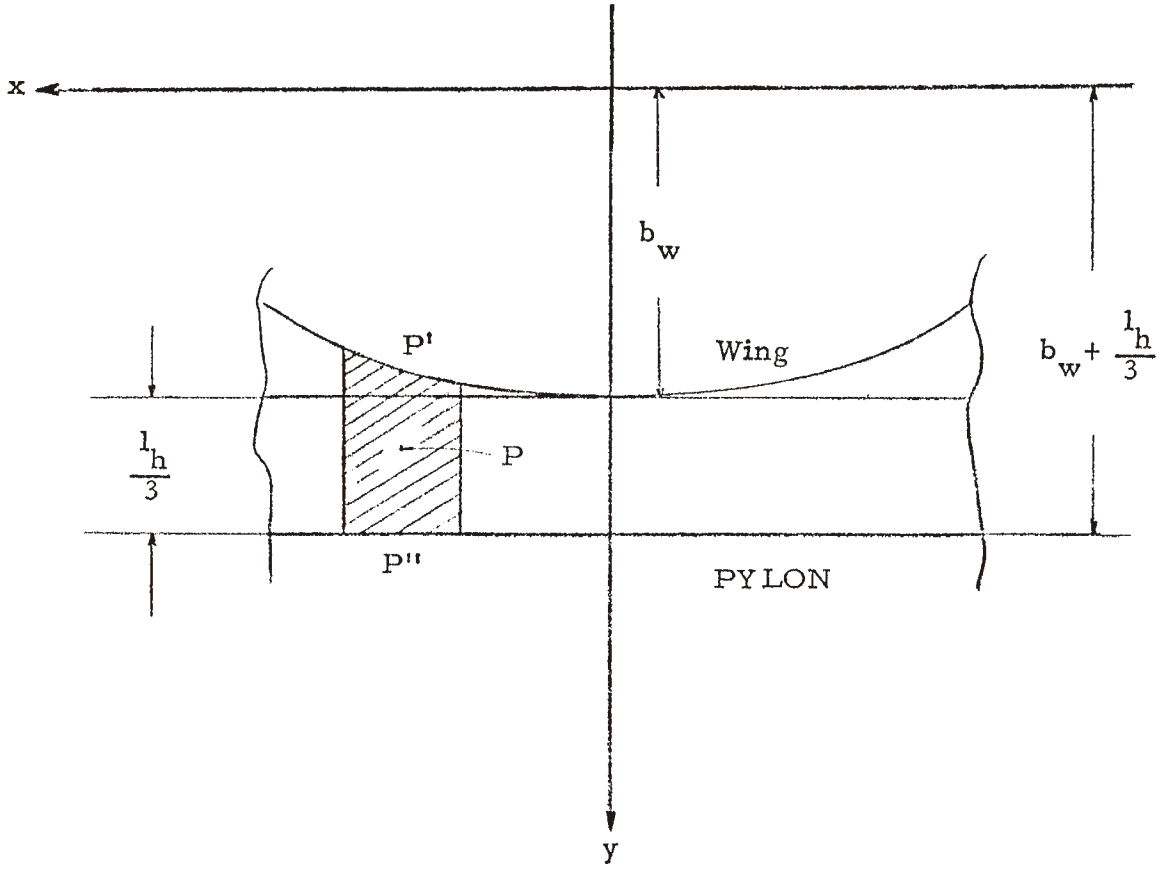

Figure 18: Calculation of the y coordinate of the center P of a pylon subzone adjacent to the wing-pylon intersection.

where u is determined by

$$\frac{\ell_p}{6}(2\alpha - 1) = \int_0^u (a_p^2 \sin^2 u + b_p^2 \cos u)^{\frac{1}{2}}\, du \qquad \text{(A-26)}$$

To understand the above relationships we refer to figures 14 and 18. The x and z coordinates at the center P of the subzone can be obtained with the aid of figure 14, whereas from figure 18 we see that

$$y_\alpha = y_P = \tfrac{1}{2}(y_{P'} + y_{P''}) = \tfrac{1}{2}\left[b_w\left(1 - \frac{x_\alpha^2}{a_w^2}\right)^{\frac{1}{2}} + b_w + \frac{\ell_h}{3}\right]$$

To calculate the areas of the above subzones we first recall that N_p is an even integer and consequently there are $(3/2)N_p$ subzones for $x > 0$ and also $(3/2)N_p$ for $x < 0$. It is easy to see (fig. 10) that subzones positioned symmetrically about the $x = 0$ plane have equal areas. If a subzone ($x > 0$) is characterized by an index α the symmetric subzone will correspond to an index β such that

$$\beta = 3N_p/2 + 1, \cdots 3N_p \qquad \alpha = 3N_p - \beta + 1 \qquad (\alpha = 1, \ldots, 3N_p/2) \qquad \text{(A-27)}$$

Thus it suffices to only calculate areas for

$$\alpha = 1, \cdots, 3N_p/2$$

$$(\Delta S)_\alpha = \frac{1}{9}\ell_p\ell_h + \int_{x_{\alpha+1}^*}^{x_\alpha^*} (b_w - y)\left[\frac{a_p^4 + x^2(b_p^2 - a_p^2)}{a_p^2(a_p^2 - x^2)}\right]^{\frac{1}{2}} dx \qquad \text{(A-28)}$$

where

$$y = b_w\left(1 - \frac{x^2}{a_w^2}\right)^{\frac{1}{2}} \qquad \text{(A-29)}$$

$$x_\gamma^* = a_p \cos u_\gamma \quad (\gamma = \alpha, \alpha + 1)$$

and u_γ is determined by

$$\frac{\ell_p}{3}(\gamma - 1) = \int_o^{u_\gamma} (a_p^2 \sin^2 u + b_p^2 \cos^2 u)^{\frac{1}{2}}\, du \qquad \text{(A-30)}$$

To derive (A-28) we refer to figures 19 and 20. From figure 20 the shaded area is

$$dS = (b_w - y)ds \qquad \text{(A-31)}$$

and

$$\left.\begin{aligned} ds &= \left[(dx^2) + (dz)^2\right]^{\frac{1}{2}} = dx\left[1 + (dz/dx)^2\right]^{\frac{1}{2}} \\ \frac{dz}{dx} &= -\frac{x}{z}\frac{b_p^2}{a_p^2} = -\frac{x}{b_p(1 - x^2/a_p^2)^{\frac{1}{2}}}\frac{b_p^2}{a_p^2} \end{aligned}\right\} \qquad \text{(A-32)}$$

With the aid of (A-31) and (A-32) we can easily arrive at (A-28).

From the numerical accuracy point of view (A-28) is not suitable for numerical integration when $x_\alpha^* = a_p$ even though the resulting singularity is integrable. To secure sufficient accuracy we can rewrite (A-28) as

$$(DS)_\alpha = \frac{1}{9}\ell_p\ell_h + b_w \int_{x_\alpha^* + 1}^{x_\alpha^*} \left\{\left[1 - \left(1 - \frac{x^2}{a_w^2}\right)^{\frac{1}{2}}\right]\left[\frac{a_p^4 + x^2(b_p^2 - a_p^2)}{a_p^2(a_p^2 - x^2)}\right] - K(a_p - x)^{\frac{1}{2}}\right\} dx$$

$$+ 2b_w K\left[(a_p - x_\alpha^* + 1)^{\frac{1}{2}} - (a_p - x_\alpha^*)^{\frac{1}{2}}\right] \qquad \text{(A-33)}$$

where

$$K = \frac{b_p}{\sqrt{2a_p}}\left[1 - \left(1 - \frac{a_p^2}{a_w^2}\right)^{\frac{1}{2}}\right] \qquad (a_p < a_w) \qquad \text{(A-34)}$$

The integrand in (A-33) is zero at $x = a_p$ and can be evaluated numerically with sufficient accuracy.

3.1.1.2 Pylon-Body Intersection

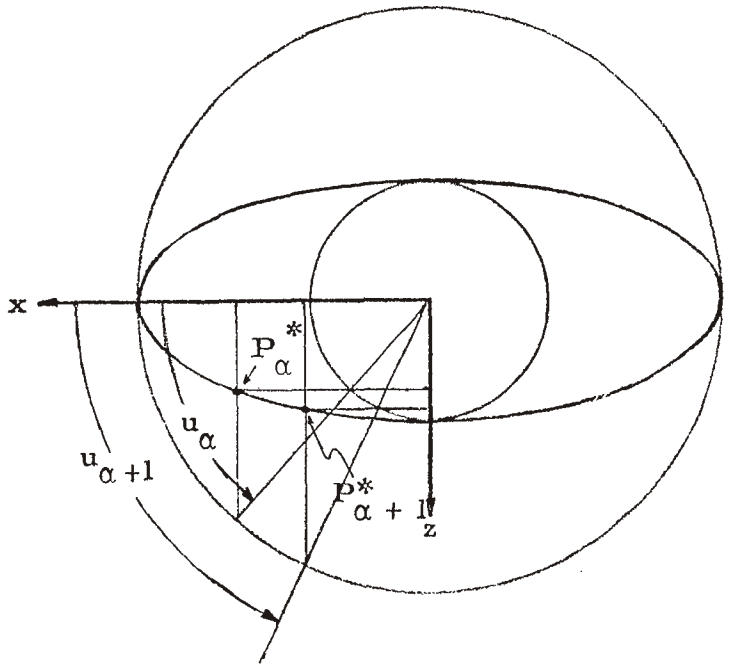

Figure 19: Cross section of pylon. P^*_α and $P^*_{\alpha+1}$ are the end points of the α th subzone.

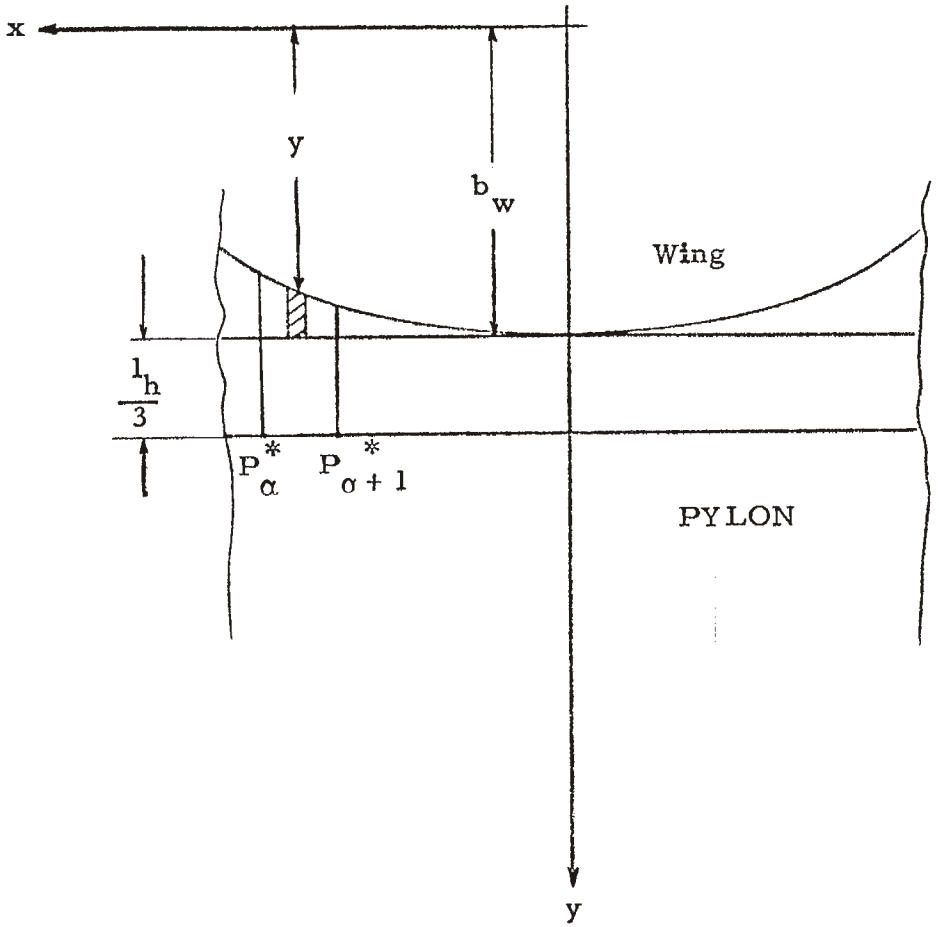

Figure 20: Calculation of the area of a pylon subzone adjacent to the wing-pylon intersection

The coordinates of the subzones adjacent to the pylon-body intersection i.e.

$$\alpha = 3N_p(3N_h - 1) + 1, \cdots, 9N_pN_h$$

are given by

$$\left.\begin{aligned} x_\alpha &= a_p \cos u \\ z_\alpha &= b_p \sin u \\ y_\alpha &= b_w + h_p - \frac{\ell_h}{6} + \frac{1}{2} a_b \left[1 - \left(1 - \frac{z_\alpha^2}{a_b^2}\right)^{\frac{1}{2}}\right] \end{aligned}\right\} \qquad \text{(A-35)}$$

and u is determined by

$$\frac{\ell_p}{6}\left\{2\left\{\alpha - (3N_h - 1)3N_p\right\} - 1\right\} = \int_o^u (a_p^2 \sin^2 u + b_p^2 \cos^2 u)^{\frac{1}{2}}\, du \qquad \text{(A-36)}$$

The x and z coordinates can be calculated with the aid of figure 14 whereas from figure 21 we see that

$$\begin{aligned} y_\alpha &= y_P = y_{P'} + \tfrac{1}{2}(P'P'') \\ &= b_w + h_p - \frac{\ell_h}{3} + \frac{1}{2}\left\{\frac{\ell_h}{3} + a_b\left[1 - \left(1 - \frac{z_\alpha^2}{a_b^2}\right)\right]^{\frac{1}{2}}\right\} \end{aligned}$$

Notice that P'' lies on the body and it has the same z coordinate as the center P of the pylon subzone.

To calculate the areas of the subzones we first recall that N_p is an even integer and consequently there are $(3/2)N_p$ subzones for $x > 0$ and also $(3/2)N_p$ for $x < 0$. Because of symmetry about the $x = 0$ plane, if a subzone ($x > 0$) is characterized by an index α the symmetric subzone will correspond to an index β such that

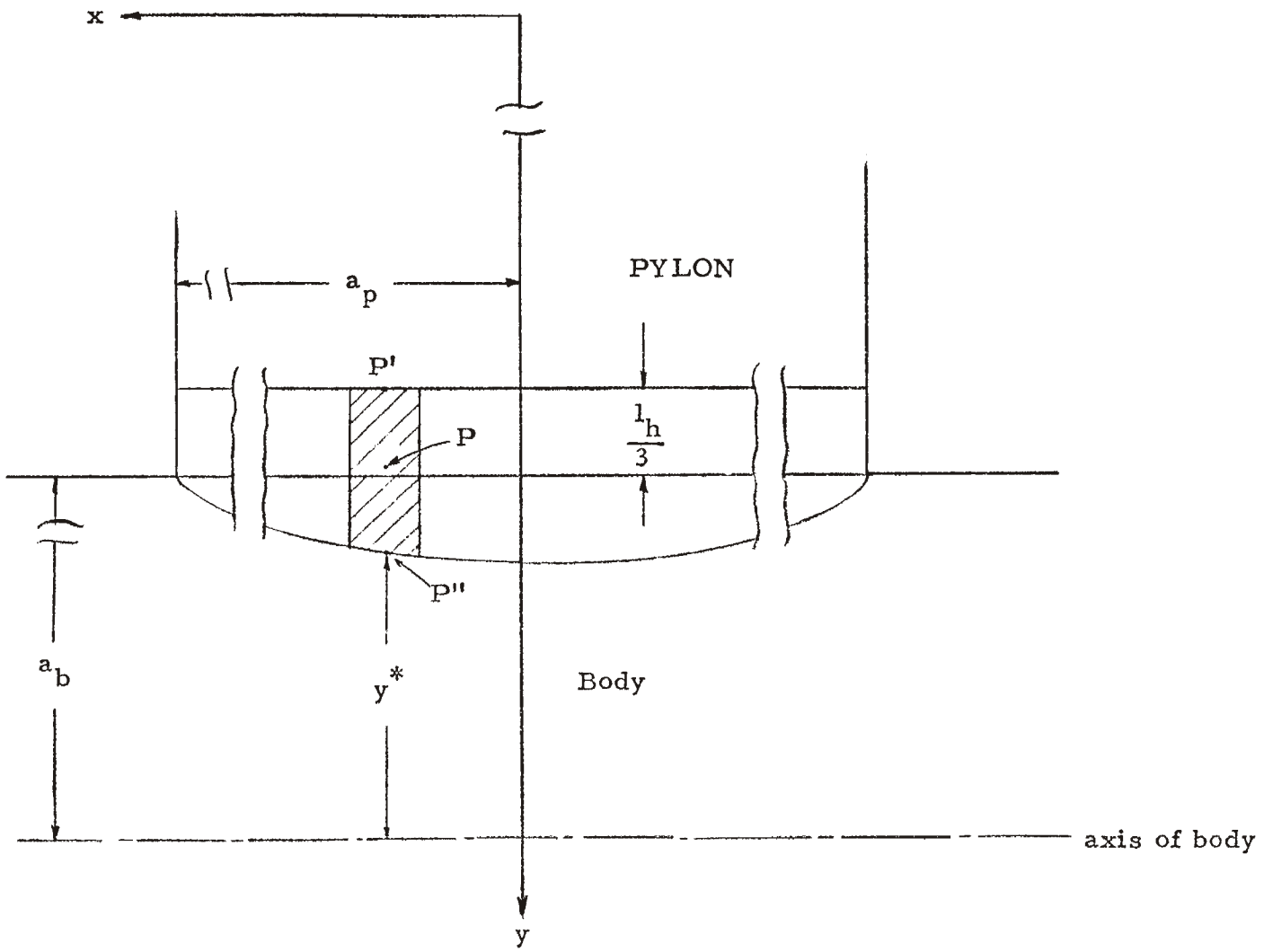

Figure 21: Calculation of the y coordinate at the center P of a pylon subzone adjacent to the pylon-body intersection

$$\beta = (3N_h - 1)3N_p + \frac{3N_p}{2} + 1, \cdots, 3N_h N_p$$

$$\alpha = 2(3N_h - 1)3N_p + 3N_p - \beta + 1$$

$$\left(\alpha = (3N_h - 1)3N_p + 1, \cdots, (3N_h - 1)3N_p + \frac{3N_p}{2}\right)$$

Thus it suffices to only calculate areas for:

$$\alpha = (3N_h - 1)3N_p + 1, \cdots, (3N_h - 1)3N_p + (3N_p/2).$$

$$(\Delta S)_\alpha = \frac{1}{9}\ell_p \ell_h + \int_{z_\alpha^*}^{z_{\alpha+1}^*} (a_b - y^*)\left[\frac{b_p^4 + z^2(a_p^2 - b_p^2)}{b_p^2(b_p^2 - z^2)}\right]^{\frac{1}{2}} dz \qquad \text{(A-37)}$$

where

$$\left.\begin{aligned} y^* &= a_b\left(1 - \frac{z^2}{a_b^2}\right)^{\frac{1}{2}} \\ z_\gamma^* &= b_p \sin u_\gamma \qquad (\gamma = \alpha, \alpha + 1) \end{aligned}\right\} \qquad \text{(A-38)}$$

and u_γ is determined by

$$[\gamma - (3N_h - 1)3N_p - 1]\frac{\ell_p}{3} = \int_0^{u_\gamma} (a_p^2 \sin^2 u + b_p^2 \cos^2 u)^{\frac{1}{2}}\, du \qquad \text{(A-39)}$$

Equation (A-37) can be derived with the aid of figures 19 and 22. From figure 22 the shaded area is

$$dS = (a_b - y^*)\, ds \qquad \text{(A-40)}$$

and

$$\left.\begin{aligned} ds &= [1 + (dx/dz)^2]\, dz \\ \frac{dx}{dz} &= -\frac{z}{x}\frac{a_p^2}{b_p^2} = -\frac{z}{a_p(1 - z^2/b_p^2)^{\frac{1}{2}}}\frac{a_p^2}{b_p^2} \end{aligned}\right\} \qquad \text{(A-41)}$$

Using (A-40) and (A-41) we can easily arrive at (A-37). Notice that when

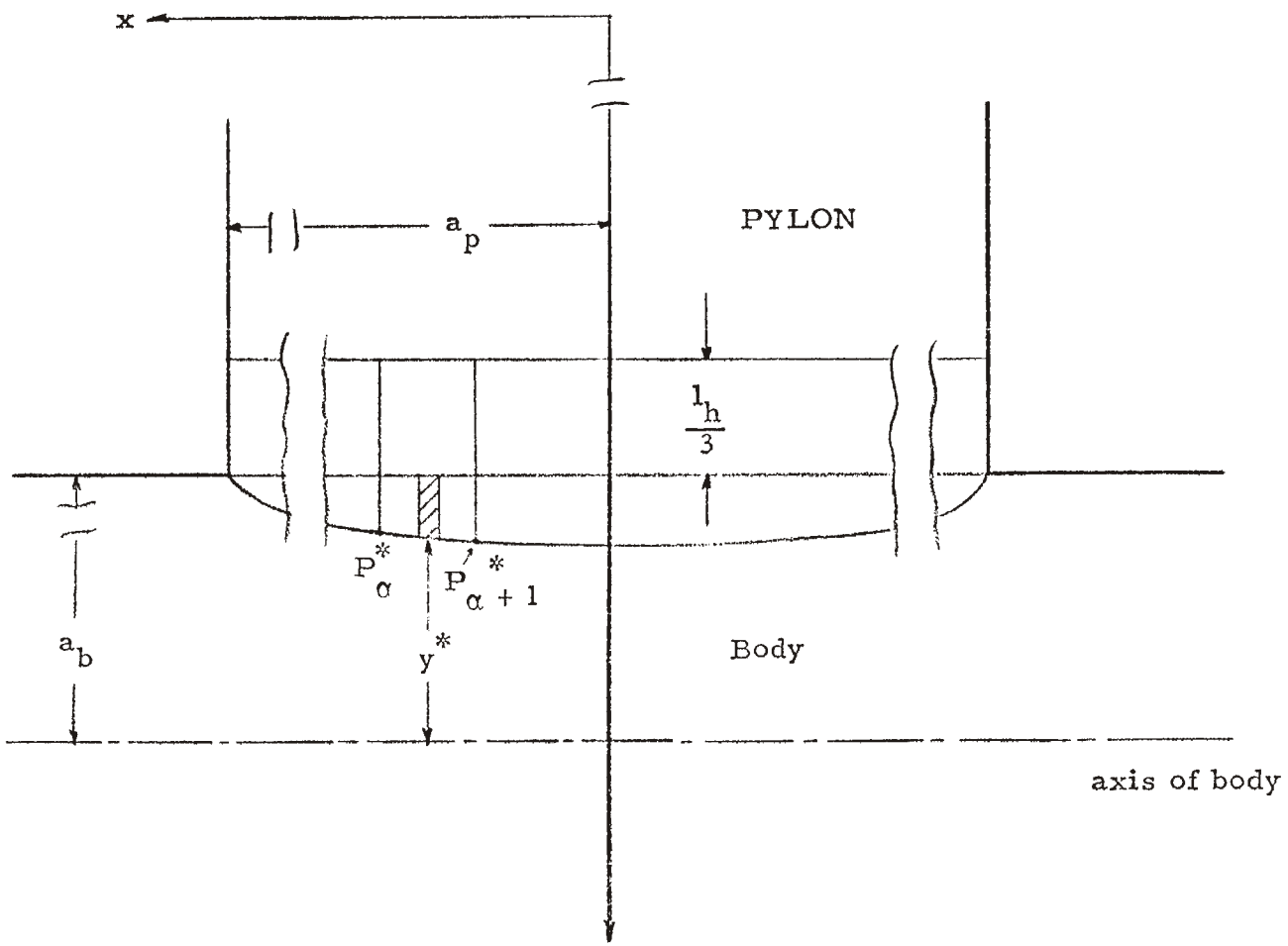

Figure 22: Geometry for the calculation of the area of a pylon subzone adjacent to the pylon-body intersection

$z^*_{\alpha+1} = b_p$, the integrand in (A-37) has an integrable singularity and consequently to allow for accurate numerical integration we should rewrite (A-37) as

$$(\Delta S)_\alpha = \frac{1}{9}\ell_p\ell_h + a_b \int_{z^*_\alpha}^{z^*_{\alpha+1}} \left\{ \left[1 - \left(1 - \frac{z^2}{a_b^2} \right)^{\frac{1}{2}} \right] \left[\frac{b_p^4 + z^2(a_p^2 - b_p^2}{b_p^2(b_p^2 - z^2)} \right]^{\frac{1}{2}} \right.$$

$$\left. - K_1 (b_p - z)^{-\frac{1}{2}} \right\} dz - 2K_1 a_b \left[(b_p - z^*_{\alpha+1})^{\frac{1}{2}} - (b_p - z^*_\alpha)^{\frac{1}{2}} \right] \qquad \text{(A-42)}$$

The integrand in (A-35) is zero at $z = b_p$ and the numerical integration can be performed accurately.

3.1.2 Body (Cylindrical Surface). Body-Pylon Intersection

In what follows we assume that $\sin^{-1}(b_p/a_b)$ is smaller than 30° and consequently the intersection does not reach beyond the first row of subzones. The subzones adjacent to the body-pylon intersection correspond to

$$A_1 \le \alpha^\dagger \le A_2$$

where A_1, A_2 have been defined by (A-14). We first present the coordinates of subzones for $x > 0$, i.e.

$$\left.\begin{aligned} A_1 &\le \alpha^\dagger \le 3N_b^{(1)} \\ x_{\alpha^\dagger} &= L_1 - \alpha^\dagger \frac{\ell_b^{(1)}}{3} + \frac{\ell_b^{(1)}}{6} \\ z_{\alpha^\dagger} &= a_b \sin\left(\frac{\pi}{12} + \frac{\varphi^*}{2} \right) \\ y_{\alpha^\dagger} &= b_w + h_p + a_b \left[1 - \cos\left(\frac{\pi}{12} + \frac{\varphi^*}{2} \right) \right] \end{aligned}\right\} \qquad \text{(A-43)}$$

where

$$\left.\begin{aligned} \varphi^* &= \sin^{-1}(z^*/a_b) \\ z^* &= b_p\left[1-\left(\frac{x_{\alpha^\dagger}}{a_p}\right)^2\right]^{\frac{1}{2}} \qquad \left(\text{for } x_{\alpha^\dagger} \le a_p\right) \end{aligned}\right\} \tag{A-44}$$

Equations (A-43) can be understood with the aid of figures 23a, 23b. Notice that when the $x_{\alpha^\dagger}$ coordinate at the center of the $\alpha^\dagger = A_1$ subzone is larger than a_p, z^* in (A-44) is not defined, i.e. point P' (fig. 23) does not belong to the pylon surface. For $x_\alpha > a_p$ the y and z coordinates for the $\alpha^\dagger = A_1$ subzone can be defined as follows

$$\left.\begin{aligned} y_{\alpha^\dagger} &= b_w + h_p + a_b\left(1-\cos\frac{\pi}{12}\right) \\ z_{\alpha^\dagger} &= a_b \sin\frac{\pi}{12} \\ \left(x_{\alpha^\dagger} = L_1 - \alpha\ \frac{\ell_b^{(1)}}{3} + \frac{\ell_b^{(1)}}{6} \ge a_p\right) \end{aligned}\right\} \alpha^\dagger = A_1,\ x_\alpha \ge a_p \tag{A-45}$$

Notice that for $x_{\alpha^\dagger} = a_p$, φ^* in (A-44) is zero and (A-43) is identical with (A-45).

The coordinates at the center of a subzone for $x < 0$ such that

$$3N_b^{(1)} + 1 \le \alpha^\dagger \le A_2$$

can be derived similarly

$$\left.\begin{aligned} x_{\alpha^\dagger} &= -\left(\alpha^\dagger - 3N_b^{(1)}\right)\frac{\ell_b^{(2)}}{3} + \frac{\ell_b^{(2)}}{6} \\ z_{\alpha^\dagger} &= a_b \sin\left(\frac{\pi}{12} + \frac{\varphi^*}{2}\right) \\ y_{\alpha^\dagger} &= b_w + h_p + a_b\left[1-\cos\left(\frac{\pi}{12} + \frac{\varphi^*}{2}\right)\right] \end{aligned}\right\} \tag{A-46}$$

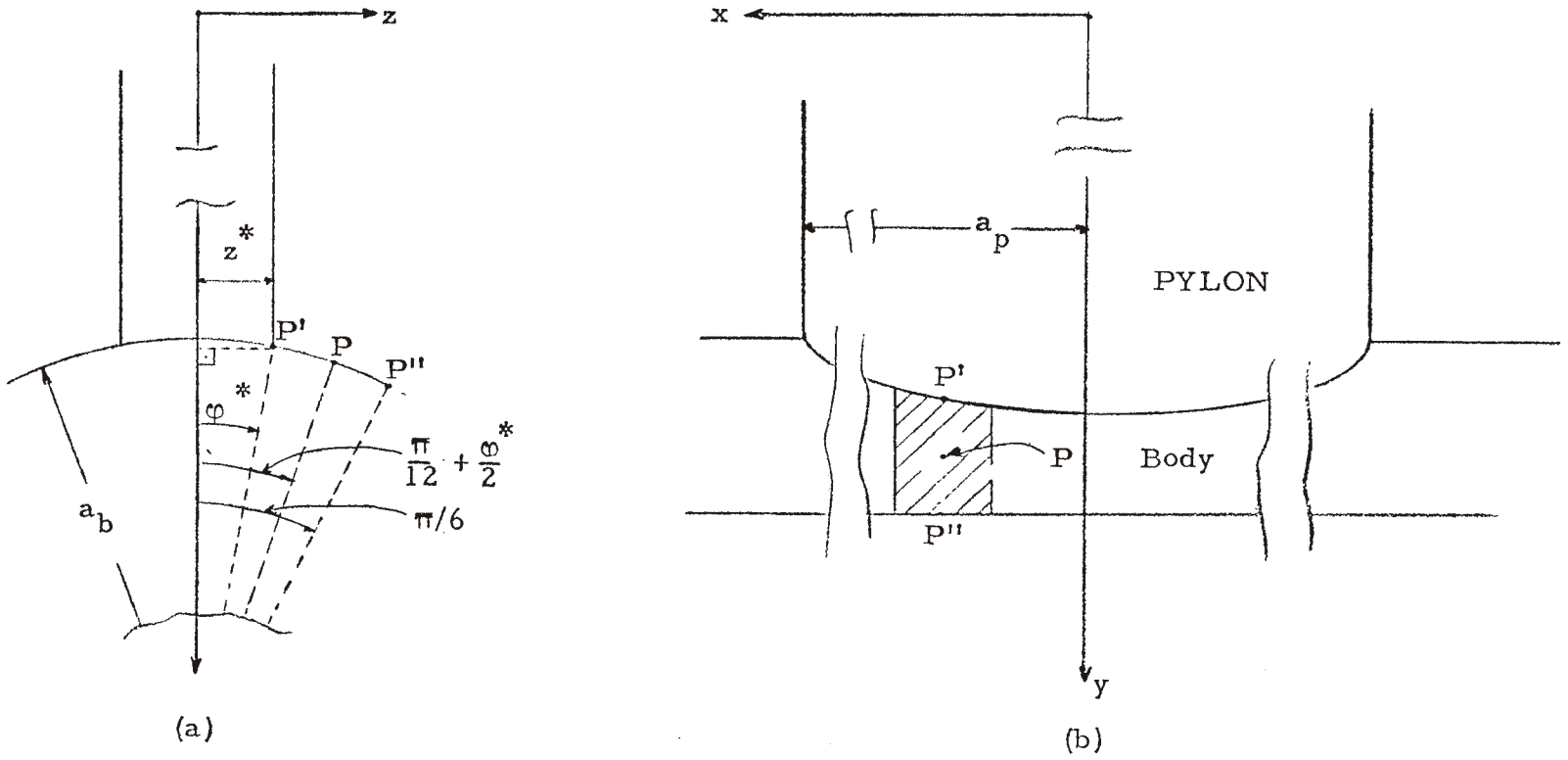

Figure 23: Geometry for the calculation of the coordinates of the center P of a body subzone adjacent to the body-pylon intersection. (Scales of figures (a) and (b) are not the same.)

$$\varphi^* = \sin^{-1}(z^*/b_p)$$

$$z^* = b_p\left[1 - \left(\frac{x_{\alpha^\dagger}}{a_p}\right)^2\right]^{\frac{1}{2}} \qquad \left(\left|x_{\alpha^\dagger}\right| \le a_p\right)$$

and

$$\left.\begin{aligned} x_{\alpha^\dagger} &= -\left(\alpha^\dagger - 3N_b^{(1)}\right)\frac{\ell_b^{(2)}}{3} + \frac{\ell_b^{(2)}}{6} \\ z_{\alpha^\dagger} &= a_b \sin\frac{\pi}{12} \\ y_{\alpha^\dagger} &= b_w + h_p + a_b\left(1 - \cos\frac{\pi}{12}\right) \end{aligned}\right\} \quad \left|x_{\alpha^\dagger}\right| \ge a_p, \quad \alpha^\dagger = A_2 \qquad \text{(A-47)}$$

Next we present the areas of the subzones starting with

$$\alpha^\dagger = A_1 = \left[\frac{L_1 - a_p}{\ell_b^{(1)}/3}\right]^* + 1$$

$$(\Delta S)_{\alpha^\dagger} = \left[L_1 - (A_1 - 1)\frac{\ell_b^{(1)}}{3} - a_p\right] a_b\varphi^* + \frac{\ell_b^{(1)}}{3}\, a_b\left(\frac{\pi}{6} - \varphi^*\right)$$

$$+ \int_{x^*}^{a_p} a_b\left(\varphi^* - \sin^{-1}\frac{z}{a_b}\right) dx \qquad \text{(A-48)}$$

where

$$\left.\begin{aligned} z &= b_p\left(1 - \frac{x^2}{a_p^2}\right)^{\frac{1}{2}} \\ x^* &= L_1 - A_1\,\frac{\ell_b^{(1)}}{3} \\ \varphi^* &= \sin^{-1}\frac{b_p}{a_b} \end{aligned}\right\} \qquad \text{(A-49)}$$

Equation (A-48) can be derived with the aid of figures 24 and 25 . From figure 25 we see that

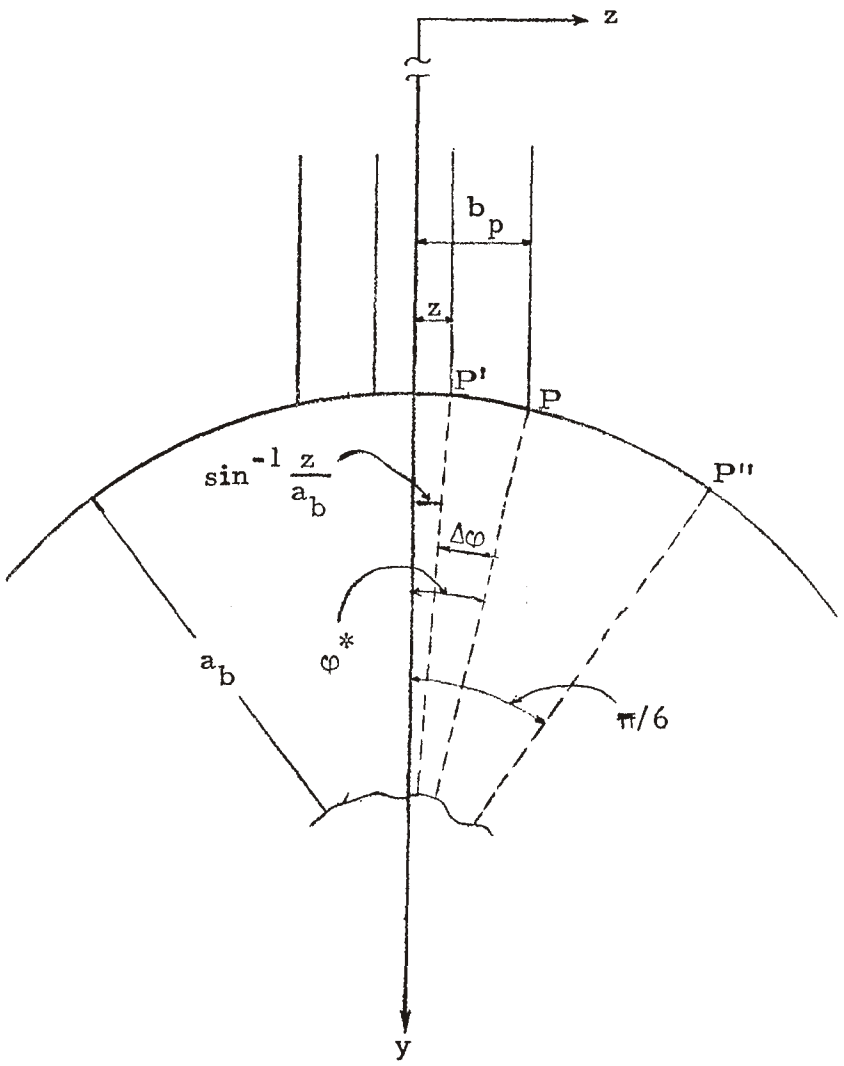

Figure 24: Geometry in the zy plane for the calculation of the area of the first body subzone adjacent to the body-pylon intersection. (Scales of figures 24 and 25 are not the same.)

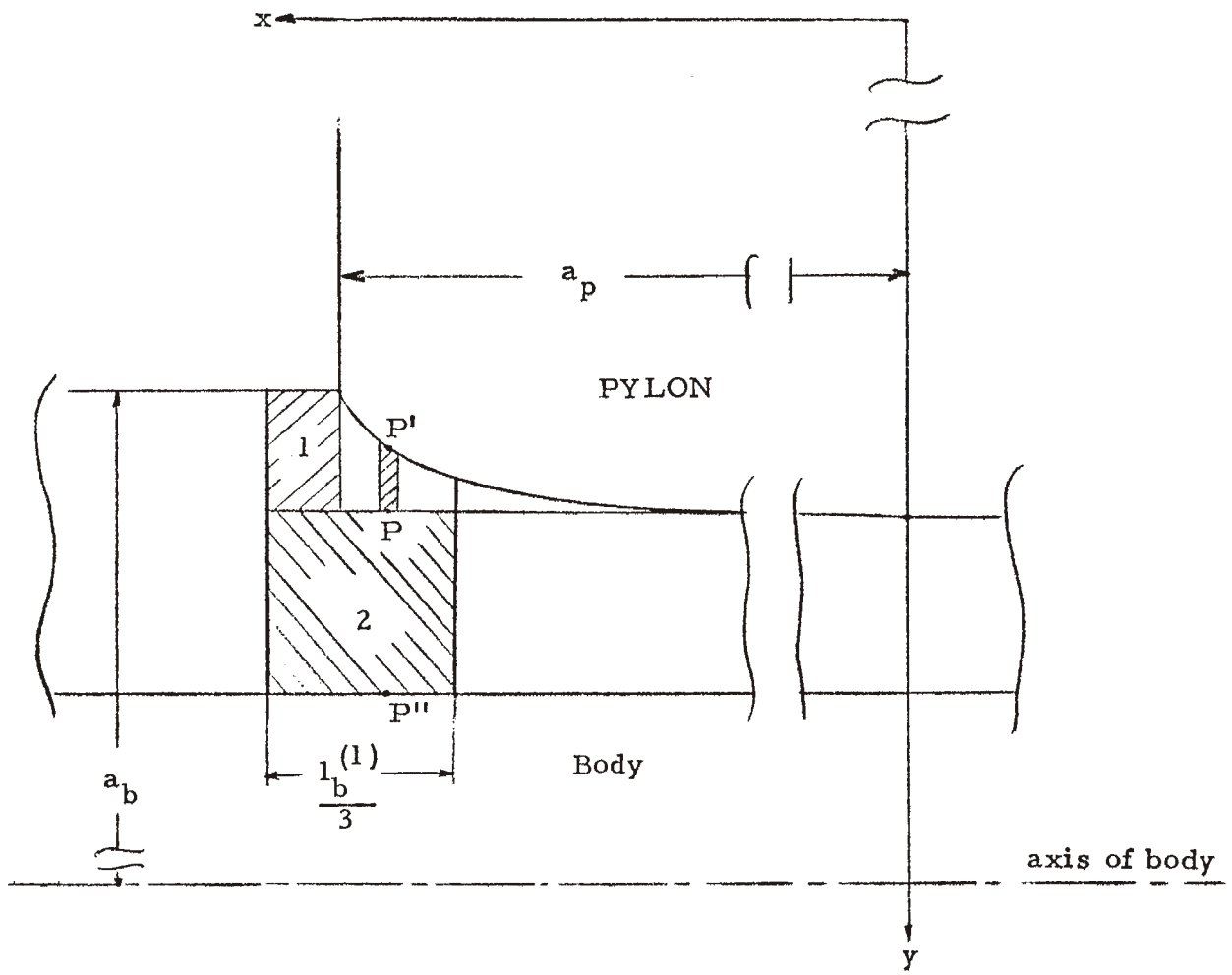

Figure 25: Geometry for the calculation of the area of the first body subzone adjacent to the body-pylon intersection

$$\text{Area 1} \doteq \left[L_1 - (A_1 - 1) \frac{\ell_b^{(1)}}{3} \right] a_b \varphi^*$$

$$\text{Area 2} = \frac{\ell_b^{(1)}}{3} a_b \left(\frac{\pi}{6} - \varphi^* \right)$$

$$\text{Differential Area} = a_b \, \Delta\varphi \, dx = a_b \left(\varphi^* - \sin^{-1} \frac{z}{a_b} \right) dx$$

With the help of the above relationships we can easily derive (A-48).

We proceed now by presenting the areas of subzones such that

$$A_1 + 1 \le \alpha^\dagger \le 3N_b^{(1)}$$

$$(\Delta S)_{\alpha^\dagger} = \frac{\ell_b^{(1)}}{3} a_b \left(\frac{\pi}{6} - \varphi^* \right) + \int_{x^*_{\alpha+1}}^{x^*_\alpha} a_b \left(\varphi^* - \sin^{-1} \frac{z}{a_b} \right) dx \qquad \text{(A-50)}$$

where

$$\left.\begin{aligned} z &= b_p \left(1 - \frac{x^2}{a_p^2} \right)^{\frac{1}{2}} \\ x^*_{\gamma^\dagger} &= L_1 - (\gamma^\dagger - 1) \frac{\ell_b^{(1)}}{3} \qquad (\gamma^\dagger = \alpha^\dagger, \alpha^\dagger + 1) \\ \varphi^* &= \sin^{-1} \frac{b_p}{a_p} \end{aligned}\right\} \qquad \text{(A-51)}$$

Equation (A-50) can be derived with the aid of figures 24 and 26 and in a similar manner as (A-48).

Next we consider subzones for $x < 0$ such that

$$3N_b^{(1)} + 1 \le \alpha^\dagger \le A_2 - 1$$

$$(\Delta S)_{\alpha^\dagger} = \frac{\ell_b^{(1)}}{3} a_b \left(\frac{\pi}{6} - \varphi^* \right) + \int_{x^*_\alpha}^{x^*_{\alpha+1}} a_b \left(\varphi^* - \sin^{-1} \frac{z}{a_b} \right) dx \qquad \text{(A-52)}$$

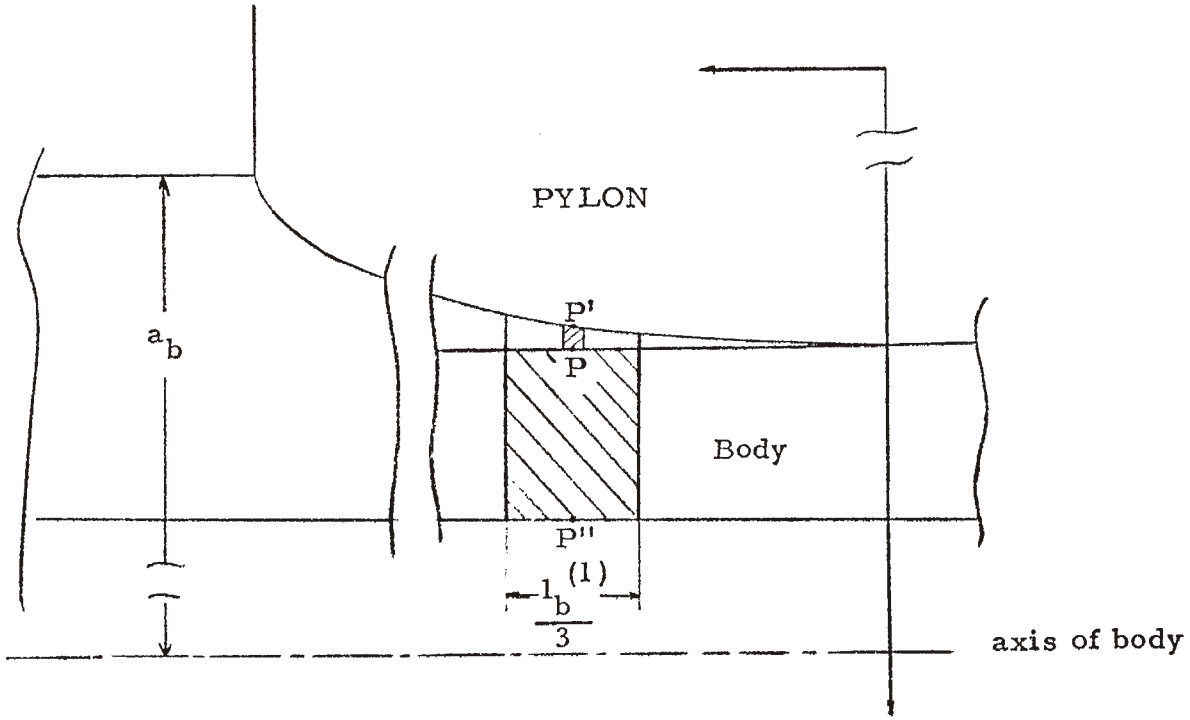

Figure 26: Geometry for the calculation of the area of a body subzone adjacent to the body-pylon intersection

where

$$\left.\begin{aligned} z &= b_p\left(1-\frac{x^2}{a_p^2}\right)^{\frac{1}{2}} \\ x^*_{\gamma^\dagger} &= (\gamma^\dagger - 3N_b^{(1)} - 1)\frac{\ell_b^{(2)}}{3} \qquad (\gamma^\dagger = \alpha^\dagger, \alpha^\dagger + 1) \\ \varphi^* &= \sin^{-1}\frac{b_p}{a_b} \end{aligned}\right\} \tag{A-53}$$

The area of the last subzone adjacent to the body-pylon intersection, i.e.

$$\alpha^\dagger = A_2 = 3N_b^{(1)} + \left[\frac{a_p}{\ell_b^{(2)}/3}\right]^* + 1$$

is given by

$$(\Delta S)_{\alpha^\dagger} = \left[\left(A_2 - 3N_b^{(1)}\right)\frac{\ell_b^{(2)}}{3} - a_p\right] a_b \varphi^* + \frac{\ell_b^{(2)}}{3} a_b \left(\frac{\pi}{6} - \varphi^*\right) + \int_{x^*_{\alpha^\dagger}}^{a_p} a_b \left(\varphi^* - \sin^{-1}\frac{z}{a_b}\right) dx \tag{A-52}$$

where

$$\left.\begin{aligned} z &= b_p\left(1-\frac{x^2}{a_p^2}\right)^{\frac{1}{2}} \\ x^*_{\alpha^\dagger} &= \left(A_2 - 3N_b^{(1)} - 1\right)\frac{\ell_b^{(2)}}{3} \\ \varphi^* &= \sin^{-1}\frac{b_p}{a_p} \end{aligned}\right\} \tag{A-53}$$

3.2 Coordinates and Areas of Zones

3.2.1 Pylon

3.2.1.1 Wing-Pylon Intersection

The coordinates at the center of a zone are the same as the coordinates at the center of the central subzone and this subzone is not adjacent to the intersection. Thus the coordinates of a zone i are given by (A-11) with α equal to $\alpha(i, k = 0)$ and related to i by the relationship

$$\alpha(i, k = 0) = 3N_p + 3k - 1, \quad 1 \le i \le N_p \tag{A-54}$$

To calculate the area of a zone we notice that only three subzones are adjacent to the wing-pylon intersection and consequently

$$(\Delta S)_i = \frac{2}{3} \ell_p \ell_h + (\Delta S)_{\alpha(i, k=1)} + (\Delta S)_{\alpha(i, k=2)} + (\Delta S)_{\alpha(i, k=3)} \tag{A-55}$$

where $(DS)_\alpha$ is given by (A-33)

$$\left.\begin{aligned} \alpha(i, k = 1) &= 3i - 2 \\ \alpha(i, k = 2) &= 3i - 1 \\ \alpha(i, k = 3) &= 3i \end{aligned}\right\} \quad 1 \le i \le N_p \tag{A-56}$$

3.2.1.2 Pylon-Body Intersection

The coordinates at the center of a zone are the same as the coordinates at the center of the central subzone, and this subzone is not adjacent to the intersection. Thus the coordinates are given by (A-11) with α equal to $\alpha(i, k = 0)$ and related to i by

$$\alpha(i, k = 0) = 3N_p(2N_h - 1) + 3i - 1, \quad N_p(N_h - 1) + 1 \le i \le N_p N_h \tag{A-57}$$

The area of a zone is equal to

$$(\Delta S)_i = \frac{2}{3} \ell_p \ell_h + (\Delta S)_{\alpha(i,k=6)} + (\Delta S)_{\alpha(i,k=7)} + (\Delta S)_{\alpha(i,k=8)} \qquad \text{(A-58)}$$

where $(\Delta S)_\alpha$ is given by (A-42) and

$$\left.\begin{aligned} \alpha(i,k=6) &= \alpha(i,k=0) + 3N_p - 1 \\ \alpha(i,k=7) &= \alpha(i,k=0) + 3N_p \\ \alpha(i,k=8) &= \alpha(i,k=0) + 3N_p + 1 \end{aligned}\right\} \qquad \text{(A-59)}$$

The relationship of $\alpha(i,k=0)$ to i is given by (A-57).

3.2.2 Body (Cylindrical Surface)

The coordinates at the center of a zone are given by (A-14) with $\alpha^\dagger$ equal to $\alpha^\dagger(i,k=0)$ and related to i by

$$\begin{aligned} &\alpha^\dagger(i,k=0) = 3N_b + 3i - 1 \\ &N_p N_h + \left[\frac{L_1 - a_p}{\ell_b^{(1)}}\right]^* + 1 \le i \le N_p N_h + N_b^{(1)} + \left[\frac{a_p}{\ell_b^2}\right]^* + 1 \end{aligned} \qquad \text{(A-60)}$$

The area of a zone is given by

$$(\Delta S)_i = \frac{\ell_b^{(m)}}{2} \pi a_b + (\Delta S)_{\alpha^\dagger(i,k=1)} + (\Delta S)_{\alpha^\dagger(i,k=2)} + (\Delta S)_{\alpha^\dagger(i,k=3)} \qquad \text{(A-61)}$$

where

$$\left.\begin{aligned} \alpha^\dagger(i,k=1) &= \alpha^\dagger(i,k=0) - 3N_b - 1 \\ \alpha^\dagger(i,k=2) &= \alpha^\dagger(i,k=0) - 3N_b \\ \alpha^\dagger(i,k=3) &= \alpha^\dagger(i,k=0) - 3N_b + 1 \end{aligned}\right\} \qquad \text{(A-62)}$$

and $\alpha^\dagger(i,k=0)$ is given by (A-60). The superscript m is equal to 1 for $x>0$ and 2 for $x<0$.

Finally we would like to make the following observations. In this work we have treated subzones adjacent to surface intersections as consisting of a "usual" subzone plus or minus some additional area because of the changing geometrical configuration at the intersection. When the additional area is <u>added</u> we assume that the additional maximum longitudinal length is less than $.5\ell_h/3$, i.e.

Wing-Pylon Intersection

$$b_w\left\{1 - [1 - (a_p/a_w)^2]^{\frac{1}{2}}\right\} \leq .5\ell_h/3$$

Pylon-Body Intersection

$$a_b\left\{1 - [1 - (b_p/a_b)^2]^{\frac{1}{2}}\right\} \leq .5\ell_h/3$$

When the additional area is <u>subtracted</u> we assume that

Body-Pylon Intersection

$$\sin^{-1}(b_p/a_b) \leq 30^\circ$$

This condition means that the intersection curve is confined within the first row of subzones on the body.

APPENDIX B

In this Appendix we derive explicit expressions for Z_{ii}^{K} (K = A, B, C, D) which appear in (94) and contain the integrable singularity arising from the free-space part of the Green's function. To accomplish this we first calculate the t, s components of $\underline{\underline{D}}_o$ defined by (91).

$$
\begin{aligned}
-\hat{t}\cdot\underline{\underline{D}}_o(\underline{r},\underline{r}_o)\cdot\hat{s}_o &= -\hat{t}\cdot[\nabla G_o(\underline{r},\underline{r}_o)\times\underline{\underline{I}}]\cdot\hat{s}_o = -\hat{t}\cdot[\nabla G_o(\underline{r},\underline{r}_o)\times\hat{s}_o] \\
&= (\hat{t}\times\hat{s}_o)\cdot\nabla G_o(\underline{r},\underline{r}_o) \\
-\hat{t}\cdot\underline{\underline{D}}_o(\underline{r},\underline{r}_o)\cdot\hat{t}_o &= (\hat{t}\times\hat{t}_o)\cdot\nabla G_o(\underline{r},\underline{r}_o) = 0 \\
\hat{s}\cdot\underline{\underline{D}}_o(\underline{r},\underline{r}_o)\cdot\hat{s}_o &= (\hat{s}_o\times\hat{s})\cdot\nabla G_o(\underline{r},\underline{r}_o) \\
\hat{s}\cdot\underline{\underline{D}}_o(\underline{r},\underline{r}_o)\cdot\hat{t}_o &= (\hat{t}_o\times\hat{s})\cdot\nabla G_o(\underline{r},\underline{r}_o)
\end{aligned}
\tag{B-1}
$$

To further simplify (B-1) we recall (35)

$$
\nabla G_o(\underline{r},\underline{r}_o) = \frac{\underline{r}-\underline{r}_o}{|\underline{r}-\underline{r}_o|}\left(ik_o-\frac{1}{R}\right)G_o(\underline{r},\underline{r}_o) \tag{B-2}
$$

$$
\underline{R} = \underline{r}-\underline{r}_o, \quad R = |\underline{r}-\underline{r}_o| \tag{B-3}
$$

and notice that $\underline{R}$ can be decomposed into two appropriate cylindrical coordinates

$$
\underline{R} = \underline{r}-\underline{r}_o = \underline{\rho}-\underline{\rho}_o + (t-t_o)\hat{t} \tag{B-4}
$$

where

$$
\left.\begin{aligned}
\underline{\rho} &= x\hat{x}+z\hat{z} \\
\hat{t} &= -\hat{y}, \quad t = -y
\end{aligned}\right\} \text{ Pylon} \tag{B-5}
$$

$$\left.\begin{aligned} \underline{\rho} &= y\,\hat{y} + z\,\hat{z} \\ \hat{t} &= -\hat{x},\quad t = -x \end{aligned}\right\} \quad \begin{matrix}\text{Body} \\ \text{(Cylindrical Surface)}\end{matrix} \tag{B-6}$$

Thus we can rewrite (B-1) as follows

Pylon

$$\begin{aligned} -\hat{t}\cdot \underline{\underline{D}}_o(\underline{r},\underline{r}_o)\cdot \hat{s}_o &= \left\{(\hat{t}\times\hat{s}_o)\cdot[\underline{\rho}-\underline{\rho}_o+(t-t_o)\hat{t}]\right\}(ik_o-\frac{1}{R})\frac{G_o}{R} \\ &= \left\{(\hat{t}\times\hat{s}_o)\cdot(\underline{\rho}-\underline{\rho}_o)+(\hat{t}\times\hat{s}_o)\cdot\hat{t}\,(t-t_o)\right\}(ik_o-\frac{1}{R})\frac{G_o}{R} \\ &= (\hat{t}\times\hat{s}_o)\cdot(\underline{\rho}-\underline{\rho}_o)\,(ik_o-\frac{1}{R})\frac{G_o}{R} \end{aligned} \tag{B-7}$$

To evaluate the triple product $(\hat{t}, \hat{s}_o, \underline{\rho}-\underline{\rho}_o)$ we use figure 27 to obtain the following relationships

$$\left.\begin{aligned} x &= a_p\cos\theta \\ y &= b_p\sin\theta \\ \underline{ds} &= -\hat{x}\,a_p\sin\theta\,d\theta + \hat{z}\,b_p\cos\theta\,d\theta \\ \hat{s} &= \underline{ds}/|\underline{ds}| \\ \underline{\rho} &= a_p\cos\theta\,\hat{x} + b_p\sin\theta\,\hat{z} \\ \hat{s} &= (-a_p\sin\theta\,\hat{x} + b_p\cos\theta\,\hat{z})/(a_p^2\sin^2\theta + b_p^2\cos^2\theta)^{\frac{1}{2}} \\ \hat{t} &= -\hat{y} \end{aligned}\right\} \tag{B-8}$$

Using (B-8) we can rewrite (B-7) as

$$-\hat{t}\cdot\underline{\underline{D}}_o(\underline{r},\underline{r}_o)\cdot\hat{s}_o = \frac{a_p b_p[1-\cos(\theta-\theta_o)]}{(a_p^2\sin^2\theta_o + b_p^2\cos^2\theta_o)^{\frac{1}{2}}}\,(ik_o-\frac{1}{R})\,\frac{G_o(\underline{r},\underline{r}_o)}{R} \tag{B-9}$$

Similarly,

$$(\hat{s}_o\times\hat{s})\cdot\underline{R} = (\hat{s}_o\times\hat{s})\cdot[(\underline{\rho}-\underline{\rho}_o)+(t-t_o)\hat{t}]$$

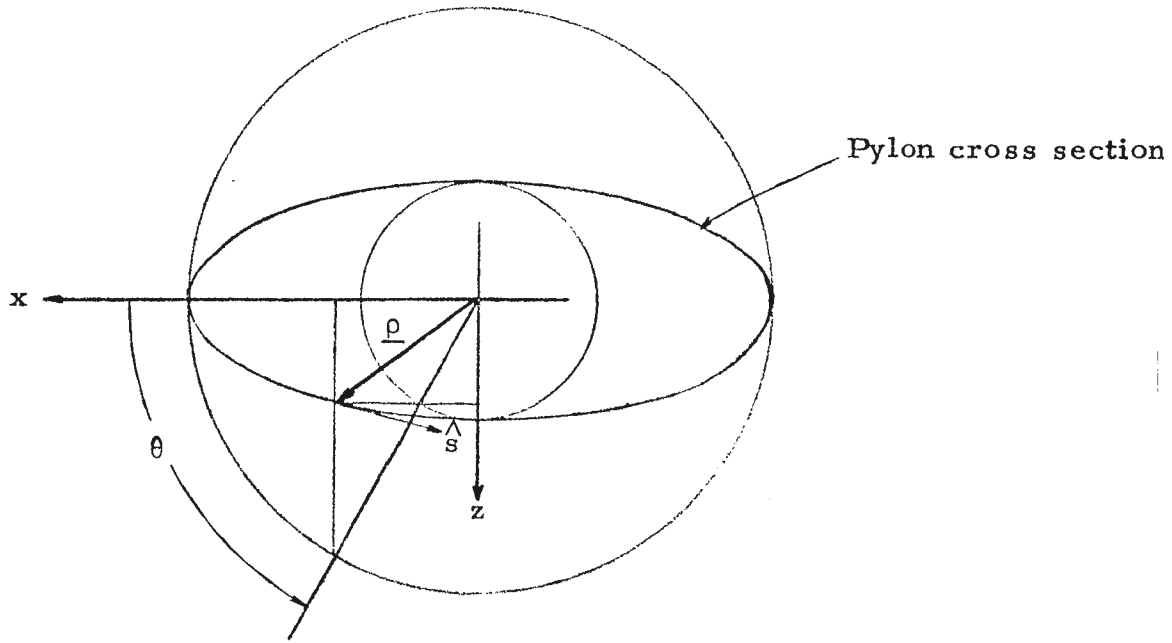

Figure 27: Geometry for the definition of $\underline{\rho}$, $\hat{s}$, and θ on the pylon elliptic cross section

$$= (\hat{s}_o \times \hat{s}) \cdot (\underline{\rho} - \underline{\rho}_o) + (t - t_o)(\hat{s} \times \hat{s}_o) \cdot \hat{t}$$

$$= (t - t_o)(\hat{s}_o \times \hat{s}) \cdot \hat{t}$$

The triple product $(\hat{s}_o, \hat{s}, \underline{\rho} - \underline{\rho}_o)$ is zero because all the vectors are coplanar and the last triple product can be evaluated with the aid of (B-8). Thus

$$\hat{s} \cdot \underline{\underline{D}}_o(\underline{r}, \underline{r}_o) \cdot \hat{s}_o = \left[(t - t_o) \frac{a_p b_p \sin(\theta - \theta_o)}{(a_p^2 \sin^2\theta + b_p^2 \cos^2\theta)^{\frac{1}{2}} (a_p^2 \sin^2\theta_o + b_p^2 \cos^2\theta_o)^{\frac{1}{2}}}\right] (ik_o - \frac{1}{R}) \frac{G_o(\underline{r}, \underline{r}_o)}{R} \qquad \text{(B-10)}$$

The last expression in (B-1) can be evaluated in a similar manner

$$(\hat{t}_o \times \hat{s}) \cdot \underline{R} = (\hat{t}_o \times \hat{s}) \cdot [\underline{\rho} - \underline{\rho}_o + (t - t_o)\hat{t}]$$

$$= (\hat{t}_o \times \hat{s}) \cdot (\underline{\rho} - \underline{\rho}_o)$$

and

$$\hat{s} \cdot \underline{\underline{D}}_o(\underline{r}, \underline{r}_o) \cdot \hat{t}_o = \frac{a_p b_p [\cos(\theta - \theta_o) - 1]}{(a_p^2 \sin^2\theta + b_p^2 \cos^2\theta)^{\frac{1}{2}}} \cdot (ik_o - \frac{1}{R}) \frac{G_o(\underline{r}, \underline{r}_o)}{R} \qquad \text{(B-11)}$$

Body (Cylindrical Surface)

For the body we can easily obtain (fig. 28)

$$\left.\begin{aligned} -\hat{t} \cdot \underline{\underline{D}}_o(\underline{r}, \underline{r}_o) \cdot \hat{s}_o &= a_b[1 - \cos(\theta - \theta_o)](ik_o - \frac{1}{R}) \frac{G_o}{R} \\ \hat{s} \cdot \underline{\underline{D}}_o(\underline{r}, \underline{r}_o) \cdot \hat{s}_o &= (t - t_o) \sin(\theta_o - \theta)(ik_o - \frac{1}{R}) \frac{G_o}{R} \\ \hat{s} \cdot \underline{\underline{D}}_o(\underline{r}, \underline{r}_o) \cdot \hat{t}_o &= a_b[\cos(\theta - \theta_o) - 1](ik_o - \frac{1}{R}) \frac{G_o}{R} \end{aligned}\right\} \qquad \text{(B-12)}$$

Body (End Caps)

For the end caps the $\underline{R}$ vector lies in the yz plane and the exterior product of any $\hat{t}$ or $\hat{s}$ with any $\hat{s}$ or $\hat{t}$ yields a vector perpendicular to this plane. Consequently, (B-1) shows that all the t, s components of $\underline{\underline{D}}_o$ are zero, i.e. there is no contribution to the submatrix elements from the integrable singularity.

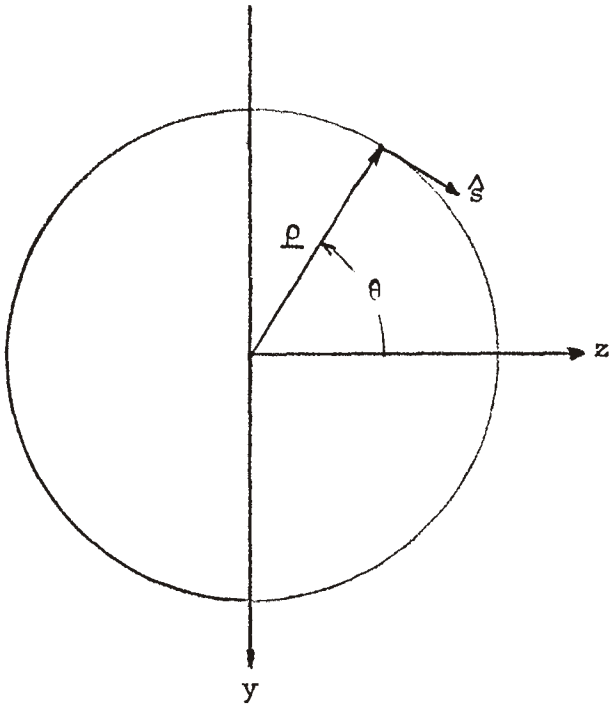

Figure 28: Geometry for the definition of $\underline{\rho}$, $\hat{s}$, and θ on the body cross section

Next we proceed to split $\underline{D}_o$ in order to treat the singularity in a numerically accurate manner. We start with integrals of the form

$$I = \int_S dS_o \, f(\theta, \theta_o) g(t, t_o)(ik_o - \frac{1}{R}) \frac{e^{ikR}}{4\pi R^2} \tag{B-13}$$

where the explicit form of f and g depends on the location of the zone over which we integrate and the specific component of $\underline{\underline{D}}_o$. When $t = t_o$ and $\theta = \theta_o$, then $R = o$ and $f(\theta_o, \theta_o) = o$, $g(t_o, t_o) = o$ but one can show that the integrand is singular. As we mentioned elsewhere this is an integrable singularity i. e. if we perform the t_o integration we obtain a one-dimensional integral with an integrand free of singularity. However, because of the presence of $\exp[ik_o R]$, the t_o integration is complicated and for this reason we rewrite (B-13) as

$$I = \int_S dS_o \, f(\theta, \theta_o) \, g(t, t_o) \left[(ik_o R - 1)e^{ik_o R} + 1\right] (1/4\pi R^3)$$

$$- \int_S dS_o \, f(\theta, \theta_o) \, g(t, t_o) \, (1/4\pi R^3) \tag{B-14}$$

We can easily show that the integrand of the first integral goes to zero as $\theta_o \to \theta$ and $t_o \to t$, whereas the second integral is simple enough to allow the t_o integration to be done explicitly. (The division of I in (B-14) corresponds to the division of $\underline{D}_o$ in (92).) The first integral in (B-14) will be treated as the other integrals occuring in the expressions for A_{ij}^{α}, B_{ij}^{α}, C_{ij}^{α}, and D_{ij}^{α} (see remarks preceding (89).) The second integral in (B-14) will be first converted into a one-dimensional integral. The exact form depends on the location of the zone.

1. Zones not Adjacent to Surface Intersections

1.1 Pylon

Consider a zone not adjacent to a surface intersection. For such a zone the ranges of t_o and θ_o are

$$\left.\begin{aligned} t_o &: t_i - \frac{l_h}{2},\ t_i + \frac{l_h}{2} \\ \theta_o &: \theta_i^{(1)},\ \theta_i^{(2)} \end{aligned}\right\} \qquad \text{(B-15)}$$

where l_h is the length of a zone along the height of the pylon and $\theta_i^{(1)}$, $\theta_i^{(2)}$ are determined by

$$\left(i - \left[\frac{i-1}{N_p}\right]^* N_p - 1\right) l_p = \int_o^{\theta_i^{(1)}} (a_p^2 \sin^2 u + b_p^2 \cos^2 u)^{\frac{1}{2}} du$$

and

$$\left(i - \left[\frac{i-1}{N_p}\right]^* N_p\right) l_p = \int_o^{\theta_i^{(2)}} (a_p^2 \sin^2 u + b_p^2 \cos^2 u)^{\frac{1}{2}}\, du$$

$$\left(i - \left[\frac{i-1}{N_p}\right]^* N_p - \frac{1}{2}\right) l_p = \int_o^{\theta_i} (a_p^2 \sin^2 u + b_p^2 \cos^2 u)\, du$$

as we explained in Appendix A.

If we take the previous relationships into account and remember that $dS_o = dt_o\,(a^2 \sin^2\theta_o + b^2 \cos^2\theta_o)^{\frac{1}{2}} d\theta_o$ we obtain

$$Z_{ii}^A = -\frac{1}{4\pi} \int_{\theta_i^{(1)}}^{\theta_i^{(2)}} d\theta_o (a^2 \sin^2\theta_o + b^2 \cos^2\theta_o)^{\frac{1}{2}} f(\theta_i, \theta_o) \int_{t_i - l_h/2}^{t_i + l_h/2} dt_o / R^3 \qquad \text{(B-17)}$$

where

$$R = \left[a_p^2 (\cos\theta_i - \cos\theta_o)^2 + b_p^2 (\sin\theta_i - \sin\theta_o)^2 + (t_i - t_o)^2\right]^{\frac{1}{2}} \qquad \text{(B-18)}$$

and Z_{ii}^A appears in (94).

Performing the t_o integration we obtain the following expression for Z_{ii}^A.

$$Z_{ii}^{A} = -\frac{l_h}{4\pi}\int_{\theta_i^{(1)}}^{\theta_i^{(2)}} d\theta_o F_A(\theta_i, \theta_o)(1/R_1) \tag{B-19}$$

where

$$F_A(\theta_i, \theta_o) = a_p b_p[1 - \cos(\theta_i - \theta_o)]$$

$$\left[a_p^2(\cos\theta_i - \cos\theta_o)^2 + b_p^2(\sin\theta_i - \sin\theta_o)^2\right]^{-1} \tag{B-20}$$

and

$$R_1 = \left[a_p^2(\cos\theta_i - \cos\theta_o^2) + b_p^2(\sin\theta_i - \sin\theta_o)^2 + (l_h/2)^2\right]^{\frac{1}{2}} \tag{B-21}$$

As we mentioned before $Z_{ii}^{B} = 0$, and because of the oddness with respect to the integrand in the expression for Z_{ii}^{C} we also have

$$Z_{ii}^{C} = 0 \tag{B-22}$$

Finally

$$Z_{ii}^{D} = \frac{l_h}{4\pi}\int_{\theta_i^{(1)}}^{\theta_i^{(2)}} d\theta_o F_D(\theta_i, \theta_o)(1/R_1) \tag{B-23}$$

where

$$F_D = \frac{a_p b_p(a_p^2\sin^2\theta_o + b_p^2\cos^2\theta_o)^{\frac{1}{2}}}{(a_p^2\sin^2\theta_i + b_p^2\cos^2\theta_i)^{\frac{1}{2}}}[1 - \cos(\theta - \theta_o)]$$

$$\left[a_p^2(\cos\theta_i - \cos\theta_o)^2 + b_p^2(\sin\theta_i - \sin\theta_o)^2\right]^{-1} \tag{B-24}$$

and R_1 is given by (B-21).

1.2 Body (Cylindrical Surface)

The limits of integration on the cylindrical surface of the body are

$$t_o : t - \frac{l_b}{2}, \; t + \frac{l_b}{2}$$

$$\theta_o : \theta - \frac{\pi}{4}, \; \theta + \frac{\pi}{4} \qquad \text{(B-25)}$$

where l_b is the longitudinal length of a zone ($l_b = l_b^{(1)}$ for $x > 0$ and $l_b = l_b^{(2)}$ for $x < 0$ as we explained in Appendix A).

We can use the results for the pylon to obtain

$$\left.\begin{aligned} -Z_{ii}^A = Z_{ii}^D &= \frac{l_b}{4\pi} \int_o^{\pi/4} \frac{d\theta}{\left[2a_b^2(1-\cos\theta)+l_b^2/4\right]^{\frac{1}{2}}} \\ Z_{ii}^B = Z_{ii}^C &= 0 \end{aligned}\right\} \qquad \text{(B-26)}$$

From (B-26) we see that unlike for the pylon zones the self-term corrections on the body are independent of the zone location (except for the fact that l_b is different in the two sections $x>0$ and $x<0$). We also observe that the integral in (B-26) has the form of an elliptic integral and can be easily calculated numerically.

1.3 Body (End Caps)

As we already mentioned

$$Z_{ii}^A = Z_{ii}^B = Z_{ii}^C = Z_{ii}^D = 0$$

2. Zones Adjacent to Surface Intersections

2.1 Pylon

2.1.1 Wing-Pylon Interface

With the aid of figure 29 we can find

$$Z_{ii}^{A} = -\frac{1}{4\pi}\int_{\theta_i^{(1)}}^{\theta_i^{(2)}} d\theta_o F_A(\theta_i,\theta_o)\ F_A^{*}(\theta_i,\theta_o) \tag{B-27}$$

$$Z_{ii}^{B} = 0 \tag{B-28}$$

$$Z_{ii}^{C} = \frac{1}{2\pi}\int_{\theta_i^{(1)}}^{\theta_i^{(2)}} d\theta_o F_C(\theta_i,\theta_o)(1/R_1 - 1/R_2) \tag{B-29}$$

$$Z_{ii}^{D} = \frac{1}{4\pi}\int_{\theta_i^{(1)}}^{\theta_i^{(2)}} d\theta_o F_D(\theta_i,\theta_o)\ F_A^{*}(\theta_i,\theta_o) \tag{B-30}$$

where F_A, R_1, F_D are given by (B-20), (B-21), and (B-24) respectively, F_C is given by

$$F_C = \frac{a_p b_p \sin(\theta_i - \theta_o)}{(a_p^2\sin^2\theta_i + b_p^2\cos^2\theta_i)^{\frac{1}{2}}} \tag{B-31}$$

$$F_A^{*}(\theta_i,\theta_o) = \frac{l_h}{2R_1} + \frac{2b_w\left[1-\left(1-\frac{a_p^2\cos^2\theta_o}{a_w^2}\right)^{\frac{1}{2}}\right]+l_h}{R_2} \tag{B-32}$$

and

$$R_2 = \left\{a_p^2(\cos\theta_i - \cos\theta_o)^2 + b_p^2(\sin\theta_i - \sin\theta_o)^2 + \left[b_w\left[1-\left(1-\frac{a_p^2\cos^2\theta_o}{a_w^2}\right)^{\frac{1}{2}}\right]+\frac{l_h}{2}\right]^2\right\}^{\frac{1}{2}} \tag{B-33}$$

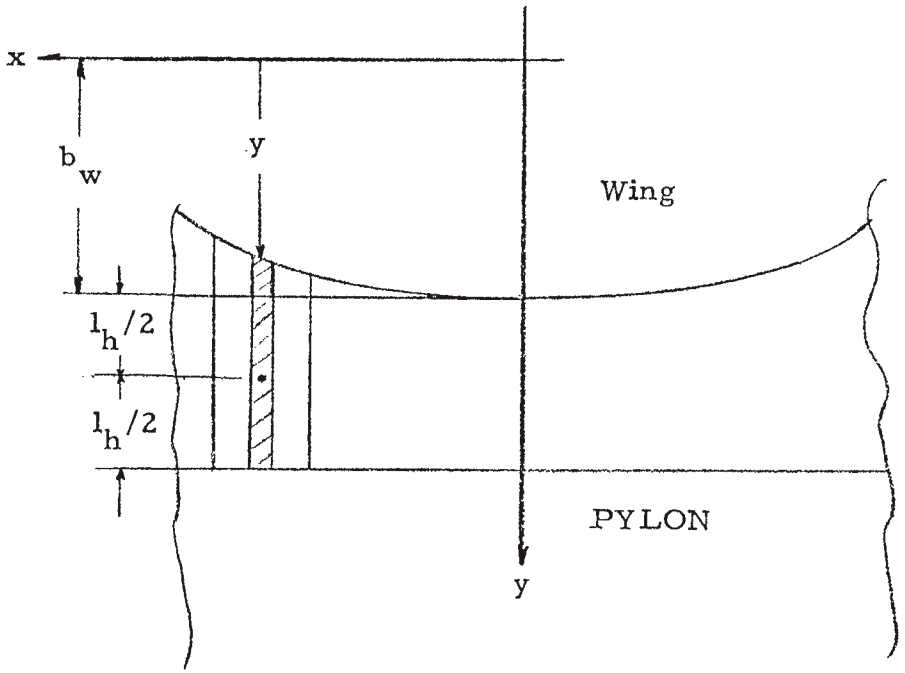

Figure 29: Geometry for the calculation of the self-contribution for zones adjacent to wing-pylon intersection.

2.1.2 Pylon-Body Interface

With the aid of figure 30 we obtain

$$Z_{ii}^{A} = -\frac{1}{4\pi}\int_{\theta_i^{(1)}}^{\theta_i^{(2)}} d\theta_o \, F_A(\theta_i, \theta_o) \; F_A^{+}(\theta_i, \theta_o) \tag{B-34}$$

$$Z_{ii}^{B} = 0 \tag{B-35}$$

$$Z_{ii}^{C} = \frac{1}{2\pi}\int_{\theta_i^{(1)}}^{\theta_i^{(2)}} d\theta_o \, F_C(\theta_i, \theta_o)(1/R_3 - 1/R_1) \tag{B-36}$$

$$Z_{ii}^{D} = \frac{1}{4\pi}\int_{\theta_i^{(1)}}^{\theta_i^{(1)}} d\theta_o \, F_D(\theta_i, \theta_o) \, F_A^{+}(\theta_i, \theta_o) \tag{B-37}$$

where F_A, R_1, F_D, F_C are given by (B-20), (B-21), (B-24), and (B-31) respectively and

$$F_A^{+} = \frac{l_h}{2R_1} + \frac{2a_b\left[1-\left(1-\frac{b_p^2\sin^2\theta_o}{a_b^2}\right)^{\frac{1}{2}}\right]+l_h}{2R_3} \tag{B-38}$$

$$R_3 = \left\{a_p^2(\cos\theta_i - \cos\theta_o)^2 + b_p^2(\sin\theta_i - \sin\theta_o)^2 + \left[a_b\left[1-\left(1-\frac{b_p^2\sin^2\theta_o}{a_b^2}\right)^{\frac{1}{2}}\right]+\frac{l_h}{2}\right]^2\right\}^{\frac{1}{2}} \tag{B-39}$$

2.2 Body (Cylindrical Surface)

2.2.1 Body-Pylon Interface

We start by considering the first zone adjacent to the interface as depicted in figure 31. This zone is characterized by an index i equal to

$$i = N_p N_h + \left[\frac{L_1 - a_p}{l_b^{(1)}}\right] + 1 \tag{B-40}$$

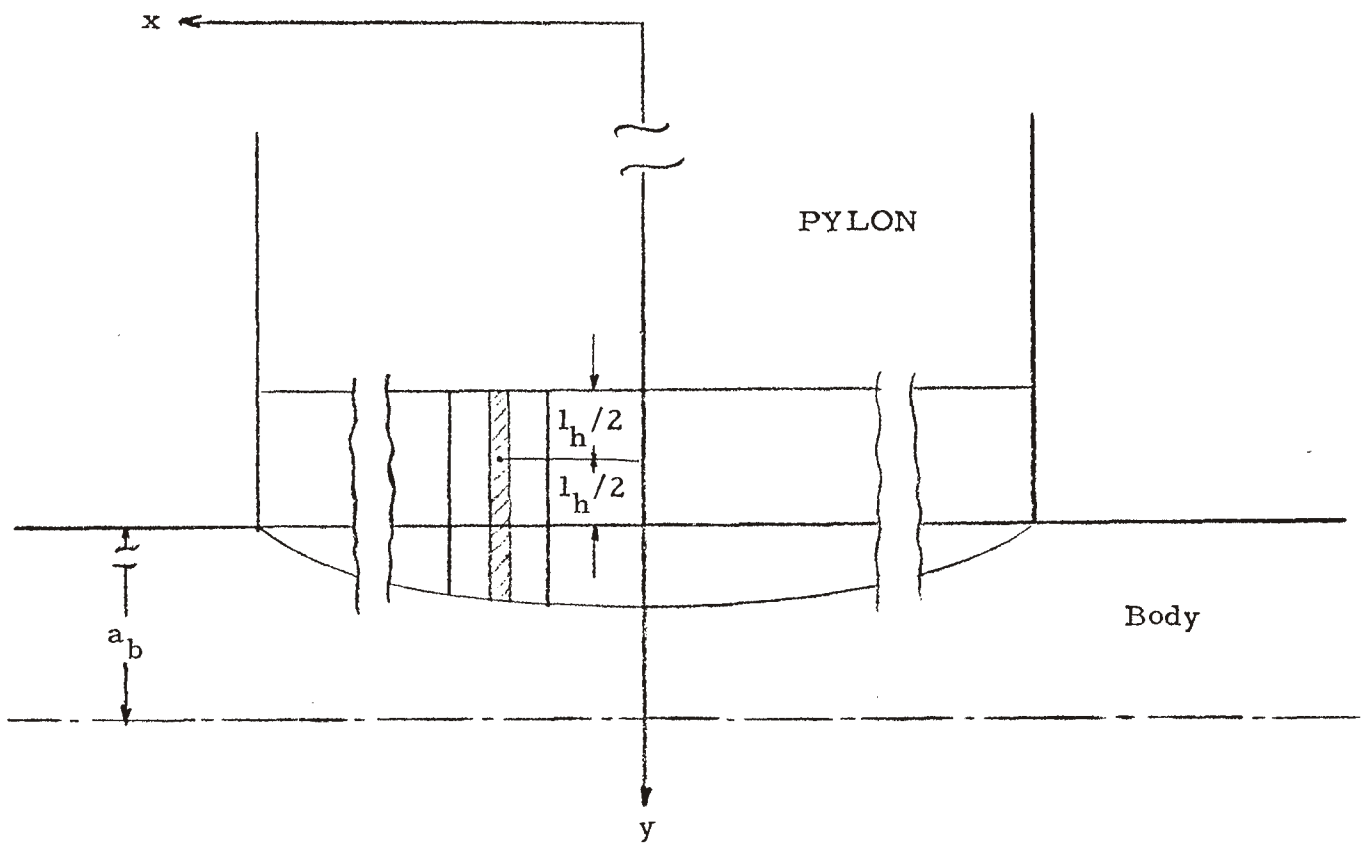

Figure 30: Geometry for the calculation of the self-contribution for zones adjacent to pylon-body intersection.

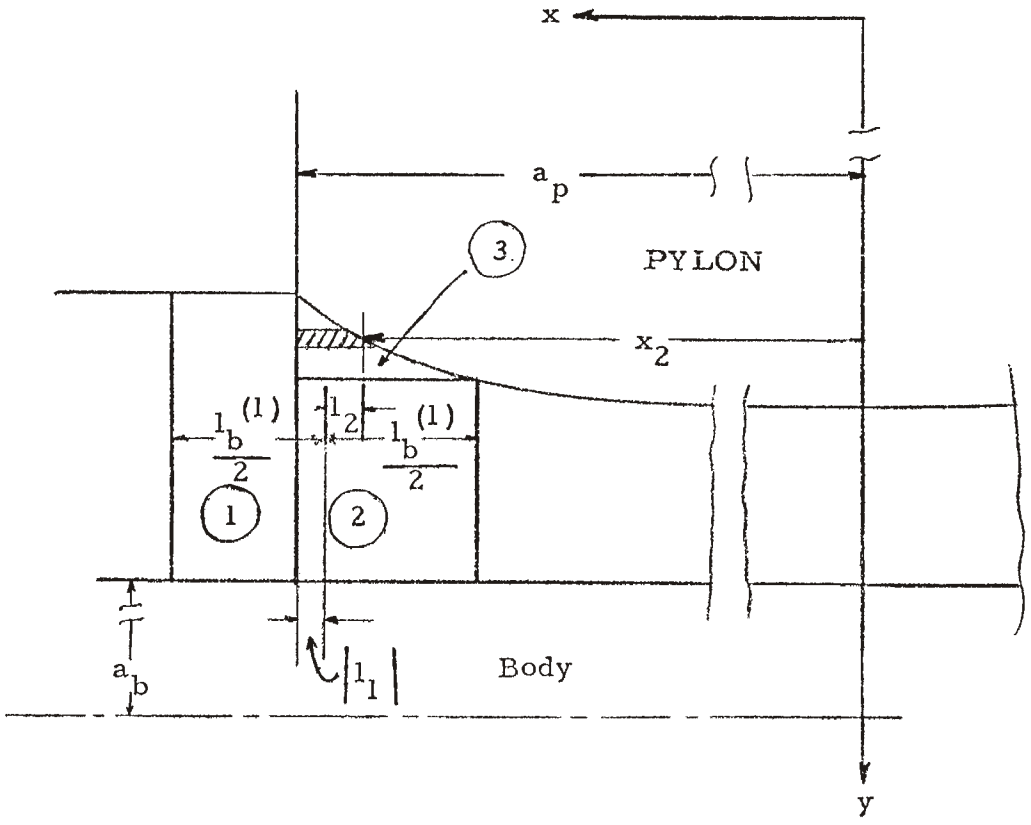

Figure 31: Geometry for the calculation of the self-contribution of the zone adjacent to body-pylon intersection ($x > 0$).

The self-term correction is given by

$$-Z_{ii}^{A} = Z_{ii}^{D} = (Z_{ii}^{D})_1 + (Z_{ii}^{D})_2 + (Z_{ii}^{D})_3 \tag{B-41}$$

$$Z_{ii}^{B} = 0 \tag{B-42}$$

$$Z_{ii}^{C} = (Z_{ii}^{C})_2 + (Z_{ii}^{C})_3 \tag{B-43}$$

$$(Z_{ii}^{D})_1 = \frac{1}{4\pi} \int_0^{\pi/4} d\theta \left\{ \frac{l_b^{(1)}}{2\left[2a_b^2(1-\cos\theta)+(l_b^{(1)}/2)^2\right]^{\frac{1}{2}}} - \frac{l_1}{\left[2a_b^2(1-\cos\theta)+l_1^2\right]^{\frac{1}{2}}} \right\} \tag{B-44}$$

$$(Z_{ii}^{D})_2 = \frac{1}{8\pi} \int_{-\pi/4}^{\theta^*} d\theta \left\{ \frac{l_1}{\left[2a_b^2(1-\cos\theta)+l_1^2\right]^{\frac{1}{2}}} + \frac{l_b^{(1)}}{2\left[2a_b^2(1-\cos\theta)+(l_b^{(1)}/2)^2\right]^{\frac{1}{2}}} \right\} \tag{B-45}$$

$$(Z_{ii}^{D})_3 = \frac{1}{8\pi} \int_{\theta^*}^{\pi/4} d\theta \left\{ \frac{l_1}{\left[2a_b^2(1-\cos\theta)+l_1^2\right]^{\frac{1}{2}}} - \frac{l_2}{\left[2a_b^2(1-\cos\theta)+l_2^2\right]^{\frac{1}{2}}} \right\} \tag{B-46}$$

$$(Z_{ii}^{C})_2 = \frac{a_b}{2\pi} \int_{-\pi/4}^{\theta^*} d\theta \sin\theta \left\{ \frac{1}{\left[2a_b^2(1-\cos\theta)+l_1^2\right]^{\frac{1}{2}}} - \frac{1}{\left[2a_b^2(1-\cos\theta)+(l_b^{(1)}/2)^2\right]^{\frac{1}{2}}} \right\} \tag{B-47}$$

$$(Z_{ii}^{C})_3 = \frac{a_b}{2\pi} \int_{\theta^*}^{\pi/4} d\theta \sin\theta \left\{ \frac{1}{\left[2a_b^2(1-\cos\theta)+l_1^2\right]^{\frac{1}{2}}} - \frac{1}{\left[2a_b^2(1-\cos\theta)+l_2^2\right]^{\frac{1}{2}}} \right\} \tag{B-48}$$

$$l_1 = a_p - \left[L_1 - (i-N_pN_h)l_b^{(1)} + \frac{1}{2}l_b^{(1)}\right] \tag{B-49}$$

$$l_2 = x_2 - \left[L_1 - (i-N_pN_h)l_b^{(1)} + \frac{1}{2}l_b^{(1)}\right] \tag{B-50}$$

$$x_2 = a_p\left[1 - (z_2/b_p)^2\right]^{\frac{1}{2}} \tag{B-51}$$

$$z_2 = a_b \cos(\theta + \pi/4) \tag{B-52}$$

$$\theta^* = \cos^{-1}(z^*/a_b) - \pi/4 \tag{B-53}$$

$$z^* = b_p\left[1-(x^*/a_p)^2\right]^{\frac{1}{2}} \tag{B-54}$$

$$x^* = L_1 - (i-N_pN_h)l_b^{(1)} \tag{B-55}$$

Next we consider zones such that

$$N_pN_h + \left[\frac{L_1-a_p}{l_b^{(1)}}\right] + 1 < i \leq N_pN_h + N_b^{(1)} \tag{B-56}$$

With the aid of figure 32 we can derive the following expressions

$$-Z_{ii}^A = Z_{ii}^D = (Z_{ii}^D)_2 + (Z_{ii}^D)_3 \tag{B-57}$$

$$Z_{ii}^B = o \tag{B-58}$$

$$Z_{ii}^C = (Z_{ii}^C)_3 \tag{B-59}$$

$$(Z_{ii}^D)_2 = \frac{l_b^{(1)}}{8\pi}\int_{-\pi/4}^{\theta_{i+1}^+}\frac{d\theta}{\left[2a_b^2(1-\cos\theta)+(l_b^{(1)}/2)^2\right]^{\frac{1}{2}}} \tag{B-60}$$

$$(Z_{ii}^D)_3 = \frac{1}{8\pi}\int_{\theta_{i+1}^+}^{\theta_i^+} d\theta\left\{\frac{l_b^{(1)}}{2\left[2a_b^2(1-\cos\theta)+l_b^{(1)}/2)^2\right]^{\frac{1}{2}}} - \frac{l_3}{\left[2a_b^2(1-\cos\theta)+l_3^2\right]^{\frac{1}{2}}}\right\} \tag{B-61}$$

$$(Z_{ii}^C)_3 = \frac{a_b}{2\pi}\int_{\theta_{i+1}^+}^{\theta_i^+} d\theta\sin\theta\left\{\frac{1}{\left[2a_b^2(1-\cos\theta)+(l_b^{(1)}/2)^2\right]^{\frac{1}{2}}} - \frac{1}{\left[2a_b^2(1-\cos\theta)+l_3^2\right]^{\frac{1}{2}}}\right\} \tag{B-62}$$

$$l_3 = x_3 - \left[L_1 - (i - N_pN_h)l_b^{(1)} + \frac{l_b^{(1)}}{2}\right] \tag{B-63}$$

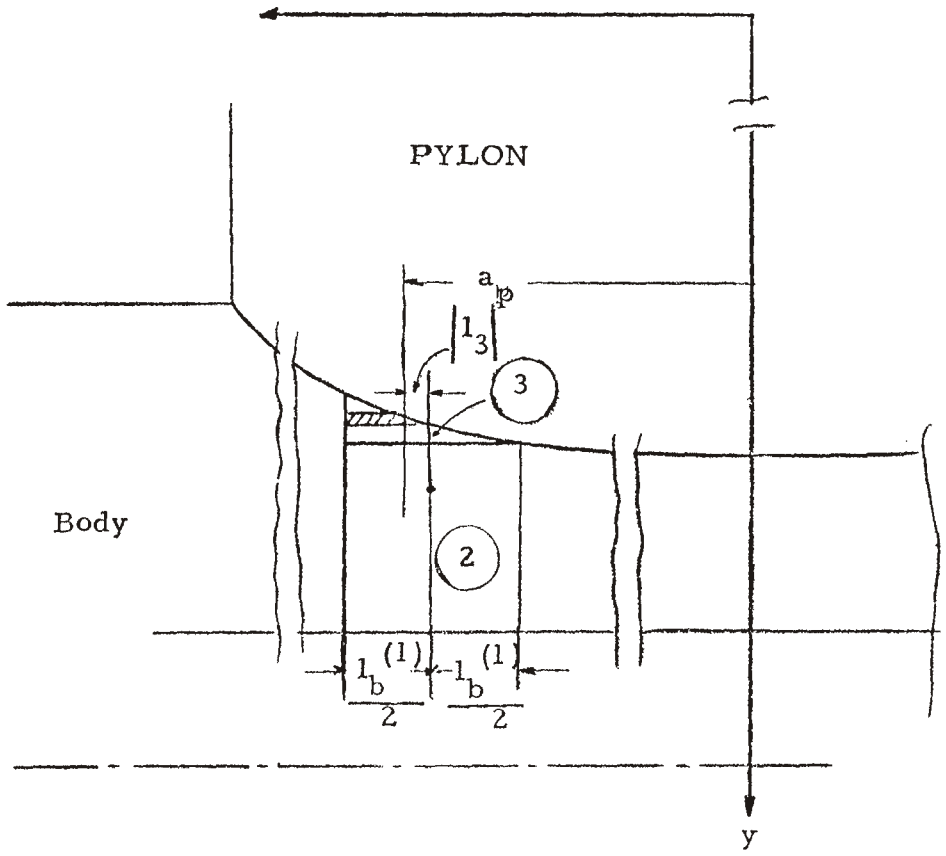

Figure 32: Geometry for the calculation of the self-contribution for zones adjacent to body-pylon intersection ($x > 0$).

$$x_3 = a_p\left[1-(z_3/b_p)^2\right]^{\frac{1}{2}} \tag{B-64}$$

$$z_3 = a_b\cos(\theta + \pi/4) \tag{B-65}$$

$$\left.\begin{aligned} \theta_m^+ &= \cos^{-1}(z_m^+/a_b) - \pi/4 \qquad (B\text{-}66)\\ z_m^+ &= b_p\left[1 - (x_m^+/a_p)^2\right]^{\frac{1}{2}} \qquad (B\text{-}67)\\ x_m^+ &= L_1 - (m - N_pN_h - 1)\, l_b^{(1)} \qquad (B\text{-}68) \end{aligned}\right\} \quad m = i, i+1$$

For zones adjacent to the body-pylon intersection and $x < o$ we can easily derive the following results

$$N_b^{(1)} + N_pN_h + 1 \le i \le N_b^{(1)} + N_pN_h + \left[\frac{a_p}{l_b^{(2)}}\right] \tag{B-69}$$

$$-Z_{ii}^A = Z_{ii}^D = (Z_{ii}^D)_2 + (Z_{ii}^D)_3 \tag{B-70}$$

$$Z_{ii}^B = o \tag{B-71}$$

$$Z_{ii}^C = (Z_{ii}^C)_3 \tag{B-72}$$

$$(Z_{ii}^D)_2 = \frac{l_b^{(2)}}{8\pi}\int_{-\pi/4}^{\theta_i'} \frac{d\theta}{\left[2a_b^2(1-\cos\theta) + (l_b^{(2)}/2)^2\right]^{\frac{1}{2}}} \tag{B-73}$$

$$(Z_{ii}^D)_3 = \frac{1}{8\pi}\int_{\theta_i}^{\theta_{i+1}'} d\theta \left\{\frac{l_b^{(2)}}{2\left[2a_b^2(1-\cos\theta)+(l_b^{(2)}/2)^2\right]^{\frac{1}{2}}} - \frac{l_4}{\left[2a_b^2(1-\cos\theta)+l_4^2\right]^{\frac{1}{2}}}\right\} \tag{B-74}$$

$$(Z_{ii}^C)_3 = -\frac{a_b}{2\pi}\int_{\theta_i}^{\theta_{i+1}'} d\theta \sin\theta \left\{\frac{1}{\left[2a_b^2(1-\cos\theta)+(l_b^{(2)}/2)^2\right]^{\frac{1}{2}}} - \frac{1}{\left[2a_b^2(1-\cos\theta)+l_4^2\right]^{\frac{1}{2}}}\right\} \tag{B-75}$$

$$l_4 = x_4 - \left[(i - N_p N_h - N_b^{(1)}) l_b^{(2)} - l_b^{(2)}/2\right] \tag{B-76}$$

$$x_4 = a_p \left[1 - (z_4/b_p)^2\right]^{\frac{1}{2}} \tag{B-77}$$

$$z_4 = a_b \cos(\theta + \pi/4) \tag{B-78}$$

$$\theta_m' = \cos^{-1}(z_m'/a_b) - \pi/4 \tag{B-79}$$

$$z_m' = b_p \left[1 - (x_m'/a_p)^2\right]^{\frac{1}{2}} \tag{B-80}$$

$$x_m' = (m - N_p N_h - N_b^{(1)} - 1) l_b^{(2)} \tag{B-8.1}$$

$$i = N_b^{(1)} + N_p N_h + \left[\frac{a_p}{l_b^{(2)}}\right] + 1 \tag{B-82}$$

$$-Z_{ii}^A = Z_{ii}^D = (Z_{ii}^D)_1 + (Z_{ii}^D)_2 + (Z_{ii}^D)_3 \tag{B-83}$$

$$Z_{ii}^B = o \tag{B-84}$$

$$Z_{ii}^C = (Z_{ii}^C)_2 + (Z_{ii}^C)_3 \tag{B-85}$$

$$(Z_{ii}^D)_1 = \frac{1}{4\pi} \int_o^{\pi/4} d\theta \left\{ \frac{l_b^{(2)}}{2\left[2a_b^2(1-\cos\theta) + (l_b^{(2)}/2)^2\right]^{\frac{1}{2}}} - \frac{l_5}{\left[2a_b^2(1-\cos\theta) + l_5^2\right]^{\frac{1}{2}}} \right\} \tag{B-86}$$

$$(Z_{ii}^D)_2 = \frac{1}{8\pi} \int_{-\pi/4}^{\theta^*} d\theta \left\{ \frac{l_5}{\left[2a_b^2(1-\cos\theta) + l_5^2\right]^{\frac{1}{2}}} + \frac{l_b^{(2)}}{2\left[2a_b^2(1-\cos\theta) + (l_b^{(2)}/2)^2\right]^{\frac{1}{2}}} \right\} \tag{B-87}$$

$$(Z_{ii}^D)_3 = \frac{1}{8\pi} \int_{\theta^*}^{\pi/4} \left\{ \frac{l_5}{\left[2a_b^2(1-\cos\theta) + l_5^2\right]^{\frac{1}{2}}} - \frac{l_6}{\left[2a_b^2(1-\cos\theta) + l_6\right]^{\frac{1}{2}}} \right\} \tag{B-88}$$

$$(Z_{ii}^{C})_2 = -\frac{a_b}{2\pi}\int_{-\pi/4}^{\theta^*} d\theta \sin\theta\left\{\frac{1}{\left[2a_b^2(1-\cos\theta)+l_5^2\right]^{\frac{1}{2}}} - \frac{1}{\left[2a_b^2(1-\cos\theta)+(l_b^{(2)}/2)^2\right]^{\frac{1}{2}}}\right\} \quad \text{(B-89)}$$

$$(Z_{ii}^{C})_3 = -\frac{a_b}{2\pi}\int_{\theta^*}^{\pi/4} d\theta \sin\theta\left\{\frac{1}{\left[2a_b^2(1-\cos\theta)+l_5^2\right]^{\frac{1}{2}}} - \frac{1}{\left[2a_b^2(1-\cos\theta)+l_6^2\right]^{\frac{1}{2}}}\right\} \quad \text{(B-90)}$$

$$l_5 = a_p - \left[(i - N_p N_h - N_b^{(1)})\, l_b^{(2)} - \frac{1}{2} l_b^{(2)}\right] \quad \text{(B-91)}$$

$$l_6 = x_6 - \left[(i - N_p N_h - N_b^{(1)}) l_b^{(2)} - \frac{1}{2} l_b^{(2)}\right] \quad \text{(B-92)}$$

$$x_6 = a_p\left[1 - (z_6/b_p)^2\right]^{\frac{1}{2}} \quad \text{(B-93)}$$

$$z_6 = a_b \cos(\theta + \pi/4) \quad \text{(B-94)}$$

$$\theta^* = \cos^{-1}(z^*/a_b) - \pi/4 \quad \text{(B-95)}$$

$$z^* = b_p\left[1 - (x^*/a_p)^2\right]^{\frac{1}{2}} \quad \text{(B-96)}$$

$$x^* = (i - N_p N_h - N_b^{(1)} - 1)\, l_b^{(2)} \quad \text{(B-97)}$$

REFERENCES

1. Sancer, M.I., and A. D. Varvatsis, "Surface currents induced on structures attached to an infinite elliptic cylinder, Part I, Detailed magnetic field integral equation for an attached structure having an arbitrary shape," AFWL Interaction Notes, Note 148, December 1973.

2. Sassman, R. W., "The current induced on a finite, perfectly conducting, solid cylinder in free space by an electromagnetic pulse," AFWL Interaction Notes, Note 11, July 1967.

3. Sancer, M. I., and A. D. Varvatsis, " Calculation of the induced surface current density on a perfectly conducting body of revolution," AFWL Interaction Notes, Note 101, April 1972.

4. Baum, C. E., "Interaction of electromagnetic fields with an object which has an electromagnetic symmetry plane," AFWL Interaction Notes, Note 63, March 1971.

5. Latham, R.W., "Small holes in cable shields," AFWL Interaction Notes, Note 118, September 1972.